Experimental Investigation of Cylindrical Grinding Inconel 718 Alloy and Multi-Objective Optimization of Cutting Parameters Using Grey Relational Analysis and Genetic Algorithm

Abdena Zewude Abdissa

A Thesis Submitted to the Department of Mechanical Engineering

School of Mechanical, Chemical, and Material Engineering

Presented in Partial Fulfillment of the Requirement for the Degree of Master's in Manufacturing Engineering

Office of Graduate Studies

Adama Science and Technology University

June, 2024

Adama, Ethiopia

Experimental Investigation of Cylindrical Grinding Inconel 718 Alloy and Multi-Objective Optimization of Cutting Parameters Using Grey Relational Analysis and Genetic Algorithm

Abdena Zewude Abdissa

Advisor: Dr. Moera Gutu Jiru (Associate Professor)

A Thesis Submitted to the Department of Mechanical Engineering

School of Mechanical, Chemical, and Material Engineering

Presented in Partial Fulfillment of the Requirement for the Degree of Master's in Manufacturing Engineering

Office of Graduate Studies

Adama Science and Technology University

June, 2024

Adama, Ethiopia

DECLARATION

I hereby declare that this Master Thesis entitled **“Experimental Investigation of Cylindrical Grinding Inconel 718 Alloy and Multi-Objective Optimization of Cutting Parameters Using Grey Relational Analysis and Genetic Algorithm”** is my original work. That is, it has not been submitted for the award of any academic degree, diploma, or certificate in any other university. All sources of materials that are used for this thesis have been duly acknowledged through citation.

Abdena Zewude Abdissa	______________________	____________________
Name of student	Signature	Date

RECOMMENDATION OF ADVISOR

I, the advisor of this thesis, at this moment, certify that I have read the revised version of the thesis entitled **“Experimental Investigation of Cylindrical Grinding Inconel 718 Alloy and Multi-Objective Optimization of Cutting Parameters Using Grey Relational Analysis and Genetic Algorithm”** prepared under my guidance by Abdena Zewude Abdissa submitted in partial fulfillment of the requirements for the degree of Master of Science in Manufacturing Engineering. Therefore, I recommend the submission of a revised version of the thesis to the department following the applicable procedures.

______________________	______________________	______________
Major Advisor	Signature	Date

APPROVAL

I, the advisor of the thesis entitled **"Experimental Investigation of Cylindrical Grinding Inconel 718 Alloy and Multi-Objective Optimization of Cutting Parameters Using Grey Relational Analysis and Genetic Algorithm"** developed by Abdena Zewude Abdissa at this moment, certify that the recommendations and suggestions made by the board of examiners are appropriately incorporated into the final version of the thesis.

Major Advisor	Signature	Date

We, the undersigned members of the Board of Examiners of the thesis by Abdena Zewude Abdissa, have read and evaluated the thesis entitled **"Experimental Investigation of Cylindrical Grinding Inconel 718 Alloy and Multi-Objective Optimization of Cutting Parameters Using Grey Relational Analysis and Genetic Algorithm"** and examined the candidate during an open defense. This is, therefore, to certify that the thesis is accepted for partial fulfillment of the requirement for the degree of Master of Science in Manufacturing Engineering.

Chairperson	Signature	Date
Internal Examiner	Signature	Date
Eternal Examiner	Signature	Date

Finally, approval and acceptance of the thesis are contingent upon submission of its final copy to the Office of Postgraduate Studies (OPGS) through the Department Graduate Council (DGC) and School Graduate Committee (SGC).

Department Head	Signature	Date
School Dean	Signature	Date
Office of Postgraduate Studies	Signature	Date

ACKNOWLEDGMENT

Above all, I want to express my gratitude and thankfulness to God, the Almighty, for all of the favors that I have received while completing research for my thesis.

I want to sincerely thank **Dr. Moera Gutu**, an associate professor at Adama Science and Technology University, who has been my thesis advisor. She has allowed me to conduct research and has given me vital advice during this thesis work. I have been greatly inspired by his dynamism, vision, genuineness, and motivation. Being able to work and study under his direction was a huge honor. I am incredibly appreciative of what he has provided for me. The invaluable guidance and assistance he provided me with in completing this research project. I also appreciate his friendliness, understanding, and wonderful sense of humor. I would want to express my sincere gratitude to his family and friends for their understanding and tolerance during our discussions about this thesis work.

I would like to sincerely thank Adama Science and Technology University for enabling me to pursue my dream of attending a technology university, the School of Research and Graduate Studies administration for their kind assistance in helping me pursue and finish my education, and the administration of the School of Mechanical, Material, and Chemical Engineering.

This thesis is fully devoted to my parents, my mother Warki Nagasa, and my father Zewude Abdissa, who have always supported me financially, emotionally, spiritually, and morally and have been my source of inspiration and strength when I've felt like giving up. I also want to thank my brothers and sisters for their important prayers and support.

Adama Science and Technology University friends. I consider each of you to be a relative and really grateful to all of you!

TABLE OF CONTENTS

LIST OF TABLES

LIST OF FIGURES

ABBREVIATIONS AND ACRONYMS

ANN	Artificial Neural Network
ANOVA	Analysis of Variance
CBN	Cubic Boron Nitride
CCD	Central Composite Design
CNC	Computer Numerical Control
CVD	Chemical Vapor Deposition
D	Diameter
d	Depth of Cut
DOE	Design of Experiments
f	feed rate
FEA	Finite Element Analysis
FEM	Finite Element Methods
GA	Genetic Algorithm
GC	Grinding Wheel Generated Higher Cutting Temperatures
GRA	Grey Relational Analysis
GRG	Grey Relational Grade
HSTR	High Strength Temperature Resistant
MQL	Minimum Quantity Lubrication
MRR	Material Removal Rate
N	Wheel speed
Ra	Average surface roughness
RSM	Response Surface Methodology
Rz	Maximum Surface Roughness
SEM	Scanning Electron Microscopy
S/N	Signal to Noise Ratio
T	Temperature
TL	Tool life
UAG	Ultrasonic Assisted Grinding
WA	Grinding Wheels, Regardless of the Depth of Cut
v	Cutting Speed
μm	Micro-meter
m	Meter

ABSTRACT

Cylindrical grinding is a complex machining process, and optimizing grinding parameters is crucial to achieving the desired surface finish and productivity. Inconel 718 alloys can be challenging during grinding procedures because these materials are poorly machine-able due to their low heat conductivity and extreme hardness. This research was to investigate the influence of process parameters, such as grinding wheel speed, feed rate, and depth of cut, on the response variables of surface roughness, material removal rate, temperature, and tool life. Experiments were performed on a CNC machine on a work piece of Inconel 718, which was commonly used in the aerospace and gas turbine manufacturing industries. A multi-objective optimization problem was solved using a Taguchi-based grey relational analysis and genetic algorithm program in MATLAB R2021. The sample was meshed using the FEM based on heat analysis of temperature by Abaqus software. An analysis of variance was used to assess the validity of the developed model. The findings showed that wheel speed contributed 78.18% and that it was the most significant parameter affecting surface roughness. A minimum surface roughness of 0.080µm was achieved at the lowest value of grinding parameters (0.01mm depth of cut, 0.02mm/rev, and 1200m/min of wheel speed), and a maximum surface roughness of 0.98µm was achieved at the highest value of grinding parameters (0.05mm depth of cut, 0.06mm/rev, and 2100m/min of wheel speed). Feed rate had a significant effect on the material removal rate (36.65%), followed by wheel speed at a percentage contribution of 22.14%. The highest temperature (119.6°C) was observed for higher grinding parameters, and the lowest temperature was obtained for the lowest grinding parameters (85.4°C). A maximum tool life of 1.48 minutes was achieved at the lowest grinding parameters, and a minimum tool life of 1.09 minutes was achieved at the highest grinding parameters. All confirmation tests were carried out using the optimum set point to confirm the standard qualities for cylindrical grinding of the work piece as suggested by the experimental results.

Keywords: *Multi-Objective Optimization, Grey Relational Analysis, Genetic Algorithm, Cylindrical Grinding, Inconel 718, Surface Roughness.*

CHAPTER-1

INTRODUCTION

1.1 Background of the Study

Machining is one type of manufacturing process, and it is most commonly used to give shape, dimensions, and sometimes properties to raw materials to produce the desired shape. Machining, collectively referred to as cutting, is the process by which a hard material, used as a cutting tool, removes unwanted portions from a material to obtain the desired shape and size. Machinability refers to the ease with which a work material is machined under a given set of cutting conditions. The main parameters considered for the assessment of machinability are surface roughness, cutting force, and tool life. The machining process can be classified into two categories: traditional and non-traditional, based on chip formation (Figure 1-1). Among the traditional machining processes, grinding is a chip-removal process that uses an individual abrasive grain as the cutting tool. It is a term used in modern manufacturing practices to describe machining with high-speed abrasive wheels, pads, and belts Code, (2018), Materials, (2017): Zahoor et al., (2020).

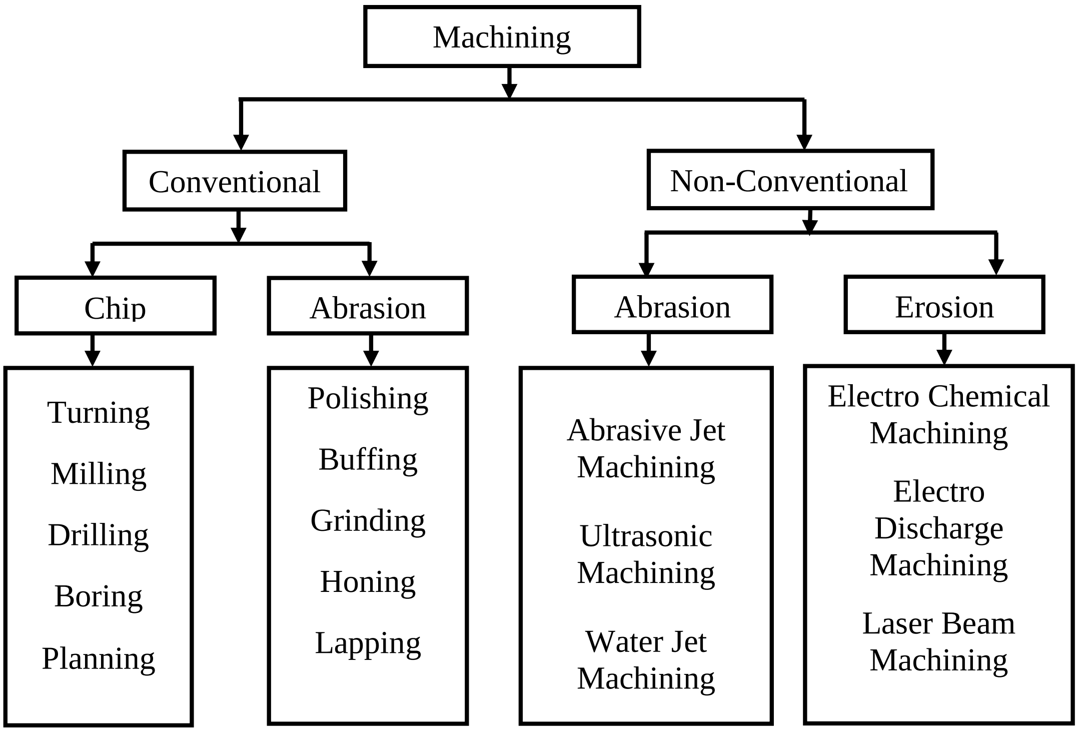

Figure 1-1: Classification of material removal process (Nukman et al., 2017).

There are two types of grinding processes: surface grinding and cylindrical grinding. Cylindrical grinding is mainly used to obtain a high surface finish, and any machining process aims to maximize the material removal rate and minimize the surface roughness. In today's world, especially in engineering applications, the demand for components with a high surface finish is increasing. Increasing productivity and quality of machined parts are the main challenges of any machining operation in the metalworking industries (Varma et al., 2018).

1.1.1 Cylindrical grinding

Cylindrical grinding machines are very common in various production sites and machinery manufacturing factories. With convenience and high efficiency, cylindrical grinding machines have become important equipment for the machinery industry. Strong and resistant to corrosion, Inconel 718 is a nickel-based superalloy that finds extensive application in gas turbines, aerospace, and other industries requiring exceptional mechanical properties under demanding conditions. The necessary dimensional accuracy, surface quality, and tight tolerances are achieved in Inconel 718 components using a variety of machining techniques, among which cylindrical grinding is one of the main methods. The cylindrical grinding precision machining method removes material off the outside surface of cylindrical work pieces to produce a smooth and accurately dimensioned item. This procedure entails spinning the workpiece on its axis as a grinding wheel typically composed of bonded abrasive particles removing material in a regulated fashion. Material is removed through heat and friction produced by the abrasive particles on the grinding wheel interacting with the workpiece surface. But if the high temperature produced during grinding is not adequately controlled, it can lead to surface damage, residual tensions, and work piece distortion (Sinha, Madarkar, et al., 2019).

1.1.2 Inconel materials

Inconel is a family of nickel-based superalloys that has exceptional strength, high temperature resistance, and corrosion resistance. They are widely used in various industries, especially in extreme environments, including aerospace, gas turbines, nuclear reactors, chemical processing, and marine engineering. There are different types of Inconel alloys, and one of them is Inconel 718. It is known for its high thermal stability and work-hardening ability, making it one of the most difficult-to-cut materials. Inconel 718 is a high-strength temperature-resistant alloy with a nickel-chromium basis that is regarded as being very challenging to process. Many previous studies have reported the poor machinability of this nickel-based alloy (Canacoo, 2022); (Liu et al., 2024).

De Bartolomeis et al.,(2021) stated that grinding can be a cost-effective alternative for roughing operations of some hard-to-machine materials. Due to the hardness of Inconel 718, with the type of grinding wheel, the depth of cut affected the surface roughness. It is important to know the relation between input parameters and their response or output characteristics. Input parameters that are usually varied in research studies are speed, feed rate, depth of cut, type of wheel, grit, usage of coolant, and force. The surface roughness of the ground part is considered an important quality measure in the industry (Curtis et al., 2021). Hence, appropriate control of cutting parameters plays a key role in the manifestation of surface quality.

1.1.3 Factors affecting surface quality

The surface roughness is mainly a result of various processes and parameters. The major factors influencing the surface quality in machining operations reported by several researchers are as follows:

- Grinding wheel selection: the selection of a grinding wheel has a major impact on surface quality. The abrasive substance, grit size, hardness, and wheel bonding type are some of the factors that affect the surface finish.
- Wheel speed: the surface finish is impacted by the grinding wheel's rotating speed. While lower wheel speeds may produce a rougher surface, higher wheel speeds typically produce finer surface finishes.
- Feed rate: the speed at which the work-piece is fed past the grinding wheel affects the surface quality. Better surface finishes are typically produced by slower feed rates because they enable more accurate material removal.
- Depth of cut: the quantity of material removed by the grinding wheel in each pass is referred to as the depth of cut. While deeper cuts may leave noticeable lines or grooves, shallower cuts usually result in smoother surface finishes.
- Work piece material: the surface quality is impacted by the substance being ground. The grinding process can be influenced by the differences in the hardness, toughness, and thermal conductivity of various materials.

- Machine rigidity and stability: to achieve superior surface quality, the grinding machine's stability and stiffness are essential. Surface imperfections could be caused by any machine's structural vibration or deflection.
- Coolant or lubrication: Surface quality can be impacted by the use of coolants or lubricants during surface grinding. Coolants aid in the process's heat dissipation, lowering the possibility of thermal damage and enhancing surface smoothness.

The prediction of the parameters of the grinding process is essential to quantify surface roughness, material removal rate, and temperature which is one of the significant quality limitations for the selection of grinding parameters in process planning (Dawood Professor, 2016a).

Kumar & Venkataramaiah, (2022a) carried out several tests to assess the effects of various process factors on the surface integrity of Inconel 718. These parameters included cutting speed, feed rate, and depth of cut. Based on surface roughness, residual stresses, and microstructural alterations, the surface integrity was evaluated.

1.1.4 Grinding operation

Grinding is one of the common abrasive machining techniques used to produce components with high surface finishes and tight tolerances. This abrasive material removal process uses an abrasive wheel with multiple grits formed of abrasive material grains. These abrasive grits are dispersed randomly throughout the wheel's volume and are incredibly hard and wear-resistant. To give the grits the appearance of a wheel, an appropriate bonding substance holds them firmly together (G. Li, Liang, Shen, Lv, Liu, Hao, & Huang, 2021). Grinding is a complex machining process, the performance of which involves several parameters related to work piece-wheel material combination along with certain machining parameters such as wheel speed, feed, table speed, and grinding mode. The environmental conditions under which grinding is carried out also play a significant role in determining the performance of the process (Sinha et al., 2023). Grind ability can be defined as the relative ease with which a particular work piece material can be ground with a specific wheel without much effort and maintaining desired surface quality. Quality of the surface includes desired surface finish and surface integrity. There is an appropriate extent of the rate of wheel wear (Sinha, Ghosh, et al., 2019a).

Due to the nature of the process, small hot chips are produced that may readily accumulate inside the inter-grit space or be re-deposited onto the work piece. Moreover, because of random grit orientation, several grits may have a large negative rake angle, low or even zero clearance angle, and may cause intense rubbing. When compared to other machining operations, the grinding process is relatively inefficient due to these two characteristics, as it requires a particular amount of energy (Halim et al., 2019).

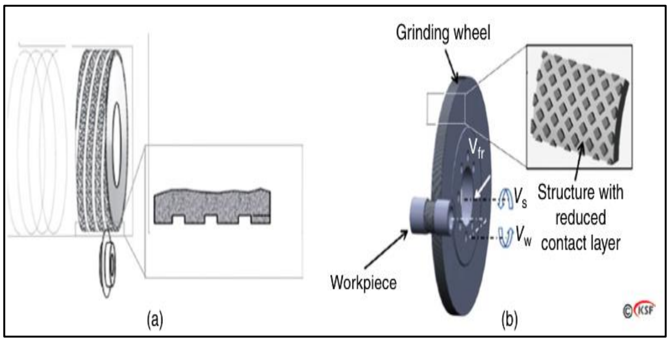

Figure 1-2: Schematic of the dressing and grinding process (Tawakoli & Daneshi, 2019).

Figure 1-2 illustrates the forces at work during the grinding process as well as the cutting effect of abrasive grits on a grinding wheel. The process of grinding is associated with a high grinding zone temperature and high specific energy (energy spent per unit volume of material removal), which are much higher than in other conventional machining operations such as turning, milling, etc. A major portion of the energy supplied is converted to heat that remains within the grinding zone. The main causes of excessive heat generation during grinding are the significant negative rake angle, the high speed of the grinding wheel, and the relatively low grit clearance angle. Elevated temperatures in the surrounding area of the grinding zone are caused by high rates of plastic deformation, grit wear, and wheel loading. In addition to reducing wheel life, these negative consequences cause several kinds of heat damage to the workpiece (Sinha, 2018).

A workpiece may suffer significant damage from excessive heat in the grinding area if it develops cracks, surface burns, or other thermal damage. Decreasing such excessive heat creation usually involves flood cooling, which involves injecting a large amount of grinding fluid into the grinding zone to transport away the heat created and regulate the temperature in the grinding zone. This makes it even easier to dispose of the chips, maintaining a clean grinding zone. However, the addition of cutting fluid frequently results in airborne dust, smoke, and other pollutants on the shop floor, which frequently has an adverse impact on the machine operator's health and the working environment (de Martini Fernandes et al., 2019). In addition, the expense of dealing with and recycling grinding fluid is a considerable worry, particularly in light of the more severe environmental rules of today. Furthermore, a lot of grinding fluid wastes away since it cannot enter the grinding zone efficiently.

As a result, when grinding, an obvious reduction in the amount of grinding fluid is preferred. Dry grinding is one option; if not, wet grinding with small quantity (SQL) or minimal quantity (MQL) lubrication may be employed. Conventional MQL/SQL uses flow rates of less than 0.05 l/h to transfer fluid as a liquid/air mix into the wheel-work contact zone, which is significantly less than typical flood cooling techniques. Even in relatively tiny amounts, MQL or SQL fluids, which are typically composed of synthetic esters and vegetable oils that are favorable to the environment, play a vital role in lubricating (Wojtewicz et al., 2019).

To standardize the grinding process, a considerable quantity of research has been conducted during the last few decades. However, working with some high-strength, temperature-resistant exotic materials present challenges for manufacturing personnel in shaping and finishing, as grinding them could intensify their hazardous properties. Among the alloys that are known to be difficult to machine are super alloys based on titanium and nickel; for this reason, it is crucial to optimize the process parameters for grinding these materials. Further study is still needed to standardize the process, even if there haven't been many studies conducted in this field previously.

1.2 Research Motivation

The machining of Inconel 718 presents numerous challenges due to its unique properties, including high strength, excellent corrosion resistance, and heat resistance. As a result, obtaining effective and affordable machining methods is a challenge for the aerospace and power generation industries, which significantly rely on this superalloy. One popular machining method that has the potential for excellent finishes and great precision is cylindrical grinding. Still, there is a lot of work to be done in the field of cutting parameter optimization for Inconel 718 cylindrical grinding. When grinding, the work piece is pressed up against a rapidly spinning grinding wheel, removing material in the shape of tiny chips using hard, sharp abrasive grits bound together with an appropriate bonding agent. The majority of the energy needed to produce chips is converted to heat, which sharply elevates the temperature at the cutting zone and boosts the possibility that the work piece was sustain considerable thermal damage (Baksa et al., 2017b).

High surface polish and accuracy are achieved through grinding, a machining technique that often results in very little material removal. However, the quality of grinding wheels and machines has improved, raising grinding to the level of abrasive machining, where material qualities do not affect the rate of material removal, precision, or polish that can be greatly enhanced (Dawood Professor, 2016b).

The key requirement for customers to accept a product for their personal use is its surface quality. This factor also increases the company's acceptance of the product as the manufacturer's surface quality rises. Inconel alloys are frequently utilized in critical industries such as aerospace, automotive, and power generation, where parts must withstand high temperatures, corrosive environments, and mechanical strains. To overcome these challenges, a thorough examination was required. Securing high-quality surface finishes, accurate dimensions, and ideal machining settings are essential to ensuring the reliability, effectiveness, and longevity of these components. It is essential to look into a technique that maximizes grinding parameters in order to handle those issues simultaneously and provide ideal input parameters.

1.3 Statement of the Problem

Aerospace, energy production, automotive, and biomedical industries require high-performance alloys, and high-load and high-pressure components must function under difficult operating circumstances. Certain industries may require their products to withstand severe mechanical and thermal loading conditions over extended periods. In these circumstances, conventional materials like steel and aluminum is not function well and have reliability and durability issues. In certain situations, employing more sophisticated materials may also be less expensive in the long term. These materials are poorly machine-able due to their low heat conductivity, quick work hardening, and capacity to react with other tool materials in an atmosphere, which limits their wider application. The other problem with surface machining is that Inconel 718 has certain qualities that make it useful at high temperatures. This may result in an improper surface finish and sudden grinding conditions. The exceptional hardness, limited heat conductivity, and work-hardening propensity of Inconel 718 alloy provide significant challenges during grinding (De Bartolomeis et al., 2021).

Optimizing the grinding parameters for cylindrical grinding by integrating RSM, GRA, GA, and FEM analysis was the primary goal of the study, which aimed to maximize machining quality and efficiency. Furthermore, the machining process was evaluated using the Johnson-Cook model and the Finite Element Method. Because of its high-speed precision, close dimensional tolerances, higher surface quality, and effective tool lubrication, a CNC grinder is one technique to use for the machining of this material. In order to improve surface finish quality, material removal rate, and overall grinding performance, this study also addresses the problems and emphasizes the need to identify the optimal grinding settings for Inconel 718 alloy.

1.4 Application of Inconel 718 Alloy

Inconel 718 is a high-temperature and corrosion-resistant nickel-based alloy commonly used in aerospace and gas turbines. Due to the strength and resistance of the material, natural heat protection because of the nickel superalloy, corrosion resistance, high mechanical strength, and good malleability and machinability, it has become a popular component for turbojet engine parts such as compressor casings, discs, and fan blades. This comprises about half of the components in conventional aircraft engine parts. Because of its efficient weldability and heat resistance, the superalloy has become an integral component of gas turbine engines (Liu et al., 2024).

1.5 Research Questions

In addition to the above, the following research questions were raised:

1. How to determine the effect of grinding parameters during cylindrical grinding of Inconel 718?
2. How to examine the effect of temperature for different grinding parameters on surface finish?
3. How to determine the optimum material removal rate for grinding parameters?
4. How to analyze the tool life for cylindrical grinding of Inconel 718 alloy?
5. How to optimize the grinding parameters by using grey relational analysis and genetic algorithm?

1.6 Objective of the Study

1.6.1 General objectives

The general objective of the study was an experimental investigation of cylindrical grinding Inconel 718 alloy and multi-objective optimization of cutting parameters using grey relational analysis and genetic algorithms.

1.6.2 Specific objectives

To meet the general objective, the following specific objectives were formulated.

1. To determine the effect of grinding parameters during cylindrical grinding of Inconel 718.
2. To examine the effect of temperature for different grinding parameters on surface finish.
3. To determine the optimum material removal rate for grinding parameters.
4. To analyze the tool life for the cylindrical grinding of Inconel 718 alloy.
5. To optimize the grinding parameters by using grey relational analysis and genetic algorithm.

1.7 Significance of the Study

The research advances the development of machining methods, especially for Inconel alloys, which are widely used in vital sectors including power generation and aircraft. The research provides better surface finish quality and material removal rate through grinding process optimization, which improves component performance and lengthens service life. The significance of this study addresses for: The study ensures efficiency and quality in grinding operations, improved grinding processes for identification of the optimal grinding parameters, Demonstrating a robust optimization approach, and reduced production costs for manufacturers. By using grey relational analysis and genetic algorithms to optimize the grinding parameters, costs can be decreased, cycle durations can be shortened, and extra post-processing steps can be avoided. In applications where components are exposed to high temperatures, corrosive conditions, and mechanical loads, this is especially important. Giving industrials the flexibility to select the best cutting parameters is another. Furthermore, the study benefits the manufacturing industry as well as the research community.

1.8 Scope of the Study

The scope of this research was to conduct experiments' performance, and to investigate the influence of process parameters, such as grinding wheel speed, feed rate, and depth of cut, on the response variables of surface roughness, material removal rate, temperature, and tool life. To develop a multi-objective optimization framework to simultaneously optimize the selected response variables by employing various optimization processes such as Grey relational analysis and Genetic Algorithm. To analyze the FE model using ABAQUS CAE software to validate the model's accuracy in predicting response, especially in terms of temperature. Generally, the integrated findings from experimental investigation, multi-objective optimization, and finite element analysis provide a comprehensive understanding of the cylindrical process for the Inconel 718 workpiece.

1.9 Limitations of the Study

The following variables were not considered in this research; it does not take into account the possibility that alternative optimization techniques, like the artificial neural network (ANN), Pareto optimization, Particle Swarm Optimization, or others, could yield different results or provide more information. The purpose of the study was to narrow down the cutting parameters of feed rate, depth of cut, and grinding wheel speed to a particular range of process parameters, or to better understand and optimize these factors. While these components are not entirely necessary for the cylindrical grinding process, additional components like as the workpiece's material characteristics, coolant flow rate, and dressing conditions may also have a big impact on how well Inconel 718 machines.

The trials were carried out in tightly controlled laboratory settings, which do not adequately reflect real-world industrial grinding situations and where other variables (such as vibrations, tool wear, and workpiece variations) may impair process efficiency. Additionally, Inconel 718, a super alloy based on nickel, was the subject of the study. The findings and optimized process parameters may not be directly transferable to other materials, as their properties and responses to the grinding process may differ significantly. The findings and conclusions drawn from this study were specific to the particular grinding setup, tool geometry, and workpiece material used.

1.10 Research Outline

The thesis report's contents were briefly introduced in the manner described below. The problem statement, study objective, applicability, limitations, and study importance were presented in the first chapter of the study. Chapter Two summarized the literature on the cylindrical grinding of Inconel 718 and associated works. Chapter Three presents the material, methods, and methodology used to accomplish the goals; Chapter Four presents the results and their discussions; and Chapter Five concludes with recommendations for further research and includes the references and appendices.

CHAPTER-2

LITERATURE REVIEW

2.1 Introduction

To focus mostly on the effective completion of the job, a review of the literature has been conducted in order to understand the issue, identify the research gap, and overcome the problems that have been mentioned. The machining of Inconel 718 cylindrical grindings was the primary focus of the current study. After a review of the summary, it was discovered that further research was needed to look into the machining behavior mentioned in the review. Additionally, an investigation and application of parametric optimization techniques to the grinding of nickel-based alloys are given.

2.2 Cylindrical Grinding Machine

The cylindrical grinding machine is a type of grinding used to shape the outside of an object. It is a precision tool used in machining to grind cylindrical surfaces and produce smooth, cylindrical workpieces. It removes material using abrasive grinding wheels, allowing for the creation of high-precision, round, and concentric shapes in a variety of industries, including manufacturing and aerospace. It can work on a variety of shapes; however, the object must have a central axis of rotation. This includes, but is not limited to, such shapes as a cylinder, an ellipse, or a crankshaft. The below figure shows a type of cylindrical grinding machine that has a direct-drive wheel speed spindle with linear motion guide ways for positioning both the table and carriage.

Figure 2-1: Cylinder grinding machine instrument (Botcha et al., 2018).

2.3 Effect of Grinding Parameters during Cylindrical Grinding

As previously mentioned, a high temperature in the grinding zone at the wheel-work piece contact is required for grinding. The chips and cutting fluid absorb most of the heat generated. Some of the heated, molten pieces could re-deposit on the ground, transferring heat to the workpiece. The heat that the workpiece absorbs causes temperatures to rise in and around the grinding zone. The methods used to grind nickel alloys are similar to those used for steel. To prevent cracking, all alloys must be in a stress-equalized state before grinding. Because Inconel 718 belongs to the D2 group of alloys, it should be rough-machined while it is annealed and finished after it has aged. The machining of these materials is increasing in frequency due to the expanding use of nickel alloys in industry. It's important to give focus to this issue because these materials are difficult (Martin et al., 2016).

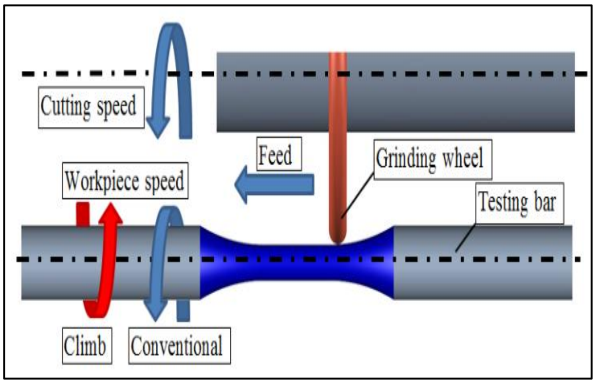

Figure 2-2: Grinding technique (Baksa et al., 2017a).

The primary goal of this effort was to determine the best grinding parameters to obtain the lowest possible surface roughness levels. As a result, the grinding parameters were determined using earlier observations. In addition, an experiment was conducted to confirm the significance of the grinding wheel clogging. Furthermore, the surface's transverse waviness was observed, as some grinding parameters cause the creation of flat faces.

2.4 Effect of Grinding Parameters on Surface Roughness

In many engineering applications, surface roughness measurement is an essential duty, and it is an important quality characteristic that override several components' functional requirements. It has a significant role in defining a machined surface's quality. Surface quality and dimensional accuracy are important factors for machine parts that come into contact with other materials or elements over their lifetime. Several studies have been carried out in the past to investigate the cylindrical grinding of Inconel 718.

Baksa et al., (2017) while performing experiments on cylindrical grinding, tried to measure the surface roughness and discussed changing the tool performance to know the best surface roughness and at the high speed of the grinding wheel and the high-speed work-piece of the workpiece, whose vectors go against to each other, cause higher friction which can lead to a higher temperature and thermal damage of the ground surface. To achieve better surface roughness it was necessary to use a grinding wheel with a smaller grain size. Two types of Inconel 718 were used for the test bars. The first was produced by conventional technology and the second by additive technology. It was confirmed that Inconel 718 produced by additive technology has the same grinding behavior as conventional Inconel 718 in terms of achieved roughness, wheel wear and spindle load. Surface roughness measurement is assessed using several factors, including Rz, Rt, and Rmax, in addition to Ra, the metric that engineering firms utilize the most. Every ground sample was taken at twelve different positions around the spinning component's circumference. The standard deviation was computed using the ten remaining measured values, which were then averaged arithmetically. The highest and lowest measured values were excluded (Martin et al., 2016).

Figure 2-3: Measurement of surface roughness (Martin et al., 2016).

Li et al., (2021) investigated Inconel 718's grind ability using alumina, green carbide, and cubic boron nitride (CBN) grinding wheels. The CBN wheel was found to produce a higher surface polish when compared to the other two. It was also seen that surface roughness increased with decreasing wheel speed, increasing table speed, and increasing feed. Because of the CBN wheel's minimal deflection and high rigidity, the work piece’s dimensional accuracy was improved. A significant rise in grinding forces makes the green carbide wheel unsuitable, whereas the alumina wheel exhibits severe wheel wear. In the case of the CBN wheel, proper dressing using an Al_2O_3 stick is extremely helpful in reducing grinding forces. Dry grinding is better for the green carbide wheel, while the CBN wheel has the longest wheel life under suitable cutting conditions. The CBN wheel is found to be the most suitable for grinding Inconel 718 if cost is not a factor.

According to (Ruzzi et al., 2020)**,** of all the output variables, wheel speed was the most important input component. With increases in wheel speed, there was a drop in the specific energy, cutting forces (Ft and Fn), and surface roughness (Ra and Rz). Plastic deformation causes both work hardening, which raises surface hardness, and degradation of the surface finish, which increases surface roughness, when wheel speed (vs) increases. The analysis showed that the depth of cut was the second most influential grinding parameter on the output variables. An increase in depth of cut led to a decrease in specific energy and a rise in cutting forces, which in turn had an undesirable effect on surface roughness. With respect to abrasive grit size (mesh), their influence on the surface roughness, the Ra parameter, and the specific grinding energy are small. Grinding with the smaller grit size (the highest mesh size) generated lower surface roughness, but on the other hand, it led to higher specific grinding energy compared to the highest abrasive grit size.

Kishore et al., (2023) investigates the grinding performance of Inconel 625 (IN 625) under dry, wet, and MQL-assisted grinding. Machine learning techniques such as multilayer perceptron (MLP), k-nearest neighbor algorithm (KNN), and support vector machine (SVM) have been implemented to predict the surface roughness (Ra) and tangential forces (Ft) under dry, wet, and MQL conditions. Further, ground surfaces and chip morphology have been critically investigated through SEM and EDS.

Hatami et al., (2022) develops the application of a compressed air jet for cleaning the wheel surface during the grinding of the nickel-based superalloy Inconel 718. The grinding of Inconel 718 poses challenges due to the material's high strength, heat resistance, and tendency to generate built-up edge and wheel loading. The study aimed to evaluate the effectiveness of using a compressed air jet to remove debris and prevent wheel clogging, thereby improving grinding performance. The jet helped remove debris, cool the grinding zone, and prevent wheel clogging during the process. This improved the cutting action and reduced the formation of built-up edge, leading to more consistent grinding performance. Additionally, the use of a compressed air jet contributed to enhanced surface quality by reducing surface roughness. The removal of debris and wheel clogging minimized the occurrence of surface defects, resulting in smoother and more uniform ground surfaces.

Kumar & Venkataramaiah, (2022b) develops the findings highlight the complex relationships between process parameters and the surface integrity of Inconel 718 during hot machining. It emphasizes the need for careful selection and optimization of process parameters to achieve the desired surface quality while considering factors such as surface roughness, residual stresses, and microstructural changes. The results provide valuable insights for improving the machining process and enhancing the surface integrity of components made from Inconel 718 in various industrial applications.

2.5 Optimization of Grinding Parameters

Numerous studies have used optimization strategies to determine the ideal combination of variables to yield the most effective outcomes for a certain process (Henry et al 2020). Modeling and optimization techniques are used in the grinding process to minimize the number of tests and obtain the optimal grinding parameters. During the modeling phase, a mathematical equation-based model that produces the optimal grinding condition can be built using the relationship between the input and response parameters. An objective function is developed, either with or without a mathematical model, in order to ascertain the grinding condition in an optimization approach.

2.5.1 Taguchi method

The simplest statistical method for optimizing input parameters to find the best possible outcomes was the Taguchi method. The standard design is transformed into a robust design using the Taguchi design of experiments. It is possible to comprehend and provide the interaction of factors influencing the output parameters thanks to this design. Orthogonal arrays (OA) of experiments that provide a set of the proper number of experimental trials are used in Taguchi analysis. The quantity of trial experiments is decreased by these orthogonal arrays (Dawood Professor, 2016a).

2.5.2 Response surface methodology (RSM)

A statistical and mathematical method called response surface methodology is used to describe and optimize the link between input variables, or components, and the response, or output, of a system or process. It is frequently used in experimental design and optimization to comprehend and enhance system or process performance. A polynomial equation, frequently quadratic or higher order, that depicts the response as a function of the components is the typical mathematical model developed from RSM. . RSM is presented in Central Composite Design (CCD) and Box-Behnken Design according to continuous factors (Adiloğlu et al., 2016).

2.5.3 Multi-objective optimization techniques

The process of optimizing systematically and simultaneously a collection of objective function is called multi objective optimization. Thus, there was many optimal solution for a multi objective problem. The exception was when the objective were not conflicting in the case where only a unique solution was expected (Serra et al 2018).

There are many types of techniques to conduct multi objective problems.

2.5.4 Grey relation analysis (GRA)

When compared to the optimization of a single performance characteristic, the optimization of numerous response characteristics is more complex. One of the key theories for discrete data, multiple input, and uncertainty is the Grey hypothesis. Between black and white is the information level of a gray system. Grey relational analysis measures the approximate correlation between sequences as well as the absolute value of the data difference between them (Sheth et al., 2021).

2.5.5 Genetic algorithm

Genetic algorithms are computerized search and optimization algorithms that fall under the evolutionary algorithms (EA) class. They operate with a collection of solutions. Using the concepts of natural selection and natural genetics, GA can evolve a series of optimum solutions centered on the global optimum solution if parameters and operators are chosen with care (Katoch et al., 2021). Genetic algorithm, which is mostly used to optimize cutting parameters in machining process, is a well-known search algorithm based on mechanics of natural and genetics. Genetic Algorithm multiple objectives and non-linear response function problems, discrete and continuous objective function. Reproduction, Crossover, and Mutation are three basic operators to generate a new population of solutions (Lu et al., 2018).

The genetic algorithm (GA) is a powerful optimization technique inspired by the principles of natural selection. It works with a population of potential solutions, mimicking the concept of "survival of the fittest." GA dynamically guides the search process by adjusting the probabilities of crossover, mutation, and selection.

This allows GA to modify the encoded information (genes) of candidate solutions, evaluate multiple individuals simultaneously, and potentially generate multiple optimal solutions (Katoch et al., 2021).

According to (Soori & Arezoo, 2022), the Taguchi optimization approach is used to modify the depth of cut and feed velocity grinding parameters during Inconel 718 super alloy grinding operations in order to minimize surface roughness and residual stress. To show how well the suggested virtual machining technology reduces surface roughness and residual stress during grinding operations, a sample work piece composed of Inconel 718 is machined.

The effect of process variables including feed, depth of cut, speed, and amplitude on output parameters is developed by (Das et al., n.d. 2021). Tangential force and surface roughness have been investigated. The input parameters have been optimized for the UAG process. Research has also been done on MQL's impact on UAG when the ideal set of parameters is used. The investigation's findings are as follows: Grey relationship analysis is used to determine the ideal set of parameters, which are as follows: amplitude of 12 microns, feed of 19 m/min, cutting speed of 30 m/s, and depth of cut of 10 microns. Experimental verification confirms the optimal values, and the outcomes match the expected outputs. When compared to the equivalent CG circumstances, the roughness values of samples ground with ultrasonic assistance in dry and MQL conditions were observed to decrease by 19.5% in dry conditions and 24.4% in MQL conditions. This outcome demonstrates that the grinding condition is improved by superimposing ultrasonic vibrations for both dry and MQL situations. For UAG with MQL values of 1.410 μm, the Ra was at its lowest. Through improved lubricant penetration and efficient heat dissipation, UAG improves MQL performance. Wheel wear and the reattachment of chips created during grinding are the reasons behind the greater levels of surface roughness and force in conventional and MQL grinding. In contrast, the work piece's vibrations caused a reduction in shear force, a reduction in friction, and a self-sharpening grinding wheel for UAG and UAG with MQL, which decreased cutting forces and improved surface smoothness. UAG provides the best condition when combined with MQL. In comparison to the other conditions, the tangential cutting forces and surface roughness were both at their lowest.

2.6 Analysis of Material Removal Rate

The material removal rate (MRR) is an important measure in grinding since it affects productivity and shows how well the operation is working. The nickel-based super alloy Inconel 718 is extremely strong and durable; therefore, maintaining surface quality while achieving a high MRR can be challenging. The weight or volume variations of the material removed before and after processing can be used to calculate the removal rate. Wb and Wa are the work piece weights before and after machining, and MRR= (Wb-Wa)/t. The processing time is shown in minutes by time t (Tufa, 2024).

Varma et al., (2018) observed and investigated as work speed and depth of cut rise, the sample's surface roughness reduces; however, an increase in feed rate has the opposite effect, while work speed increases lead to a decrease in the rate of metal removal, increases in feed rate and depth of cut have the opposite effect. The ideal machining settings for the best surface roughness were found to be 400 rpm for work speed, 400 microns for cut depth, and 1200 mm/min for feed rate. Similarly, the optimal combination is reported to be a work speed of 400 rpm, a cut depth of 300 microns, and a feed ratio of 800 mm/min based on MRR.

Esmaeili et al., (2021) examine that an increase in grain edge radius from 0.5 to 2.5 μm and an increase in maximum uncut chip thickness from 0.5 to 1.5 μm, respectively, led to an increased subsurface damage (SSD) depth by 23.86% and 129.42%. As greater negative rake angles and faster cutting rates were approached, the SSD depth did, however, first reduce and then grow. The optimal combination of influential parameters was determined using a multi-response optimization based on analysis of variance (ANOVA) and SSD predictive model. The results showed that the maximum uncut chip thickness was 0.719 μm, the cutting speed was 80 m/s, the cutting edge radius was 0.5 μm, and the rake angle was at least 30°.This lead to the minimum SSD depth of 0.406μm and the maximum removal rate of 57.493 mm^3/mm s. The experimental results confirmed the positive contribution of an ecofriendly nano-fluid minimum quantity lubrication (NMQL), containing grapheme nano plates with 0.3wt% concentration within the green fluids to the significant improvement of surface roughness (by 41.09%, relative to dry grinding) and morphology.

De Souza Ruzzi, de Paiva, Machado, et al., (2021), compares the two types of conventional abrasives (WA and GC) and discovers that, in terms of surface roughness, the GC is more appropriate for grinding Inconel 718 when utilizing a conventional cutting fluid application (wet grinding), even though it has a higher cutting region temperature. This illustrates how faster GC abrasive grit wear down elevates the temperature at the contact zone and results in a somewhat rougher ground surface than a WA wheel. Higher material removal rates, or higher values of the radial depth of cut, are the driving force behind this phenomenon.

2.7 Effect of Temperature on Surface Quality

An essential element in grinding that negatively affects the work piece's surface qualities is temperature rising. Furthermore, residual tension, deformation, and distortion of the workpiece result from the thermal stress caused by temperature variations. Three key factors contribute to tensile residual stresses in grinding: plastic deformation, thermal expansion and contraction, and phase change brought on by high grinding temperatures. The temperature differential causes tensile residual stresses, which primarily occur close to the work-piece's surface and negatively impact the material's behavior. Tensile residual stress is typically the cause of both surface and sub-surface cracks (Lyu et al., 2023).

The heat created in the contact area between the wheel and the work-piece is the major cause of the degradation of the workpiece's metallurgical qualities, surface polish, dimensional accuracy, and wheel life (Yin & Marinescu, 2017).

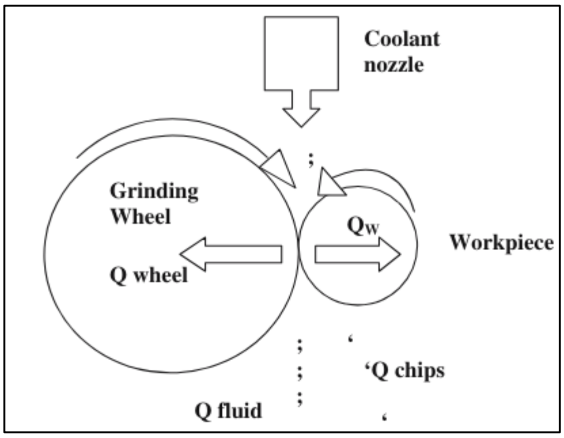

Figure 2-4: Dissipation of heat energy in cylindrical grinding (Yin & Marinescu, 2017).

The effects of temperature and force were compared for both CBN and SA wheels discussed by (X. Li et al., 2019). More work piece material was carried to the grinding region, the grinding thickness of a single grain developed, and the time required for each grinding step decreased as vw increased. Because of the incapability of the grinding heat to spread quickly, the temperature and grinding force increased, and the grinding thickness of a single grain reduced as opposed to increased. Good lubrication caused the grinding force and temperature to drop, and the grinding coolant to rise in the grinding area alongside the grinding wheel. Lastly, surface integrity was examined and assessed utilizing a SA wheel and various grinding depths, as well as grinding temperature and force. It was feasible to determine that, when grinding Inconel 718, a SA with an ap of 0.005 mm and a vw of 016 m/min and yield a superior surface than one employing a 0 25 m/s speed. The surface hardness in this grinding example was 44 HV, the surface residual stress was +700Mpa, the surface roughness was Ra 0.112µm, and the depths of the three layers were 40–60µm for the residual stress layer, 30–40µm for the softened layer, and 10–15µm for the plastic deformation layer.

2.8 Tool Life

The amount of machining time that a cutting tool has to provide a desired and acceptable performance is known as tool life. It is the amount of time, measured in minutes between tool changes, and that a tool was able to cut satisfactorily. In machining, tool life is crucial since changing and resetting a tool costs a lot of time. Higher tool life leads to higher productivity and decreased machining costs. The process of cutting tool wear and failures increases the surface roughness, and the accuracy of work piece deteriorates. Abrasive wear is strongly associated with the tool life of the Inconel 718, while adhesive and fracture wear are mostly found in the tool of the wrought Inconel 718 (Park et al., 2020).

The following variables primarily affect tool life during machining: the material of the machined component; the shape and composition of the cutting tool; the cutting circumstances; and the machining procedure.

2.8.1 Taylor tool life equation

Tool wear is always used as a life time criterion since it is easy to determine quantitatively. Most of the time flank wear land is used as the criterion because it influences work piece surface roughness and accuracy. Taylor tool life formula is as follows (Bedada et al., 2021).

$$VT^n = C \tag{2.1}$$

Where T is the tool life (min) required to develop, V is the cutting speed (m/min), n is an exponent dependent on the cutting parameters, and C is a constant. The cutting environment (application of cutting fluid) and the tool work materials are the primary determinants of the values of 'n' and 'C'. The development of numerous different materials and equipment led to the discovery that the depth of cut and grinding feed are also important factors. Taylor's tool life formula was therefore adjusted as follows to account for these modifications:

$$VT^n f^a t^b = C \tag{2.2}$$

Where f is feed (mm/rev) and t is the depth of cut (mm). It is necessary to conduct experiments to ascertain the exponents n, a, and b for every cutting circumstance.

2.9 Summary of Literature Review

For a variety of materials, many researchers have identified the optimum parameter; however, the same methodology has not yet been employed. According to the literature reviewed above and summarized in Table 2.1, most researchers focused on determining how wheel speed, feed rate, amplitude, cutting velocity, and depth of cut affect surface roughness, material removal rate, temperature, and cutting force when grinding various materials under various conditions.

Table 2-1: Summary of related literature

S. No	Author and year	Material used	Input parameters used	Output parameters	Findings	Limitations
1.	Das et al., n.d. (2021)	Inconel 718	Amplitude (6 -12) microns f= (19 – 21) m/min V= (10 -30) m/s d= (10 – 22) microns	Average surface roughness (1.410)µm, tangential and normal force.	Investigation of surface grinding on Inconel under distinct cooling conditions.	Limited the cooling condition of the experiments.
2.	Soori & Arezoo, (2022)	Inconel 718	d= 30 μm and feed velocity 130 mm/s.	Ra (0.25 μm) and Residual stress	Minimizing surface roughness and residual stress in grinding operations	Focus only feed velocity and depth of cuts.
3.	Varma et al., (2018)	Inconel 800	Work Speed 100 – 400 (rpm) d= 300 -500 (microns) f= (800 – 1600) mm/min	Surface Roughness and Material Removal Rate (MRR)	Using neural networks and ANFIS, predict to Ra and MRR.	The effect of Temp., were not explained during operations.

4.	Kishore et al., (2023)	Inconel 625	Machine learning input features (such as emission signals, cutting forces, vibration signals, or Temp.)	Surface quality (Evaluated based on Ra, surface defects (scratches, pits, cracks.	Application of machine learning techniques in environmentally benign surface grinding of Inconel 625.	It focuses the limited machine learning and environmental benignity.
5.	de Souza Ruzzi, de Paiva, da (2021)	Inconel 718	N= (10-30)m/s Work speed (5000-10,000)mm/min Depth of cut (0.01-0.03)mm Abrasive Mesh (60-100).	Surface Roughness, Wear and Force analysis.	Temperature and surface finish were analyzed when grinding with various grinding wheels.	Limited Investigation of Grinding Wheel types without optimizations.
6.	F. Li et al., (2020)	Inconel 718	Current intensity (500-1200), Current frequency (37.5)kHz Feed rate (5-10) mm/s d= (10- 40) μm	Induction heating and residual stress.	Regulating residual stresses during grinding using induction heating and magnetic flux concentrators.	The speed of the workpiece needs to be low to make the induction heating effective.
7.	Baksa et al., (2017a)	Inconel 718	d= (0.005-0.01)mm f= (5-20)mm/min Work piece speed (100-200)rpm V= (25-35)m/s	Surface Roughness and Wheel wear.	The impact of cutting conditions on surface quality and wheel.	Not focus on optimization technique simply it identify the influence parameters.

2.10 Research Gap

The parameters for grinder machines have been the subject of extensive investigation in the past. Several researchers have focused their work on the effects of grinding parameters, such as grinding wheel type, grinding wheel speed, feed rate, depth of cut, coolant type, coolant flow rate, and workpiece material properties, on the surface quality of the machined part, which affects the desired output, including surface finish, material removal rate, and overall performance on different materials, as noted in the literature. There is a lack of comprehensive experimental investigations that focus specifically on the cylindrical grinding of Inconel 718 using GRA, GA, and RSM analysis. While some studies have explored the machining of Inconel 718, they haven’t utilized these specific techniques or considered multiple performance characteristics simultaneously. Many existing studies on the machining of Inconel 718 have focused on a single performance characteristic, such as surface roughness or material removal rate. However, the simultaneous optimization of multiple performance characteristics, such as surface roughness, material removal rate, temperature, and tool life, is crucial for achieving an efficient and effective grinding process.

Insufficient investigation of the combination of gray relational analysis (GRA) and response surface methodology (RSM): There has not been much research done on the combined application of RSM and GRA for parameter optimization in the cylindrical grinding of Inconel 718. Even though RSM is an established approach for modeling and optimizing complex interactions, more research is needed to fully understand how it can be integrated with GRA and GA, two strategies that work well when handling many simultaneous goals. Even a few number of research have included ABAQUS analysis to assess workpiece properties while grinding a cylindrical surface. Incorporating ABAQUS analysis can yield a detailed understanding of the workpiece's stress distribution, temperature fluctuations, and surface integrity, which helps facilitate the optimization procedure.

CHAPTER -3

MATERIALS AND METHODS

3.1 Introduction

An investigational study was conducted to optimize grinding parameters to give the best values of surface quality, temperature, and increased material removal rate simultaneously during cylindrical grinding of Inconel 718 alloy. This chapter presents the details of the experimental procedures and properties of the material used for the study.

3.2 Experimental Procedure

This research work conducted an experimental investigation according to the research design prepared using response surface methodology, grey relational analysis, and genetic algorithms. The general procedure of an experimental investigation is presented in Fig. 3-1. Input process parameters are the workpiece material, machining parameters defined on the specific machine tool, and grinding tools located and clamped into a corresponding tool holder.

The design of the experiment was used to identify the optimum cutting parameters and the most influential parameters. Data analysis and regression model development in Analysis of Variance was conducted on Design-Expert version 13, and multi-objective optimization was conducted by using grey relational analysis and genetic algorithms. This section presents the details of the results and the discussion used for the study.

The selection of RSM and GA in this research was based on their capacity to rapidly explore, the solution space, their ability to effectively model complex systems, manage non-linear interactions, handle multiple objectives, assure strong convergence, and have practical applications in a variety of domains. RSM encompasses a set of mathematical and statistical techniques that are instrumental in the modeling and analysis of various problems. Through meticulous experimental design, the primary aim is to optimize a response, which represents the output variable that is influenced by multiple independent variables, also known as input variables. RSM is presented in Central Composite Design (CCD) and Box-Behnken Design according to continuous factors (Adiloğlu et al., 2016). GA used to modify the encoded information (genes) of candidate solutions, evaluate multiple individuals simultaneously, and potentially generate multiple optimal solutions (Katoch et al., 2021).

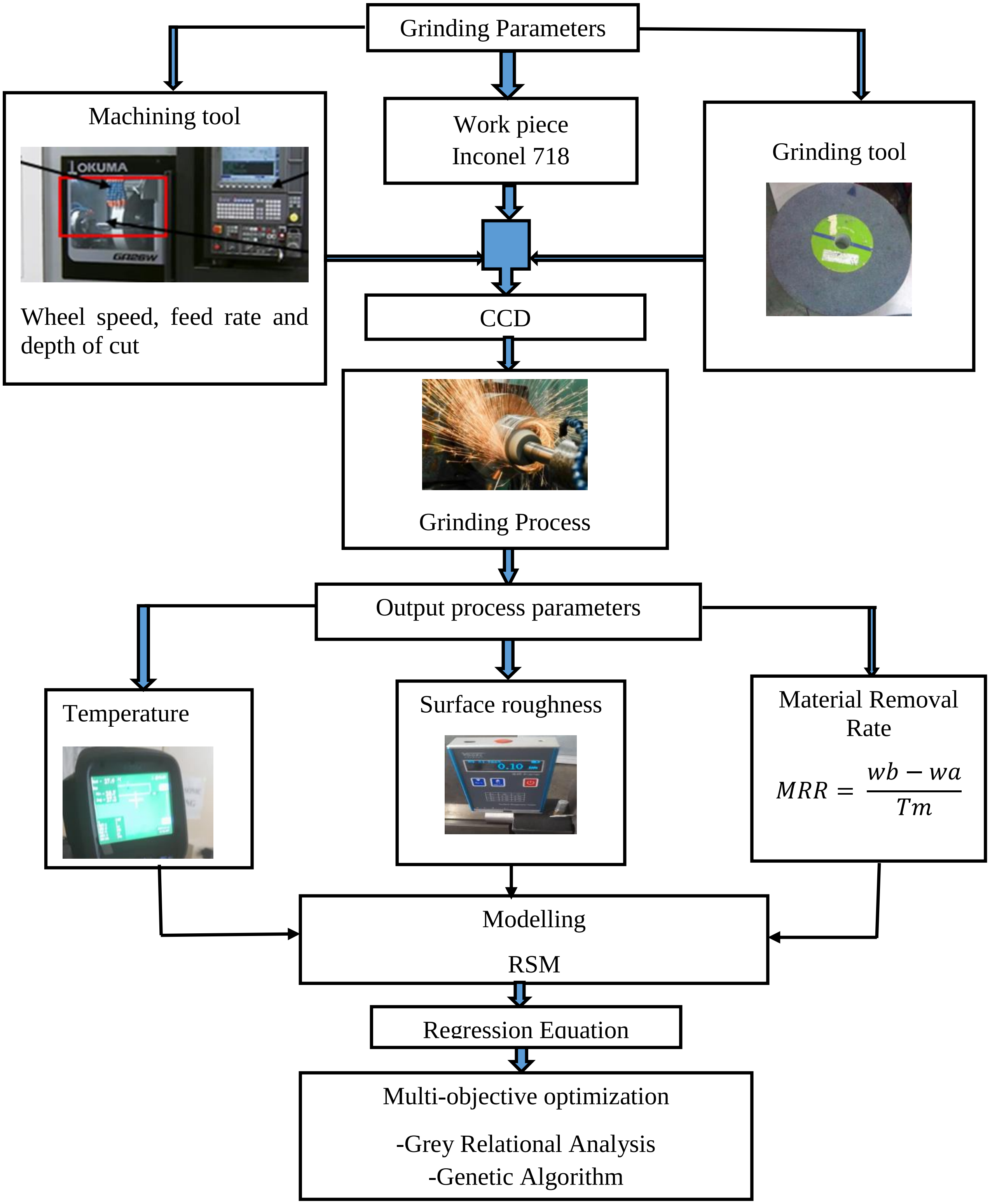

Figure 3-1: Schematic diagrams of experimental procedures

3.3 Machines and Equipment

This sub-topic describes the materials and machine tools used for the experimental investigation of the grinding of Inconel 718 under dry conditions.

3.3.1 Work piece material

The cylindrical grinding experiments were carried out using commercially available age-hardened Inconel 718 plates of the work components, manufactured with a size of 30mm x 30mm. Tables 3-1 and 3-2 provide the specimen's chemical composition and mechanical characteristics, respectively, for this experiment. Using cubic boron nitride grinding wheels, cylindrical grinding experiments have been carried out under dry conditions on an OKUMA GP-26T II two-axis CNC cylindrical grinding machine.

Figure 3-2: Work piece material used before machining

Figure 3-3: Work piece material after machining

Table 3-1: Chemical composition of Inconel 718 (Alagan et al., 2016)

Elements	C	Mn	Ti	Si	Al	Co	Mb	Cb	Fe	Cr	Ni
%age	0.08	0.35	0.6	0.35	0.8	1	3	5	17	19	52.82

Table 3-2: Mechanical properties of Inconel 718 (Alagan et al., 2016)

Yield Point (MPa)	**Hardness (HRC)**	**Elongation (%)**	**Ultimate Strength (Mpa)**
1041-1160	40-50	14-19	1260-1390

Table 3-3: Material properties of Inconel and CBN (Xie et al., 2019)

Subjects	**Inconel 718**	**CBN**
Density (kg/m^3)	8220	3400
Young's modulus (Gpa)	208	710
Young's modulus (Gpa)	0.3	0.15
Thermal conductivity (W/(m K))	11.4	80
Thermal expansion coefficient (K^{-1})	1.3×10^{-5}	2.2×10^{-6}
Specific heat (J/(kg K))	203	430

3.3.2 Grinding tool materials

Cubic Boron Nitride (CBN) was used during operations. CBN is a synthetic abrasive material known for its exceptional hardness and thermal stability. It was frequently used in grinding applications due to its resistance to heat, ability to withstand high temperatures, excellent wear resistance, high-quality surface finish as compared to other abrasives, and reduced grinding force. Using diamond and CBN grinding wheels, researchers have experimented with profile grinding while also examining the wheel wear mechanism, dimensional accuracy, surface roughness, specific grinding energy, and grinding temperature (G. Li, Liang, Shen, Lv, Liu, Hao, Huang, et al., 2021).

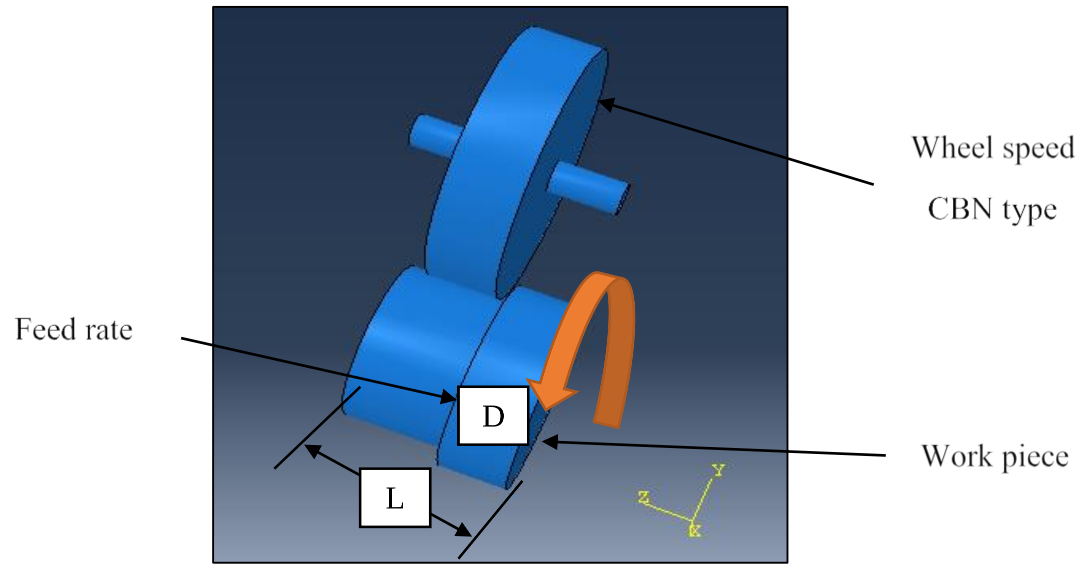

Figure 3-4: Schematic of a grinding operation in 3D using Abaqus CAE

3.3.3 Experimental setup of cylindrical grinding

In order to determine the specifications for the material used in cylindrical grinding, several researchers conducted empirical testing, which can be taken into consideration while analyzing the properties of Inconel 718 during the process. In the process of experimental investigations, several grinding settings are tested. The optimal material requirements for the grinding process can be determined using the data collected from these experiments. Below is a summary of the material specifications and experimental setups used in this research:

Grinding Wheel Type:

- Material type: Cubic Boron Nitride (CBN)
- Bond Type: Resin bond that is the bond type of the grinding wheel
- Grit Size: the grit size of the grinding wheel 120

Standards Used:

- ISO 9001: This standard ensures quality management systems are in place to meet customer requirements and continuously improve processes.
- Machine Power: the power rating of the grinding machine is 7.5KW

3.3.4 Cylindrical grinder machine

A cylindrical grinding machine is a type of machine tool used for shaping the outer surface of a workpiece. It was primarily used to grind cylindrical surfaces. The work piece is held in a chuck or between centers and rotated while a grinding wheel, mounted on a spindle, removes material to achieve the desired shape, size, and surface finish. A CNC cylindrical grinding machine is one in which the computer program directs the machine’s movements and operations to precisely grind cylindrical work pieces.

This experimental investigation was conducted on OKUMA GP-26T II CNC grinder which have capacity to grind work piece having maximum diameter of 200mm, through length capacity of 600mm, 7.5kW spindle motor. CNC grinder used for grinding process is shown on Figure 3.5.

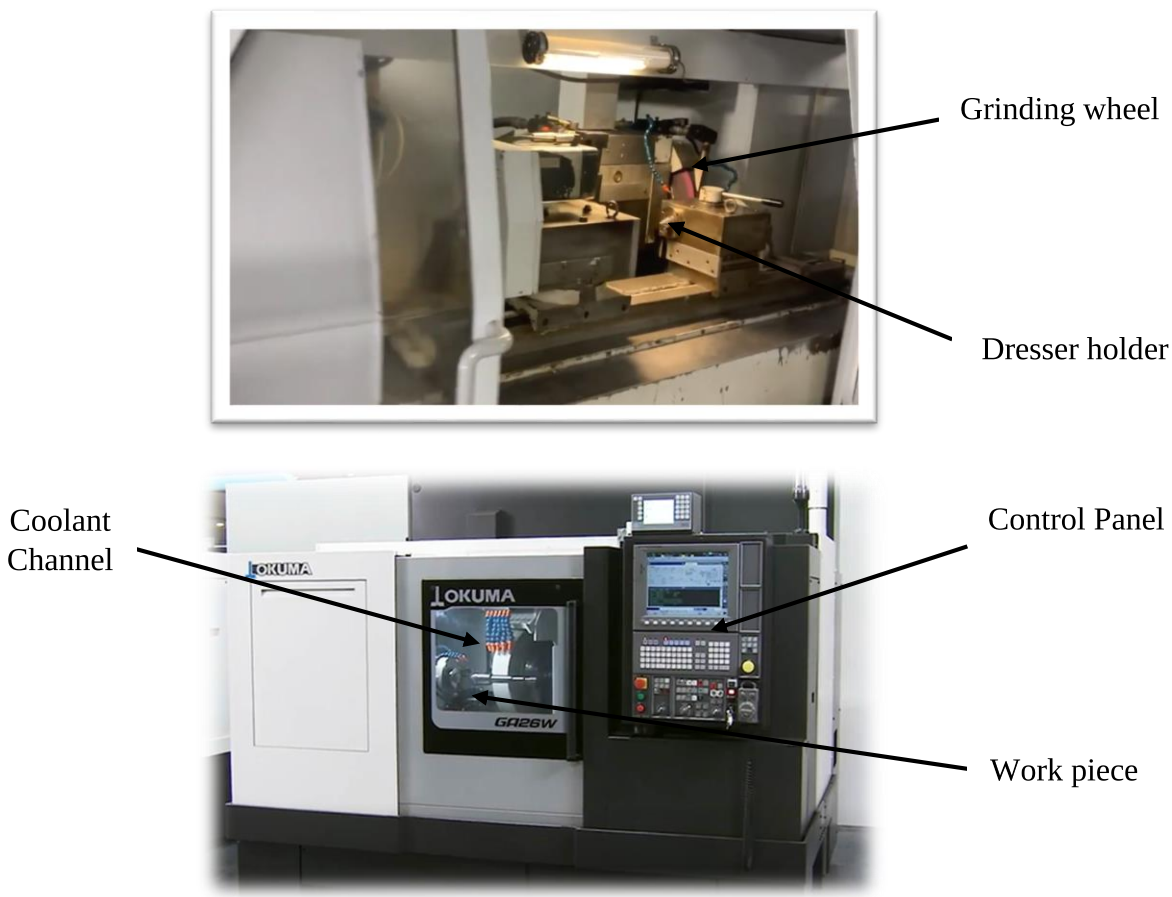

Figure 3-5: OKUMA CNC cylindrical grinder

3.3.5 Surface roughness measurement

Surface roughness was measured by a surface contact profilometer roughness tester known as the VOGEL Surface Roughness Tester with the 65711 model, which was a digital surface roughness tester, as shown in Figure 3.6. This surface roughness tester displays the roughness value in micrometers (µm). The measuring range of the VOGEL Surface Roughness Tester 65711 is 0.02µm to 10µm. A stylus attached to the detector unit of the tester was used to trace the minute irregularities of the workpiece surface. The vertical stylus displacement during the trace is processed and digitally displayed on the liquid crystal display of the instrument.

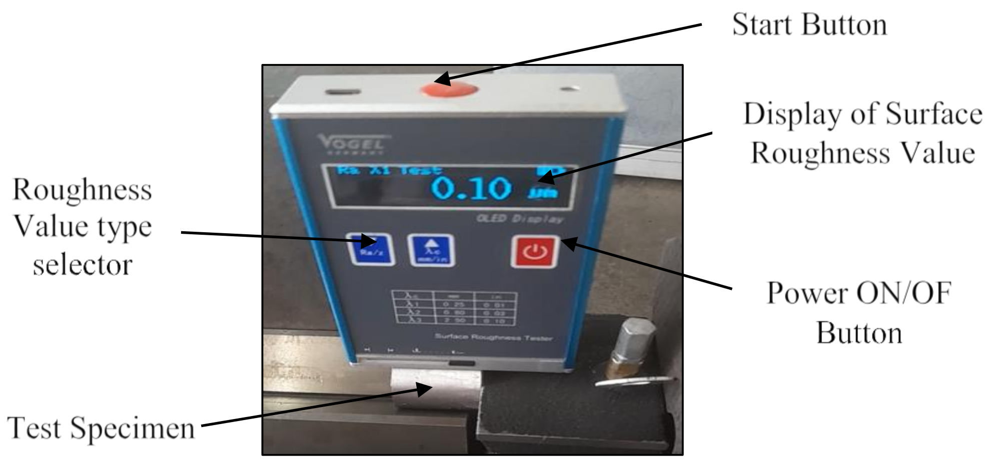

Figure 3-6: Surface-roughness testing equipment

3.3.6 Measurement of work piece temperature

The workpiece temperature was measured using an infrared thermometer to quantify and examine the link between grinding temperature. Every run's machining time was used to measure the temperature of the grinding zone. An infrared thermometer monitors an object's surface temperature and is known as a model of E30bx model. This is its basic mode of operation. The unit of optics senses emitted, reflected, and transmitted energy, which is collected and focused onto a detector. The unit electronics translate the information into a temperature reading, which is displayed on the unit. In units with a laser, the laser is used for aiming purposes only. By holding the meter by its handle grip and pointing it towards the surface to be measured. Pull and hold the trigger to turn the meter on and be tested. While continuing to push the trigger, the laser pointer is concentrated in the grinding zone. Release the trigger, and the display appeared on the LCD, indicating that the reading was being held. It can select the temperature units ^{0}C and ^{0}F. The infrared thermometer used for the temperature measurement is shown in Figure 3.7.

Figure 3-7: Infrared thermometer

3.3.7 Measurement of material removal rate (MRR)

The material removal ratio (MRR) is determined by dividing the volume of material removed by the machining time. One can determine the removal rate by measuring the weight or volume differences of the material removed before and after operation. It was measured with a model's measurement device, an HC2 pocket scale with a steel platform. Specifications: - Large load cell for reduced corner error and creep; - Capacity/Graduation: 300gx0.01g and 1000gx0.05.

Figure 3-8: Weight measurement of a work piece materials

The workpiece weights before and after machining are denoted by Wb and Wa. Time t displays the processing time in minutes.

$$MRR = \frac{wb - wa}{Tm} \quad (3.1)$$

Wb =weight of work piece material before grinding

Wa = weight of work piece material after grinding Tm = machining times (min or sec).

3.4. Methodology

This flow chart shows the steps involved in this methodology:

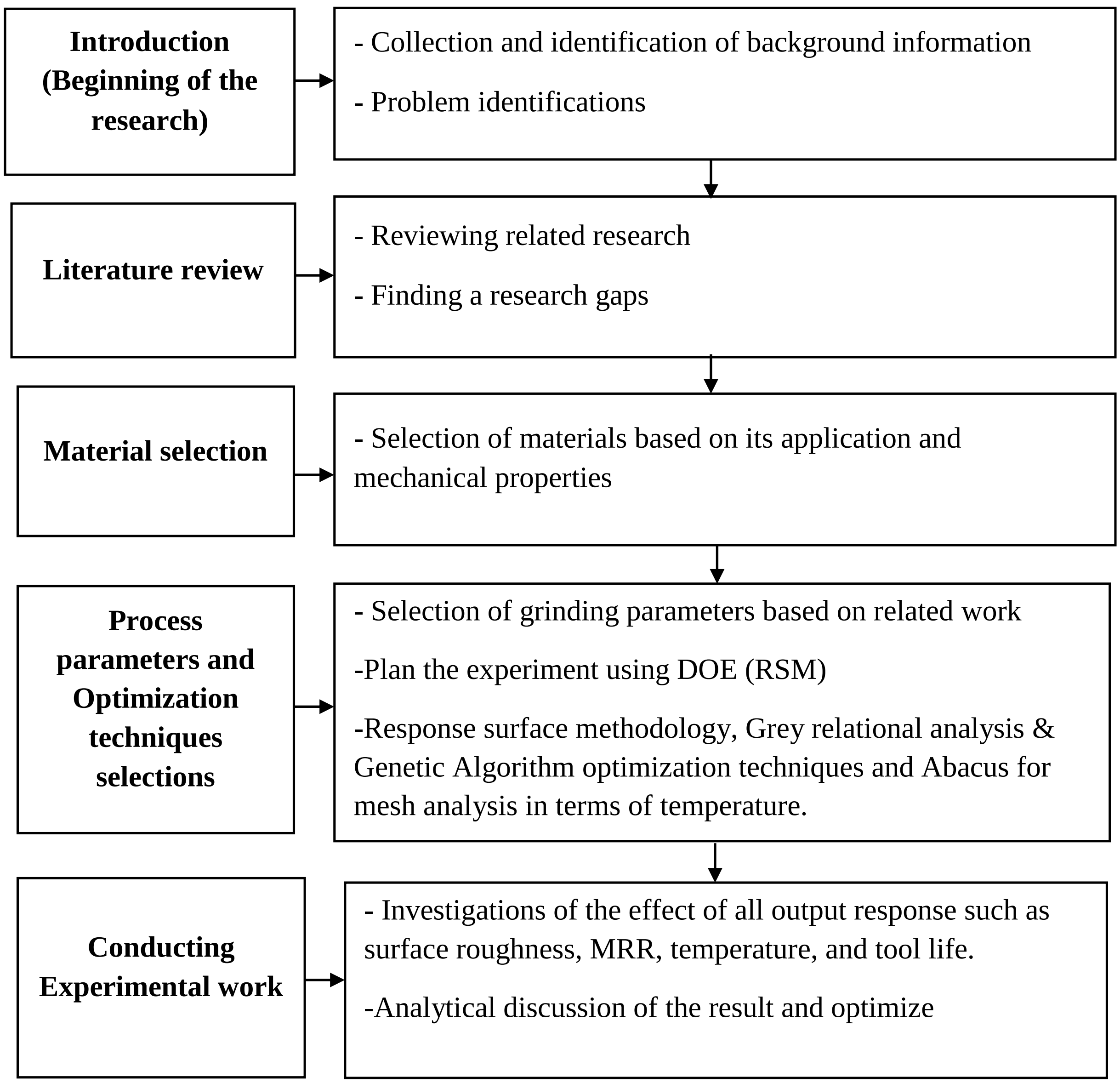

Figure 3-9: Flowchart of methodology

3.5 Selection of Process Parameter

Based on the available literature, tool manufacturer recommendations, test material manufacturer instruction manuals, industry practices, and experience, the process parameters for this Inconel 718 were chosen for experimental runs. The following grinding parameters were employed, as mentioned in Table 3-4:

Table 3-4: Process parameters selected by various researchers

Researchers	**Material**	**Tool used**	**Process parameters**		
			Wheel Speed	Feed rate	Depth of cut
Baksa et al., (2017a)	Inconel 718	CBN (Cubic Boron nitride)	(25-35)m/s or 1500-2100 (m/min) @ D=5.25mm	5-20 (mm/min) at D= 5.25mm or 0.3-0.3 (mm/rev)	0.005 – 0.01 (mm)
Varma et al., (2018)	Inconel 800	Aluminum Oxide	Another Parameter	800-1600 (mm/min)	300-500 (μm) 0.3-0.5 (mm)
de Souza Ruzzi, de Paiva, da Silva, et al., (2021)	Inconel 718	SiC (Silicon Carbide)	(10-30)m/s or (600-1800) m/min	Another parameter	0.01-0.03 (mm)
Das et al., n.d. (2021)	Inconel 718	Metal Bonded Diamond	Another parameter	19-21 (m/min) at D=20mm (0.03-0.05)mm/rev	10-22 (μm) 0.01-0.022 (mm)
Siddik et al., (2017)	Inconel 718	Aluminum Oxide	Another parameter	(0.67-6) m/min @D =30mm	0.01-0.03 (mm)
Canacoo, (2022)	Inconel 718	Aluminum Oxide	20.3m/s or 1218m/min	Another parameter	0.013-0.025 (mm)

Considering all the factors in Table 3-4, the following grinding parameters were employed for the experiment; the selected grinding parameters are shown in Tables 3–5:

Table 3-5: Levels of parameters and their range used for an experiment

Variables	Levels		
	Level I	Level II	Level III
Wheel Speed (N, m/min)	1200	1650	2100
Feed Rate (f, mm/rev)	0.02	0.04	0.06
Depth of Cut (d, mm)	0.01	0.03	0.05

3.6 Analysis and Optimization Techniques

3.6.1 Finite element analysis of grinding temperature

The investigation of thermal influences and temperature distribution in the Inconel 718 work piece during cylindrical grinding was performed. Boundary value problems are approximated using a computational technique known as finite element analysis (FEA). It employs a numerical method called the Finite Element Method (FEM). A design model is loaded into a computer and analyzed in FEA to generate preset results. It is used in situations where an accurate analytical solution is difficult to find, such as complex geometry, loads, and material characteristics. Predictions of Inconel 718 machining using FEA can greatly improve experimental evaluations when the damage and failure criteria are chosen correctly. This approach not only allows for more exact parameter calibration, but it also enhances temperature (T) prediction throughout the machining process, tool life, and surface quality assessment by analyzing surface roughness (SR) and stress state (Pedroso et al., 2024). FEA software is used in this work to do static analysis. Abaqus is used to analyses the temperature and flow stress. The temperature-dependent characteristics of Inconel 718 characterize the substance. It is believed that the substance is isotropic and opaque. Table 4-35 lists the Johnson-Cook parameter values utilized with Inconel 718. The Johnson-Cook model is a common description of the flow stress behavior of materials at high strain rates and temperatures. Figure 3-10 shows an Abaqus model of a cylindrical work item with dimensions of 30 mm in length and 30 mm in diameter.

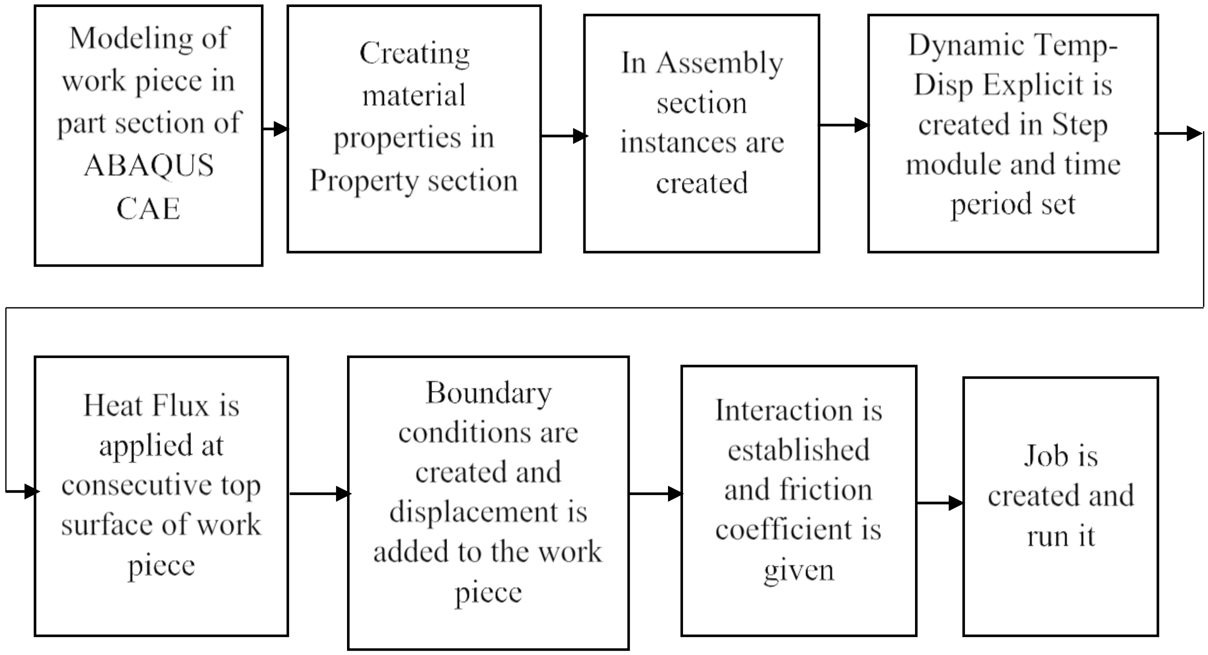

Figure 3-10: Work piece modeling flow chart in ABAQUS CAE

Figures 3-11and 3-12 show a mesh model of an Inconel 718 work component. The mesh model was most likely produced with finite element analysis (FEA) software to predict the behavior of the workpiece under various loads or situations.

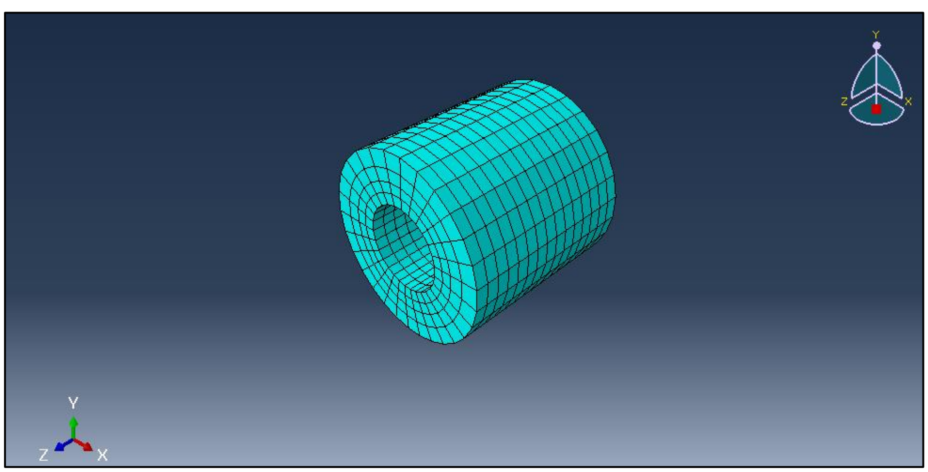

Figure 3-11: Mesh for Inconel 718 work piece

It can analyze the structural integrity, heat distribution, and other performance parameters of the workpiece by illustrating it as a mesh of microscopic parts, eliminating the need for physical prototypes.

The boundary conditions for Figure 3-12 were an initial temperature of the work piece T=85^{o}C, and the final temperature of work piece T=125^{o}C. The mesh analysis used are the thermal conductivity 11.4W/ (mk), young's modulus 208Gpa, Poisson's ratio 0.3 and specific heat 203J/(KgK).

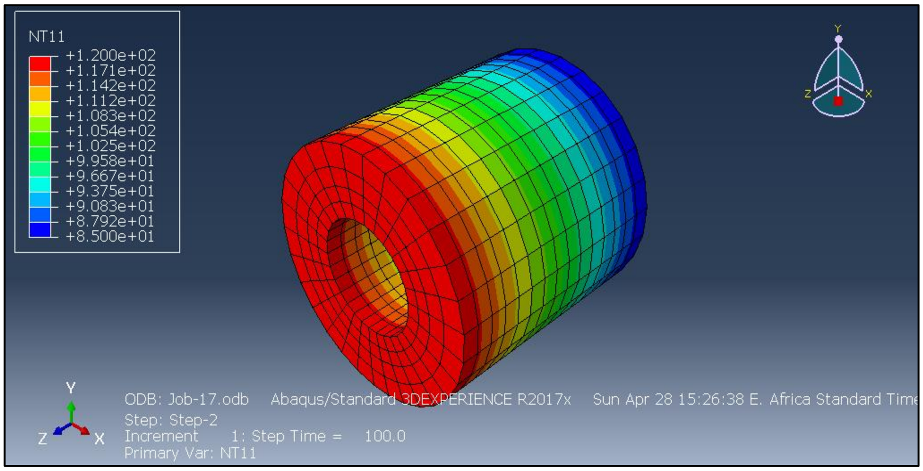

Figure 3-12: Mesh analysis Inconel 718 work piece

3.6.2 Response surface methodology (RSM)

Response Surface Methodology is an empirical optimization technique employed to assess the correlation between experimental outputs (or responses) and input variables denoted as X1, X2, X3, and so on (Khuri & Cornell, 2018).

Response Surface Methodology was used to prepare the design matrix and regression models.

The steps involved in RSM techniques are as follows:

- Designing a set of experiments for adequate and reliable measurement of the true mean response of interest.
- Following the performed experimental investigations, statistical processing, i.e. regression modelling, was developed for obtained results.
- After obtaining regression equations, transformation and reduction were performed in order to obtain models with a high coefficient of determination to predict the measured

responses (output process parameters) material removal rate (MRR), temperature, and surface roughness (Ra).

- Analysis of variance (ANOVA) was performed, as well as diagnostics and adequacy checking of regression models.

3.6.3 Analysis of variance (ANOVA)

The analysis of variance (ANOVA) was used to determine which factors had a significant impact on the quality feature. The statistical method used to determine each control parameter's influence is called an ANOVA. The percentage contributions of each control factor were employed in the analysis of variance to calculate the associated effects on the performance attributes. In this analysis, a 95% level of confidence, or a significance level of 5%, was taken into account. The output features' statistical significance can be determined by analyzing the ANOVA findings. When α values are below 0.05 and above 0.05, they are not significant in an ANOVA analysis. The percentage contribution of each model term in relation to the overall sum of squares is measured by the percent contribution. The percentage contribution is frequently a basic but reliable indicator of each model term's relative value. The percentage contribution of each influential parameter was determined using the analysis of variance (Thankachan *et al.*, 2018).

Every term used in the ANOVA table is explained here.

Block: The block row indicates the proportion of answer variance that can be ascribed to blocks. Block variance is eliminated from the examination. Blocks are regarded as non-replicated, hard-to-change factors, hence they are not tested (no F or p-value).

Model: The model row displays the overall model test for significance as well as the amount of variation in the answer that the model can account for.

Terms: The model is tested separately after being divided into individual terms.

Residual: The residual row displays the amount of response variation that remains unaccounted for.

Cor Total: The variation around the observations' mean is displayed in this row. Sum of Squares: the total of the squared discrepancies between the source of that row's variation and the general average.

Degrees of Freedom (df): The quantity of estimated parameters needed to calculate the sum of squares from the source.

The product of squares and degrees of freedom is known as the mean square. Likewise known as variance.

F Value: A test used to compare the residual mean square to the mean square of the source.

Prob > F: (p-value) Probability of seeing the observed F-value if the null hypothesis is true (there are no factor effects). Small probability values call for the rejection of the null hypothesis. The probability equals the integral under the curve of the F-distribution that lies beyond the observed F-value. i.e., if the Prob>F value is very small (less than 0.05 by default), then the source has tested significantly. Significant model terms probably have a real effect on the response. A significant lack of fit indicates the model does not fit the data within the observed replicate variation.

Mean: the sum of squares for the effect of the mean.

The column labeled "**df**" provides the degrees of freedom for each source. In response surface methodology, the total degrees of freedom equal the number of model coefficients added sequentially line by line.

For a mixture model: let q be the number of components in a mixture. The degrees of freedom for the linear terms in a mixture model is (q-1), rather than q, because the sums of squares are corrected for the mean.

3.6.4 Design of experiments

The design of experiments (DoE) technique is a very powerful tool that permits us to model and analyze the influence of process variables on the response variables. The response variable is an unknown function of the process variables, known as design factors or independent variables (Chelladurai et al., 2020). In a grinding operation, many factors can be considered as machining parameters. However, the review of the literature shows that the depth of cut (d, mm), grinding wheel speed (N, m/min), and feed rate (f, mm/rev) are the most widespread machining parameters taken by the researchers. A rotatable central composite design (CCD) was chosen for the experimentation. CCDs are built using the center and axial points to enhance 2-level factorial designs to fit quadratic models. Three levels per factor in a face-centered, central composite design were chosen. To offer superior prediction ability close to the factor space's center, four center points were employed. A DOE's sample size is based on several parameters, including process complexity, number of levels for each parameter, and required precision. Experiments were carried out according to the experimental plan based on central composite Face Centered design. The experimental design matrix consisting of experiment run order and coded values of the process parameters is shown in Table 3-6:

Table 3-6: Experimental design matrix

Run	**Wheel Speed (m/min)**	**Feed Rate (mm/rev)**	**Depth of Cut (mm)**
1	2100	0.02	0.01
2	2100	0.04	0.03
3	1650	0.04	0.03
4	2100	0.06	0.01
5	1200	0.06	0.05
6	1200	0.06	0.01
7	1650	0.02	0.03
8	2100	0.02	0.05
9	1650	0.04	0.01
10	2100	0.06	0.05
11	1200	0.02	0.05
12	1650	0.04	0.05
13	1650	0.06	0.03
14	1650	0.04	0.03
15	1200	0.02	0.01
16	1650	0.04	0.03
17	1650	0.04	0.03
18	1200	0.04	0.03

3.6.5 Multi-objective optimization by using Grey relational analysis

This multi-object optimization technique determines the interval between trial runs by correlating various sets of grinding parameters. Data preprocessing is done first in gray relational analysis in order to normalize the raw data. This process, known as gray relation generation, involves linearly normalizing the S/N ratio within the interval of 0 to 1.

For the Grey Relational Analysis (GRA), the eighteen experiments become eighteen subsystems. The influence of these subsystems on the response variable is to be analyzed using the GRA technique. The parametric conditions corresponding to the highest weighted gray relational grade give minimum values of surface roughness, and temperature. In this manner, the multi-objective problem has been converted into single-objective optimization using the GRA technique.

The quality characteristics of a control variable are evaluated using a signal-to-noise (S/N) ratio, where the signal represents the "desirable" output and noise refers to the variations in the output due to "undesirable" factors. The Taguchi method uses the signal-to-noise ratio to express the scatter around a target value. In Taguchi's experimental analysis, the output response was analyzed by considering three categories: "nominal is better, larger is better, and smaller is better." In Taguchi analysis, the mean response of the experimental data was evaluated by transforming the output data into a signal-to-noise ratio (S/N). For the present experiment, the S/N ratio of the output responses was found to be "smaller is better" since the rate of surface roughness (Ra) should be minimal. The S/N ratio condition was expressed in the logarithmic transformation of the loss function, as in Equation (Upadhyay, 2020).

- Larger - the – better

$$\text{S/N ratio}(\eta) = -10\ \log_{10}\left(\frac{1}{n}\right)\sum_{i=1}^{n}\frac{1}{y^2ij} \tag{3.2}$$

- Smaller- the better

$$\text{S/N ratio}(\eta) = -10\ \log_{10}\left(\frac{1}{n}\ \sum_{i=1}^{n} yij^2\right) \tag{3.3}$$

- Nominal -the better.

$$\text{S/N ratio}(\eta) = 10\ \log_{10}\left(\frac{\mu^2}{\sigma^2}\right) \tag{3.4}$$

$$\text{Where } \mu = \frac{y1+y2+y3+\cdots\cdots\cdots+yn}{n}$$

$$\sigma^2 = \frac{\sum(yi-\bar{y})^2}{n-1}$$

The significance of the individual parameters was determined by the Analysis of Variance (ANOVA). The ANOVA table consists of the P-value, F-value, and percentage (%) of the contribution of each parameter. The larger the F-value of a parameter, the more notable it is. The significance of a parameter can also be understood by its probability value. If the p-value is less than 0.05 for a parameter, then it is significant in the process and the percentage of contribution of each input process parameter on the quality characteristics.

In grey relational analysis, the grey relational coefficient for different process characteristics is calculated and the average of these coefficients is called grey relational grade which is used as a single response for the experimental plan, and the same is illustrated in the following steps.

Step 1: Transform the original response data into S/N ratio (Y_{ij}) using the appropriate formula depending on the type of quality characteristics using Eq. 3.2, Eq.3.3, and Eq.3.4.

Step 2: Selection of experimental design based on the levels of the process parameters normalize the performance characteristics. Using Y_{ij} is normalized as Z_{ij} ($0 \leq Z_{ij} \leq 1$) by the following formula to avoid the effect of adopting different units and to reduce the variability. It's necessary to normalize the original data before analyzing them with grey relation theory or any other methodologies. An appropriate value is deduced from the values in the same array to make the value of this array approximate to 1. Since the process of normalization affects the rank, we also analyzed the sensitivity of the normalization process on the sequencing result. Thus, we recommend that the S/N ratio value be adopted when normalizing data in grey relation analysis.

- S/N ratio with larger the better manner:

$$Zij = \frac{Yij - \min(Yij, i=1,2,....n)}{\max(Yij, i=1,2,...n) - \min(Yij, i=1,2,....n)} \tag{3.5}$$

- S/N ratio with smaller -the better manner:

$$Zij = \frac{\min(Yij, i=1,2,....n) - Yij)}{\max(Yij, i=1,2,...n) - \min(Yij, i=1,2,....n)} \tag{3.6}$$

- S/N ratio with nominal the best:

$$Zij = \frac{(Yij - Target) - \min(Yij - Target), i=1,2,....n)}{\max(Yij - Target), i=1,2,...n) - \min(Yij - Target), i=1,2,....n)} \tag{3.7}$$

Step 3: Calculation of the grey relational coefficient and the grey relational grade.

$$\gamma\big(Yo(k), Yi(k)\big) = \frac{\Delta\min + \xi\Delta max}{\Delta oj(k) + \xi\Delta max} \tag{3.8}$$

Where,

- j=1, 2…n; k=1, 2…m, n is the number of experimental data items and m is the number of responses.
- $Y_o(k)$ is the reference sequence ($Y_o(k)=1$, k=1, 2…., m; $Y_j(k)$ is the specific comparison sequence.
- $\Delta 0j = \| Yo(k) - Yi(k)$ The absolute value of the difference between $Y_o(k)$and $Y_j(k)$.
- $\nabla min = min\nabla j\ min\nabla \mathrm{k} \parallel Y0(k) - Yj(k) \parallel$ is the smallest value of Yj(k).
- $\nabla min = max\nabla jmax\nabla \mathrm{k} \parallel Y0(k) - Yj(k) \parallel$ is the largest value of Yj(k).
- ζ is the distinguishing coefficient which is defined in the range $0 \leq \zeta \leq 1$ (the value may adjust based on the practical needs of the system).

Step 4: ANOVA for grey relational grade to analyze the experimental results.

$$\bar{\gamma} = \frac{1}{k}\sum_{i=1}^{m} \gamma ij \tag{3.9}$$

Where, $\bar{\gamma}$ is the grey relational grade for the j^{th} experiment and k is the number of performance characteristics.

The grade is considered for optimizing the multi-response parameter design problem.

Step 5: Selection of optimal parameters using graph method or ANOVA response table for the grey relational grade.

The highest grey relational grade implies better product quality; therefore, based on the grey relational grade, the factor effect can be estimated and the optimal level for each controllable factor can also be determined (Unune & Mali, 2016).

3.6.6 Genetic algorithm (GA)

The genetic algorithm, a search heuristic that mimics process evaluation, is used to provide practical optimization solutions. In a genetic algorithm, a population of strings known as chromosomes represents alternative solutions to an optimization problem and evolves toward better solutions. GAs are very suitable for solving multi-objective problems (Nwobi-Okoye & Uzochukwu, 2020).

The genetic algorithm (GA) is a powerful optimization technique inspired by the principles of natural selection. It works with a population of potential solutions, mimicking the concept of "survival of the fittest." GA dynamically guides the search process by adjusting the probabilities of crossover, mutation, and selection.

This allows GA to modify the encoded information (genes) of candidate solutions, evaluate multiple individuals simultaneously, and potentially generate multiple optimal solutions (Katoch et al., 2021). In GAs, three operators are employed selection, crossover, and mutation. The selection operator involves the creation of a new population of individuals based on the fitness values of individuals from the previous generation. During crossover, specific parts of individuals are typically exchanged between two selected individuals. Mutation, on the other hand, involves randomly changing the values of particular genes (Slowik & Kwasnicka, 2020).

Steps to develop the genetic algorithm is as follows:

Step 1: Obtain mathematical model from RSM experimental design.

Step 2: Develop a Genetic algorithm MATLAB code to run the experimental data obtained from RSM

Step 3: Develop multi-objective function through MATLAB with input parameter and output response.

Step 4: Give the operation parameter of GA such as initial population, iteration number and maximum optimization time.

Step 5: Use a multi-objective function as a fitness function and run the GA.

Step 6: Obtain the optimum value for the output response.

CHAPTER-4

RESULTS AND DISCUSSIONS

4.1 Introduction

The impact of grinding parameters (wheel speed, depth cut, and feed rate) on the temperature, tool life, and surface roughness of Inconel 718 material during the cylindrical grinding process was assessed by an experimental study. The experiment was conducted on a CNC grinder machine using a CBN grinder tool. Eighteen investigations were carried out to determine the optimal condition. For each single response, measurements were obtained before, and after the machining process. After that, statistical analysis was done to identify the main effects and select the best settings following the specifications. The response values from the CCD-based response surface technique were examined using ANOVA. The software Design of Expert 13° was employed for statistical investigations. For large (numerous) optimizations, genetic algorithms and grey relational analysis were employed.

The results of each experiment were discussed in this chapter. The experiment was conducted in a controlled environment to minimize errors. The design of the experiment was used to identify the optimum cutting parameters and to identify the most influential parameters. This section presented the details of the result and discussion used for the study. Furthermore, predictive and optimization models are discussed with supporting diagrams.

4.1.1 Result values obtained from the grinding experiment

Data collection is critical in any field's statistical analysis because it determines whether the study proceeds to the best or undesirable outcome. A correct and appropriate data collecting yields better results from analysis. In such a focus, it is critical to select an appropriate data gathering technique for the analysis. In this work, the response surface methodology design, or CCD design model, was to be conducted by selecting data collecting for the grinding process. The data from each experiment wherein Inconel 718 was ground cylindrically using a CBN grinding tool is presented in Table 4-1.

Table 4-1: Experimental results

Run	N (m/min)	f (mm/rev)	d (mm)	Ra (µm)	MRR (mm^3/min)	Temp. (°C)	TL (min)
1	2100	0.02	0.01	0.48	12.54	111.5	1.16
2	2100	0.04	0.03	0.72	14.95	115.3	1.11
3	1650	0.04	0.03	0.31	9.83	103.8	1.15
4	2100	0.06	0.01	0.70	14.71	113.2	1.21
5	1200	0.06	0.05	0.23	14.14	112.7	1.18
6	1200	0.06	0.01	0.21	14.26	100.4	1.22
7	1650	0.02	0.03	0.26	6.81	101.6	1.24
8	2100	0.02	0.05	0.78	13.96	118.7	1.13
9	1650	0.04	0.01	0.27	10.56	102.4	1.19
10	2100	0.06	0.05	0.98	15.12	119.6	1.26
11	1200	0.02	0.05	0.15	8.17	98.5	1.40
12	1650	0.04	0.05	0.42	10.71	110.4	1.09
13	1650	0.06	0.03	0.45	10.83	111.1	1.17
14	1650	0.04	0.03	0.32	11.54	104.8	1.15
15	1200	0.02	0.01	0.08	7.10	85.4	1.48
16	1650	0.04	0.03	0.36	9.52	106.5	1.15
17	1650	0.04	0.03	0.37	10.63	109.9	1.15
18	1200	0.04	0.03	0.16	11.58	97.6	1.27
Min	1200	0.02	0.01	0.08	6.81	85.4	1.09
Max	2100	0.06	0.05	0.98	15.12	119.6	1.48

4.2 Surface Roughness Analysis and Discussion

Grinding wheel speed, depth of cut, and feed rate have an effect on the surface roughness of Inconel 718 when cylindrically ground. Optimization techniques and prediction models are utilized to find the best grinding parameters for achieving the desired surface finish while addressing the problems provided by Inconel 718's material attributes.

The statistical tests and descriptive statistics, such as fit summary, analysis of variance, regression equation, influence, and effect of each parameter, were discussed.

4.2.1 Fit summary

Fit Summary is a software utility that assisted in initiating the regression computation necessary to fit every polynomial model to the chosen answer. The quadratic model was suggested in Tables 4-2, 4-3, and 4-4, whereas the quadratic model was aliased. This means that the highest order model, which explains significantly more of the response variation (p-value small), has an insignificant lack of fit (p-value > 0.10), and the Adjusted R-squared and Predicted R-squared have reasonable agreement (within 0.2 of each other).

Table 4-2: Fit summary

Source	Sequential p-value	Lack of Fit p-value	Adjusted R^2	Predicted R^2	
Linear	< 0.0001	0.0447	0.8880	0.8168	
2FI	0.0978	0.0639	0.9178	0.6855	
Quadratic	**< 0.0001**	**0.9658**	**0.9932**	**0.9911**	**Suggested**
Cubic	0.8992	0.9040	0.9890	0.9757	**Aliased**

Table 4-3: Sequential model sum of squares

Source	Sum of Squares	df	Mean Square	F-value	p-value	
Mean vs Total	2.94	1	2.94			
Linear vs Mean	0.9176	3	0.3059	45.94	< 0.0001	
2FI vs Linear	0.0394	3	0.0131	2.69	0.0978	
Quadratic vs 2FI	**0.0505**	**3**	**0.0168**	**41.39**	**< 0.0001**	**Suggested**
Cubic vs Quadratic	0.0006	4	0.0002	0.2448	0.8992	Aliased
Residual	0.0026	4	0.0007			
Total	3.95	18	0.2193			

Table 4-4: Model summary statistics

Source	Std. Dev.	R^2	Adjusted R^2	Predicted R^2	PRESS	
Linear	0.0816	0.9078	0.8880	0.8168	0.1852	
2FI	0.0699	0.9468	0.9178	0.6855	0.3179	
Quadratic	**0.0202**	**0.9968**	**0.9932**	**0.9911**	**0.0090**	**Suggested**
Cubic	0.0256	0.9974	0.9890	0.9757	0.0246	Aliased

4.2.2 Analysis of variance for surface roughness

The analysis of variance (ANOVA) was performed to determine the relative relevance of the cutting parameters in relation to surface roughness during cylindrical grinding of Inconel 718 alloy. The statistical tests and descriptive statistics are shown in the ANOVA. In broad terms, look for low p-values to identify significant terms in the model. Tables 4-5's surface roughness analysis of variance revealed that the model's F-value of 275.16 indicates the model's significance. This kind of significant F-value has a 0.01% probability of being caused by noise. Model terms are considered significant when P-values are less than 0.0500. A, B, C, AB, AC, and A^2 are important model terms in this instance. The model terms are not important if the value is bigger than 0.1000. Model reduction could make your model better if it has a large number of insignificant model terms (apart from those needed to maintain structure). The F-value is not fit. There is a 96.58% chance that noise is the cause of a significant lack of fit F-value. The model should fit since it is desirable to have a non-significant lack of fit. The model fits the data and used to interpolate with confidence if the difference between the adjusted R-squared and anticipated R-squared from Table 4-6 is less than 0.2. Furthermore, it was discovered that Table 4-6's sufficient precision was greater than 4, or 58.6654, indicating that the model's signal strength was sufficient to allow optimization. This ANOVA's percentage of contribution was calculated by dividing the sum of squares for each individual source by the sum of squares for the C or Total.

Table 4-5: Analysis of variance for surface roughness

Source	Sum of Squares	df	Mean Square	F-value	p-value		% of contribution
Model	1.01	9	0.1120	275.16	< 0.0001	Significant	
A-Wheel Speed	0.7896	1	0.7896	1940.74	< 0.0001		78.18 %
B-Feed Rate	0.0640	1	0.0640	157.30	< 0.0001		6.34 %
C-Depth of Cut	0.0640	1	0.0640	157.30	< 0.0001		6.34 %
AB	0.0066	1	0.0066	16.25	0.0038		0.65 %
AC	0.0325	1	0.0325	79.91	< 0.0001		3.22 %
BC	0.0003	1	0.0003	0.7681	0.4064		0.03 %
A^2	0.0258	1	0.0258	63.47	< 0.0001		2.55 %
B^2	0.0004	1	0.0004	1.06	0.3332		0.04 %
C^2	0.0000	1	0.0000	0.0457	0.8361		-
Residual	0.0033	8	0.0004				0.33 %
Lack of Fit	0.0007	5	0.0001	0.1511	0.9658	not significant	
Pure Error	0.0026	3	0.0009				
Cor Total	1.01	17					

Table 4-6: Fit statistics

Std. Dev.	0.0202	**R^2**	0.9968
Mean	0.4039	**Adjusted R^2**	0.9932
C.V. %	4.99	**Predicted R^2**	0.9911
		Adeq Precision	58.6654

4.2.3 Regression model for surface roughness

This model used to determine the statistical relationship between cutting parameters and surface roughness. The change in grinding parameters associated with the change in the surface roughness was ascertained by using this model.

Regression Equation:

$$Ra\ (\mu m) = -0.906 + 0.000624\ N\left(\frac{m}{min}\right) + 4.00\ f\left(\frac{mm}{rev}\right) + 4.00\ d\ (mm) \tag{4.1}$$

4.2.4 Parametric influence on surface roughness

The residuals follow a normal distribution and, therefore, a straight line, according to the graph of the Normal Probability plot vs internally studentized residual in Figure 4.1a. The plot of the residuals against the ascending predicted response values on Figure 4.1 b, which is used to test the assumption of constant variance, revealed a random scatter or constant range of residuals across the graph, indicating that no transformation is required. This is the graph of residuals vs. predicted. Therefore, the model is appropriate for doing analyses on how different factors affect surface roughness.

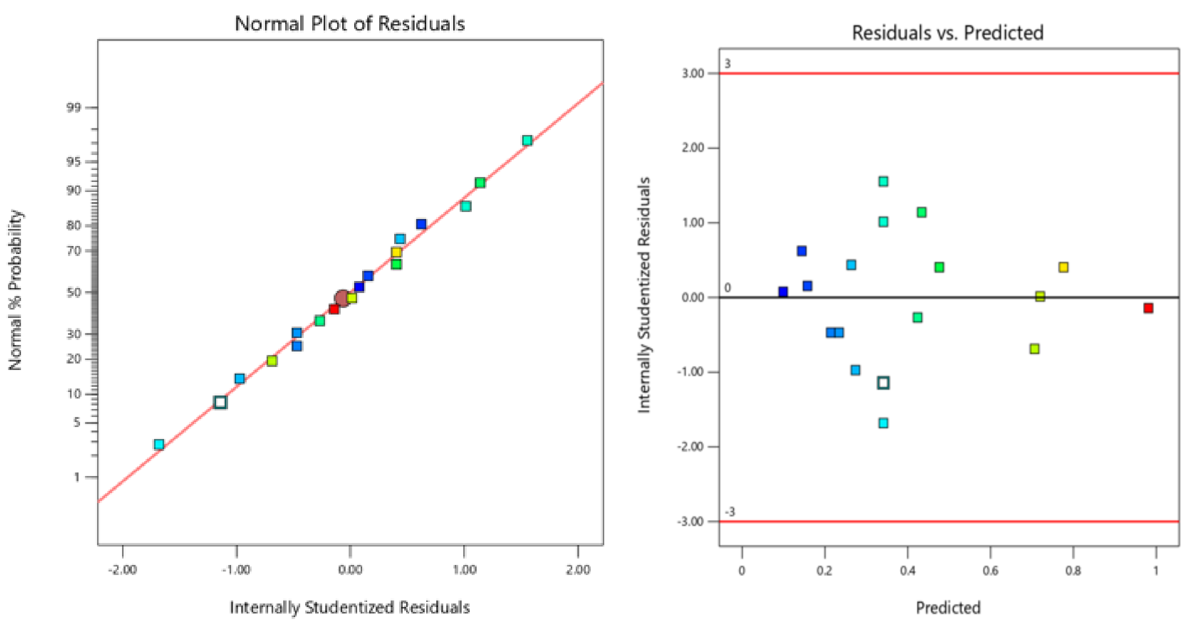

(a) (b)

Figure 4-1: (a) Normal plot of residuals and (b) Residuals vs. Predicted

4.2.5 Effect of wheel speed on surface roughness

Wheel speed is the rotational speed of the grinding wheel that affects the surface finish. The effect of wheel speed on surface roughness is shown in Figure 4-2. The minimum surface roughness was obtained at the lowest speed of 1200 m/min, and the maximum surface roughness was found at the highest feed rate of 2100 m/min, when wheel speed increased at a constant feed rate and depth of cut. The investigation and ANOVA revealed that wheel speed, which accounts for 78.12% of the variation in surface roughness, is a significant factor influencing surface roughness. Increased wheel speed means more material is in contact with the grinding work piece, which results in a higher grinding force to remove material at a faster rate, which results in the existence of vibration and friction, which leads to high surface roughness. Surface roughness and the degree of work hardening rapidly decrease with increased grinding speed, and a similar effect was obtained and discussed by (Liu et al., 2024). The relationship between wheel speed and surface roughness is quadratic, as suggested by the ANOVA model. Figure 4-2 shows a 3D surface projection of the contour plot graph for the interaction effects of wheel speed and feed rate on surface roughness.

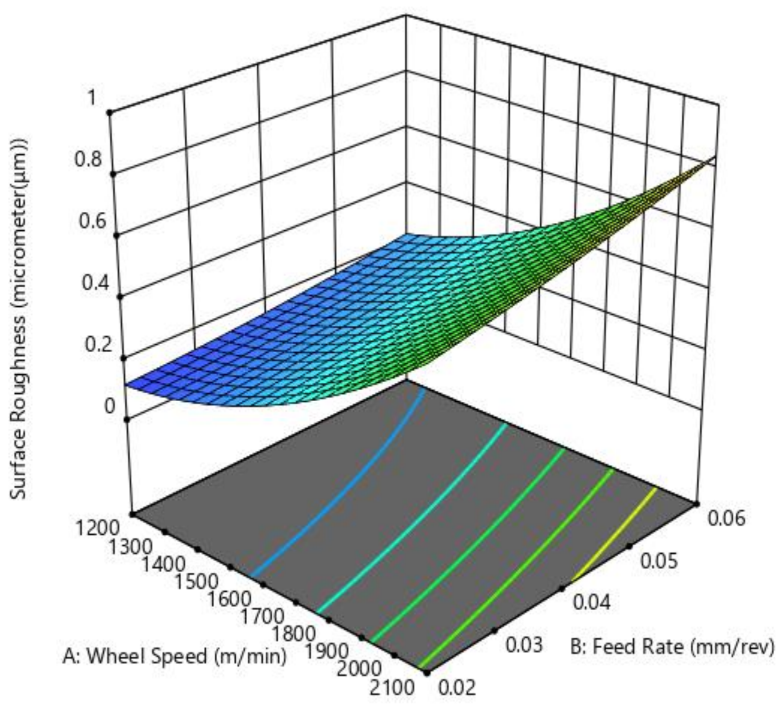

Figure 4-2: Interaction effects of wheel speed and feed rate on Ra

4.2.6 Effect of depth of cut and feed rate on surface roughness

Feed rate and depth of cut were shown to have little effects on surface roughness, contributing 6.34% and 6.34% of the total, respectively.

The figure below illustrates the relationship between the depth of cut, feed rate, and surface roughness, with constant wheel speed values indicating the effect of depth of cut and feed rate on the surface roughness for grinding Inconel 718. Figure 4-3 shows the 3D surface projection of the contour plot graph for the interaction effects of feed rate and depth of cut on surface roughness.

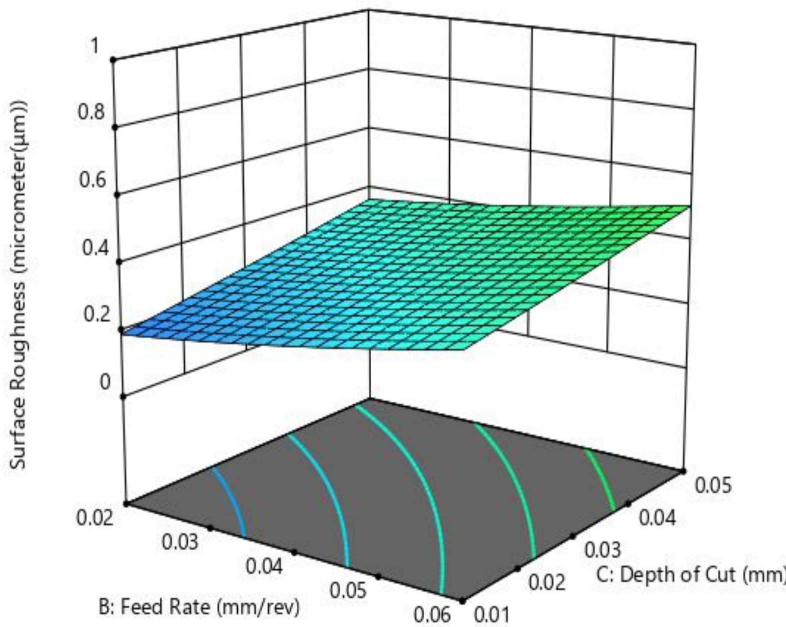

Figure 4-3: Interaction effects of feed rate and depth of cut on Ra.

4.3 Analysis of Workpiece Temperature

Friction between the tool work and the wheel interface caused heat to be produced during the machining process. The kind of material being machined and the grinding parameters employed affect how much heat is produced. Heat generation at the grinding wheel interface was confirmed by measurements and observations made throughout the experimental activity. Table 4.1 presents the recorded temperature for various parameters during the grinding process of Inconel 718, using an infrared thermometer.

4.3.1 Fit summary

Fit summary computes all model parameters and statistics, such as R-squared values for model comparison, lack of fit, and p-values. It also produced a model suggestion and the essential statistical information required to select the proper beginning point for the final model fitting. Tables 4-7 and 4-8, which clearly show that the cubic and quadratic models are aliased, support the recommendation of the 2FI model, which is the sequential sum of squares for the two-factor interaction A, B, C, AB, BC, and AC terms. This indicates that the highest order model has an insignificant lack of fit (p-value > 0.10), explains a significant amount of the response variation (p-value small), and has an acceptable degree of agreement (within 0.2) between the adjusted and predicted R-squared.

Table 4-7: Fit summary

Source	**Sequential p-value**	**Lack of Fit p-value**	**Adjusted R^2**	**Predicted R^2**	
Linear	< 0.0001	0.4206	0.8651	0.7594	
2FI	**0.0006**	**0.9846**	**0.9619**	**0.9316**	**Suggested**
Quadratic	0.6151	0.9897	0.9576	0.9568	
Cubic	0.9647	0.8654	0.9248	0.6962	**Aliased**

Table 4-8: Sequential model sum of squares

Source	**Sum of Squares**	**df**	**Mean Square**	**F-value**	**p-value**	
Mean vs Total	2.055E+05	1	2.055E+05			
Linear vs Mean	1092.04	3	364.01	37.34	< 0.0001	
2FI vs Linear	**106.17**	**3**	**35.39**	**12.85**	**0.0006**	**Suggested**
Quadratic vs 2FI	5.80	3	1.93	0.6315	0.6151	
Cubic vs Quadratic	2.76	4	0.6905	0.1271	0.9647	Aliased
Residual	21.73	4	5.43			
Total	2.068E+05	18	11486.36			

Table 4-9: Model summary statistics

Source	Std. Dev.	R^2	Adjusted R^2	Predicted R^2	PRESS	
Linear	3.12	0.8889	0.8651	0.7594	295.57	
2FI	**1.66**	**0.9753**	**0.9619**	**0.9316**	**83.97**	**Suggested**
Quadratic	1.75	0.9801	0.9576	0.9568	53.08	
Cubic	2.33	0.9823	0.9248	0.6962	373.25	Aliased

4.3.2 Analysis of variance for work piece temperature

An Analysis of Variance (ANOVA) for workpiece temperature during cylindrical grinding of Inconel 718 is a statistical method for determining the relative influence of numerous parameters on the workpiece's temperature during the grinding process. This research helps to determine which elements have a major impact on workpiece temperature and how they interact with one another. ANOVA aids in determining which factors have a statistically significant impact on temperature by assessing the variance in workpiece temperature under various combinations of these variables. This information can be used to optimize the grinding process and minimize the risk of overheating, which is critical for maintaining the integrity and quality of the workpiece, especially for materials like Inconel 718, which are known for their high strength and resistance to corrosion and oxidation.

Descriptive statistics and statistical tests were presented in this section. Low p-values identified important terms in the model. From the analysis of variance for tool tip temperature in Table 4–10, it was observed that the **model F-value** of 72.51 implies the model is significant. There is only a 0.01% chance that an F-value this large could occur due to noise. P-values less than 0.0500 indicate model terms are significant. In this case, A, B, C, AB, and AC are significant model terms. Values greater than 0.1000 indicate the model terms are not significant. If there are many insignificant model terms (not counting those required to support hierarchy), model reduction to improve the model. The lack of fit F-value of 0.15 implies the Lack of Fit is not significant relative to the pure error. There is a 98.46% chance that a lack of fit F-value this large could occur due to noise.

Table 4-10: Analysis of variance for work piece temperature

Source	Sum of Squares	df	Mean Square	F-value	p-value		% of contribution
Model	1198.21	6	199.70	72.51	< 0.0001	Significant	97.53%
A-Wheel Speed	700.57	1	700.57	254.36	< 0.0001		57.03%
B-Feed Rate	170.57	1	170.57	61.93	< 0.0001		13.88%
C-Depth of Cut	220.90	1	220.90	80.20	< 0.0001		17.98%
AB	88.44	1	88.44	32.11	0.0001		7.2%
AC	17.40	1	17.40	6.32	0.0288		1.42%
BC	0.3200	1	0.3200	0.1162	0.7396		0.026%
Residual	30.30	11	2.75				2.47%
Lack of Fit	8.81	8	1.10	0.1537	0.9846	not significant	
Pure Error	21.49	3	7.16				
Cor Total	1228.50	17					

Table 4-11: Model summary statistics

Source	Std. Dev.	R^2	Adjusted R^2	Predicted R^2	PRESS	
Linear	3.12	0.8889	0.8651	0.7594	295.57	
2FI	**1.66**	**0.9753**	**0.9619**	**0.9316**	**83.97**	**Suggested**
Quadratic	1.75	0.9801	0.9576	0.9568	53.08	
Cubic	2.33	0.9823	0.9248	0.6962	373.25	Aliased

4.3.3 Influence of grinding parameter on work piece temperature

Figure 4-4a's graph of the externally studentized residual vs the normal probability plot showed that the residuals either dropped on a straight line or extremely near to it, suggesting that the mistakes are normally distributed. The assumption of constant variance was tested using the residuals vs. predicted graph in Figure 4.4b, which plots the residuals against the ascending predicted response values. The plot showed a random scatter or constant range of residuals across the graph, indicating that no transformation was required and that all temperature values were within a reasonable range. So, the model was valid to determine the effect of individual factors on the temperature obtained during grinding.

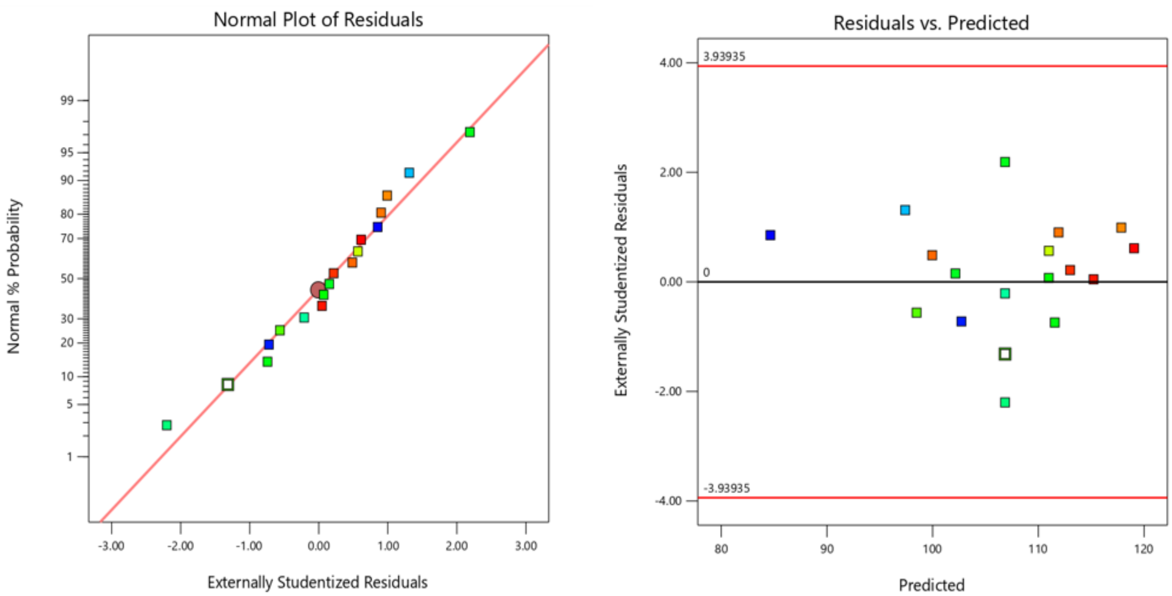

(a) (b)

Figure 4-4: (a) Normal plot of residuals and (b) Residuals vs. Predicted

As observed from Table 4-1, the maximum temperature (119.6) was established at a high wheel speed of 2100 m/min, a feed rate of 0.06 mm/rev, and a high depth of cut of 0.05mm. The minimum temperature of 85.4 °C was obtained at low grinding parameters.

From Table 4-1 As surface roughness increased, the temperature value also increased; hence, temperature increased, and a similar result has been obtained by (Deshpande et al., 2018). The grinding temperature depends greatly on the wheel characteristics, higher wheel speeds, feed rates, depth of cuts, and workpiece properties of a material. Controlling the temperature during Inconel 718 cylindrical grinding requires careful consideration and optimization of these aspects. High temperatures have the potential to cause thermal damage, alter material properties, and reduce surface integrity, all of which can have a negative impact on the quality of the finished product. Figure 4-5 shows the effect of parameters on temperatures A, B, and C, representing wheel speed, feed rate, and depth of cut, respectively.

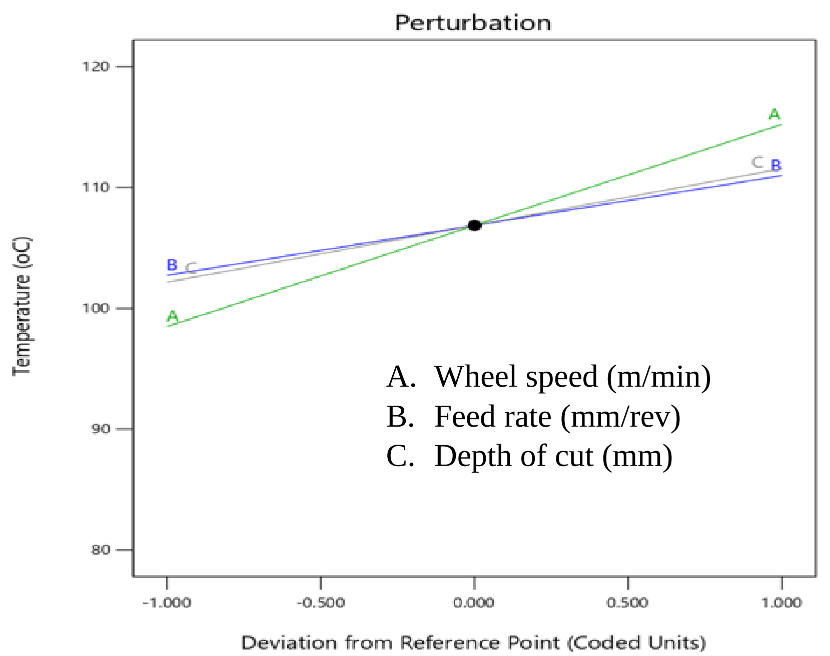

Figure 4-5: Effect of grinding parameters on temperature

To compare and display the impact of all machining parameters at the center point on the grinding temperature, a perturbation plot similar to the one in Figure 4.5 was created. The results displayed in Figure 4.5's perturbation plot are as follows:

(i) As temperatures increased, the wheel speed (A) also increased significantly, as shown by ANOVA Table 4-10. Wheel speed has a significant percentage contribution of 57.03% to the work piece temperature, meaning that a significant amount of temperature change was observed for the same amount of feed rate and depth of cut. The lowest recorded temperature of 85.4^{o}C was found at the lowest wheel speed of 1200 m/min, and the highest recorded temperature of 119.6^{o}C was found at the maximum wheel speed of 2100 m/min. Temperature increases as a result of increased friction between the work piece and the grinding wheel as well as a lack of time for the heat produced to disperse. A similar result has been obtained by (Baksa et al., 2017a) achieves and discusses this by changing the tool performance to know the best surface roughness, and at high speed, the grinding wheel and the high-speed workpiece, whose vectors go against each other, cause higher friction, which can lead to higher temperatures and thermal damage to the ground surface.

(ii) The grinding temperature also increased with an increase in the depth of cut (d) for the same reason as wheel speed, which is due to friction created at the tool work interface. It has a percentage contribution of 17.98% to temperature change as obtained from the ANOVA table and

(iii) There is no much increase in the grinding temperature due to increase in the feed rate as compared to wheel speed and depth of cut. And generally increasing wheel speed and depth of cut together has a higher effect on the grinding tool temperature than increasing the depth of cut. Depth of cut value has a smallest effect on grinded work piece temperature compared to wheel speed and feed rate.

Increased wheel speed, feed rate, and depth of cut during cylindrical grinding of Inconel 718 result in increased temperatures in the grinding zone. This is because the increased energy input from the grinding operation is almost totally transformed into heat. Increased heat generation may cause thermal expansion and distortion of the workpiece, severely impacting its dimensional accuracy and surface finish (Taylor & Slatter, 2017).

Figure 4.6(a) illustrates the main effects of varying the two factors wheel speed (A) and feed rate (B) on grinding temperature with constant depth of cut at 0.03 mm. As lower wheel speed and lower feed rate resulted in lower grinding temperature (T).

Influence of varying the two factors wheel speed (A) and depth of cut (C) on grinding temperature and keeping feed rate at constant level i.e. 0.04mm/rev was depicted in Figure 4.6(b). It was observed that lower wheel speed and lower depth of cut results in lower grinding temperature.

Figure 4.6 (c) illustrates the main effects of varying the two factors feed rate (B) and depth of cut (C) on grinding temperature with a constant level of wheel speed at 1650m/min. Figure 4-6 shows a 3D Surface projection of the contour plot of (a) 3D surface graph for the Interaction effects of feed rate and wheel speed on work piece temperature, (b) a 3D surface graph for the Interaction effects of depth of cut and wheel speed on workpiece temperature and (c) 3D surface graph for the interaction effect of depth of cut and feed rate on work piece temperature.

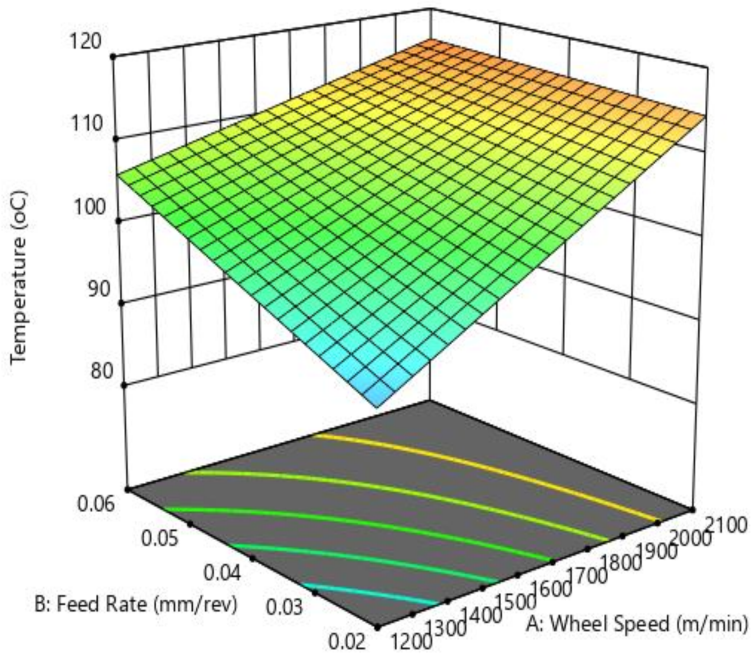

Figure 4-6a: Interaction effects of feed rate and wheel speed on temperature

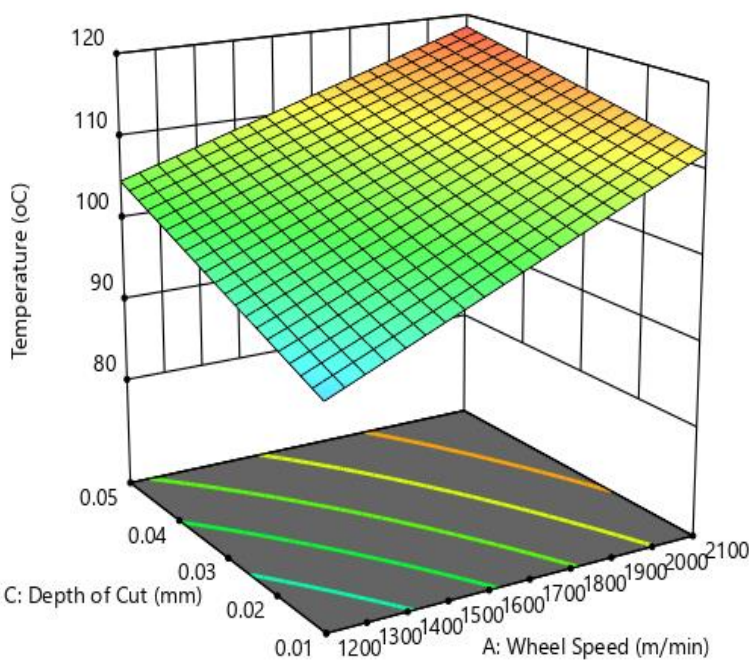

Figure 4-6b: Interaction effects of depth of cut and wheel speed on temperature

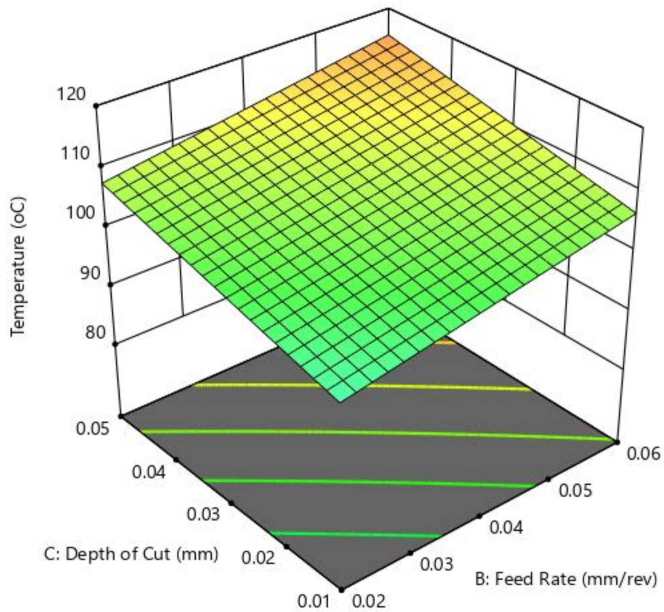

Figure 4-6c: Interaction effects of depth of cut and feed rate on temperature

4.4 Material Removal Rate Analysis and Discussion

The material removal rate (MRR) during cylindrical grinding of Inconel 718 is the amount of material removed from the workpiece per unit time. It is influenced by a variety of elements while cylindrical grinding Inconel 718, including grinding wheel speed, feed rate, and depth of cut. The statistical tests and descriptive statistics, such as fit summary, analysis of variance, regression equation, influence, and effect of each parameter, were discussed.

4.4.1 Fit summary

Fit Summary is a computer program that evaluates impacts for each model term and generates statistics (such as p-values, lack of fit, and R-squared values) for model comparison. This tool collected the vital facts required to establish the proper starting point for the final model fitting and suggested model. As demonstrated by Tables 4-12, 4-13, and 4-14, The quadratic model (sequential sum of squares for the two-factor interaction A, B, C, AB, BC, and AC terms) was suggested as the highest order model that explains significantly more of the variation in the response (p-value small), has an insignificant lack of fit (p-value > 0.10), and reasonably agrees with the predicted and adjusted R-squared (within 0.2 of each other). The cubic model was aliased.

Table 4-12: Fit summary

Source	Sequential p-value	Lack of Fit p-value	Adjusted R^2	Predicted R^2	
Linear	0.0051	0.0955	0.4992	0.2606	
2FI	0.2882	0.0999	0.5409	-0.1556	
Quadratic	**< 0.0001**	**0.9889**	**0.9519**	**0.9443**	**Suggested**
Cubic	0.9741	0.7675	0.9130	0.0005	**Aliased**

Table 4-13: Sequential model sum of squares

Source	Sum of Squares	df	Mean Square	F-value	p-value	
Mean vs Total	2367.41	1	2367.41			
Linear vs Mean	72.76	3	24.25	6.65	0.0051	
2FI vs Linear	14.29	3	4.76	1.42	0.2882	
Quadratic vs 2FI	**33.98**	**3**	**11.33**	**32.30**	**< 0.0001**	**Suggested**
Cubic vs Quadratic	0.2694	4	0.0674	0.1063	0.9741	Aliased
Residual	2.54	4	0.6339			
Total	2491.24	18	138.40			

Table 4-14: Model summary statistics

Source	Std. Dev.	R^2	Adjusted R^2	Predicted R^2	PRESS	
Linear	1.91	0.5876	0.4992	0.2606	91.56	
2FI	1.83	0.7029	0.5409	-0.1556	143.10	
Quadratic	**0.5921**	**0.9773**	**0.9519**	**0.9443**	**6.90**	**Suggested**
Cubic	0.7962	0.9795	0.9130	0.0005	123.77	Aliased

4.4.2 Analysis of variance for material removal rate

Descriptive statistics and statistical tests were presented in this section. In which low p-values identified important terms in the model. From Analysis of Variance for Material Removal Rate on Table 4-15 it was observed that **Model F-value** of 38.35 implies the model is significant. There is only a 0.01% chance that an F-value this large could occur due to noise. **P-values** less than 0.0500 indicate model terms are significant. In this case A, B, AB, A^2, B^2 are significant model terms. Values greater than 0.1000 indicate the model terms are not significant. If there are many insignificant model terms (not counting those required to support hierarchy), model reduction to improve the model. It is implied that the lack of fit is not substantial in relation to the pure error by the Lack of Fit F-value of 0.09. Noise is the most likely cause of a significant Lack of Fit F-value (98.89%). Fit is desirable; a non-significant deficiency in fit is desirable.

Table 4-15: Analysis of variance for material removal rate

Source	**Sum of Squares**	**df**	**Mean Square**	**F-value**	**p-value**		**% contribution**
Model	121.03	9	13.45	38.35	< 0.0001	Significant	97.74 %
A-Wheel Speed	27.42	1	27.42	78.21	< 0.0001		22.14 %
B-Feed Rate	44.14	1	44.14	125.89	< 0.0001		35.65 %
C-Depth of Cut	1.20	1	1.20	3.41	0.1018		0.97 %
AB	13.34	1	13.34	38.04	0.0003		10.77 %
AC	0.0153	1	0.0153	0.0437	0.8397		0.012 %
BC	0.9316	1	0.9316	2.66	0.1417		0.75 %
A^2	25.46	1	25.46	72.62	< 0.0001		20.56 %
B^2	5.16	1	5.16	14.71	0.0050		4.17 %
C^2	0.5139	1	0.5139	1.47	0.2606		0.42 %
Residual	2.81	8	0.3506				2.27 %
Lack of Fit	0.3549	5	0.0710	0.0869	0.9889	not significant	
Pure Error	2.45	3	0.8167				
Cor Total	123.83	17					

Table 4-16: Fit statistics

Std. Dev.	0.5921	**R^2**	0.9773
Mean	11.47	**Adjusted R^2**	0.9519
C.V. %	5.16	**Predicted R^2**	0.9443
		Adeq Precision	18.7869

4.4.3 Regression for material removal rate

The regression technique was employed to figure out the statistical relationship between the parameters and material removal rate and to make predictions about the response for given levels of each factor.

Regression Equation for Material Removal Rate (MRR):-

$$\begin{aligned}\mathrm{MRR}\left(\frac{\mathrm{mm3}}{\mathrm{min}}\right) = {} & 11.726 - 0.647\,\mathrm{N1} - 2.019\,\mathrm{N2} + 2.665\,\mathrm{N3} - 2.573\,\mathrm{f1} \\ & + 0.944\,\mathrm{f2} + 1.629\,\mathrm{f3} - 0.213\,\mathrm{d1} - 0.266\,\mathrm{d2} + 0.479\,\mathrm{d3}\end{aligned} \tag{4.2}$$

4.4.4 Parametric influence on material removal rate

The graph of the normal probability plot versus internally student-zed residual in Figure 4.7a showed that the residuals follow a normal distribution and thus follow a straight line. A normal plot of residuals is a graphical tool used to determine the normality of residuals in a regression model. It's a plot of the residuals vs their theoretical scale. If the residuals are regularly distributed, the points should fall close to the dotted line. If the points deviate greatly from the line, it could suggest non-normality or other problems with the model.

The graph of residuals vs. predicted values in Figure 4.7b, which is a plot of the residuals versus the ascending predicted response values used to test the assumption of constant variance, showed a random scatter or constant range of residuals across the graph, which indicates that the model is valid to conduct the effect of individual factors on material removal rate. A residuals vs. anticipated plot is a graphical tool for evaluating linear regression assumptions. It is a visualization of the residuals vs the planned values. The figure should not exhibit any obvious patterns or trends, and the residuals should be uniformly dispersed around zero. Patterns or deviations suggest model errors, such as nonlinearity or inaccurate assumptions.

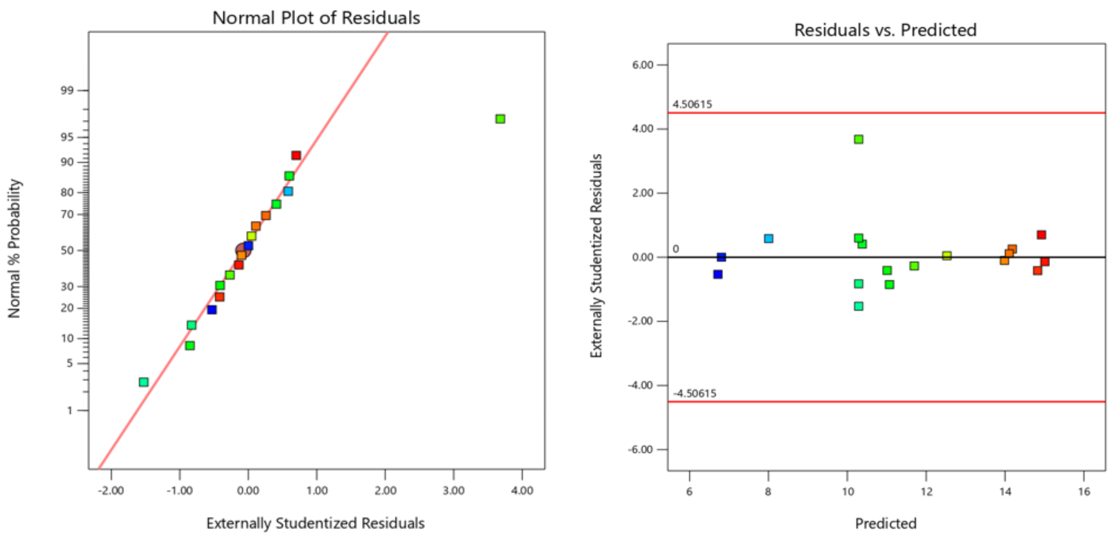

(a) (b)

Figure 4-7: (a) Normal plot of residuals and (b) Residuals vs. Predicted

4.4.5 Effect of wheel speed on material removal rate

From Figure 4.8, it was indicated that material removal rate increased as wheel speed increased, with a percentage contribution of 22.14% to material removal rate. From experimental investigation, it was observed that with too slow wheel speed, time was lost for the machining operation, resulting in a low material removal rate or production rate.

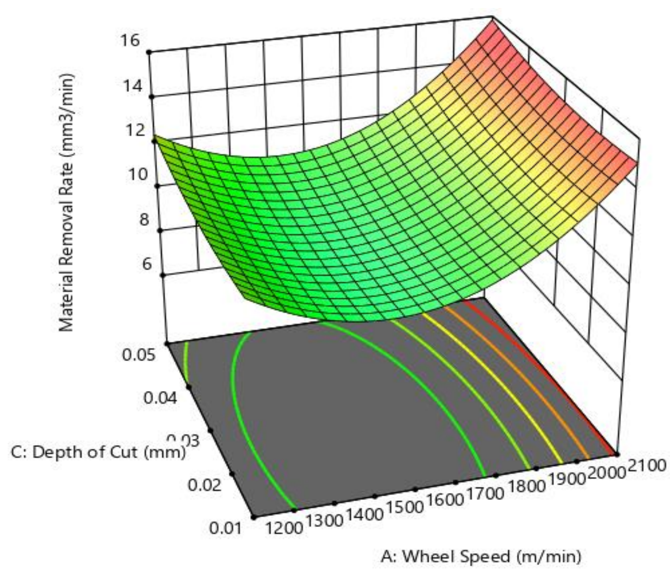

Figure 4-8: Interaction effects of depth of cut and wheel speed on MRR

4.4.6 Effect of feed rate on material removal rate

The effect of feed rate on material removal rate is shown in Figure 4-9. It was observed that as feed rate increased at a constant depth of cut, the highest material removal rate was achieved at the highest feed rate of 0.06 mm/rev, and the smallest material removal rate was found at the lowest feed rate, which is 0.02 mm/rev. ANOVA showed that feed rate was a significant factor, contributing 35.65% of the total material removal rate, which was the greatest rate of removal. Similar observation were reported by (S. Kumar & Bhatia, 2015). The higher feed rates promote the axial movement of the cutting tool, resulting in its shifting to a new location at a faster rate, thereby increasing MRR. Figure 4-9 shows the 3D surface projection of the contour plot for the interaction effects of wheel speed and feed rate on material removal rate. The maximum MRR doesn't show economical machining because tool wear increases, surface roughness increases as wheel speed increases, and feed rate increases. The acceptable or recommended MRR was at optimum wheel speed, feed rate, and depth of cut, where the minimum Ra value was obtained.

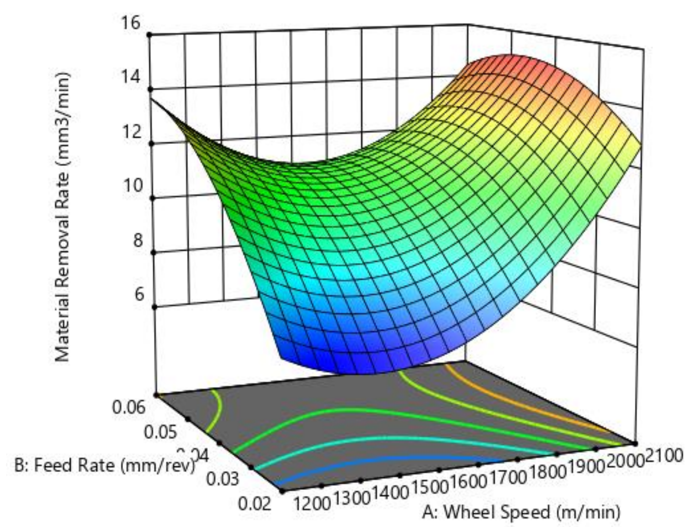

Figure 4-9: Interaction effects of feed rate and wheel speed on MRR

4.4.7 Effect of depth of cut on material removal rate

The effect of the depth of cut on the material removal rate was shown in Figure 4-10, and it was observed that as the depth of cut and wheel speed increased at a constant feed rate, the material removal rate also increased due to raised temperature, creating friction between the tool and workpiece, as shown in the temperature graph of Figures 4–6 b. ANOVA in Table 4–15, it was observed that depth of cut was the insignificant effect parameter on material removal rate with a percentage contribution of 0.97%. Higher depths of cut mean the least volume of material to erode, thus leading to the least increasing MRR. In high depths of cut in a grinding operation, the least material removal rate is achievable if the process is performed at high wheel speed. Figure 4-10 shows the 3D surface projection of the contour plot for the interaction effects of depth of cut and wheel speed on material removal rate.

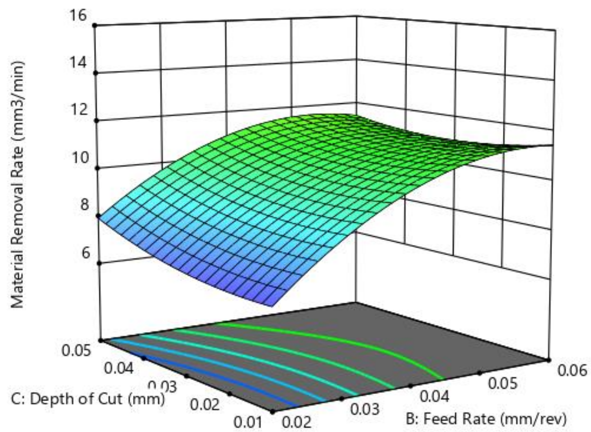

Figure 4-10: Interaction effects of depth of cut and feed rate on MRR

4.5 Tool Life Analysis and Discussions

Tool life indicates the amounts of satisfactory performance or service rendered by a fresh tool or a grinding point till it is declared failed. It is the length of cutting time. Operating the tool until final catastrophic failure is one way of defining tool life. Tool life is always assessed or expressed by a span of machining time (T) in minutes (Jafarian et al., 2016). Using the Taylor tool life equation, the tool life for cylindrical grinding was determined for each experimental run (Equation 2.2), i.e., $VT^n f^a t^b = C$. Where n, a, and b are Taylor's tool life exponents and C is a constant. The values of "n" and "C" are mostly determined by the toolwork materials, whereas "a" and "b" are determined by the toolwork material as well as the grinding environment (the application of grinding fluid). It is possible to assess the constant values by machining experiments or by consulting Machining Data Handbooks. It should be feasible to use the following formula to translate wheel speed from Equation 2.2 to cutting speed.

$$V = \frac{\pi * D * N}{1000} \ m/mi \tag{4.3}$$

Where V is cutting speed, D= diameter of workpiece and N = wheel speed of each input parameter.

Table 4-17: Taylor tool life equation constant values (Tebaldo et al., 2017).

Grinding Conditions	Taylor's Tool Life Equation Constants			
	C	n	a	b
CNC grinding	100	0.45	0.15	0.10

Tool life were calculated for each run of experiment by using the constant value in Table 4-17. As shown in the table the longer tool life was obtained when all the grinding parameter are at their minimum level conditions. At first experimental run all parameters are in their minimum (i.e 0.01 mm depth of cut, 0.02mm/rev feed rate and 1200m/min of wheel speed) and the maximum tool life 1.48min were obtained.

From Table 4-17 by using C= 100, n=0.45 , a= 0.15, b=0.10 and at a diameter of 30mm and length of 30mm evaluate the Taylors tool life for each during cylindrical grinding of machine.

4.5.1 Fit summary

A fit summary is the result of a statistical analysis performed to optimize the parameters of a cylindrical grinding process. A strong fit summary often includes high R^2 and R^2adj values, low mean squared sequence values, and significant F-values with low p-values. This shows that the model accurately captures the relationships between the input parameters and the intended output responses, allowing for successful optimization of the grinding process. The Predicted R^2 of 0.8561 is in reasonable agreement with the Adjusted R^2 of 0.9668; i.e. the difference is less than 0.2.

Table 4-18: Fit summary

Source	**Sequential P-value**	**Adjusted R^2**	**Predicted R^2**	
Linear	0.0861	0.2301	-0.3470	
2FI	0.0197	0.5863	-0.7475	
Quadratic	**< 0.0001**	**0.9668**	**0.8561**	**Suggested**
Cubic		1.0000		**Aliased**

Table 4-19: Sequential model sum of squares

Source	Sum of Squares	df	Mean Square	F-value	p-value	
Mean vs Total	26.28	1	26.28			
Linear vs Mean	0.0586	3	0.0195	2.69	0.0861	
2FI vs Linear	0.0587	3	0.0196	5.02	0.0197	
Quadratic vs 2FI	**0.0404**	**3**	**0.0135**	**43.09**	**< 0.0001**	**Suggested**
Cubic vs Quadratic	0.0025	4	0.0006			Aliased
Residual	0.0000	4	0.0000			
Total	26.44	18	1.47			

Table 4-20: Model summary statistics

Source	Std. Dev.	R^2	Adjusted R^2	Predicted R^2	PRESS	
Linear	0.0852	0.3660	0.2301	-0.3470	0.2159	
2FI	0.0624	0.7323	0.5863	-0.7475	0.2800	
Quadratic	**0.0177**	**0.9844**	**0.9668**	**0.8561**	**0.0231**	**Suggested**
Cubic	0.0000	1.0000	1.0000		*	Aliased

4.5.2 Analysis of variance for tool life

The ANOVA is where the descriptive statistics and statistical tests are presented. From the analysis of variance for tool life in Table 4-21, it is observed that the model F-value of 56.09 implies the model is significant. There is only a 0.01% chance that an F-value this large could occur due to noise. **P-values** less than 0.0500 indicate model terms are significant. In this case, A, B, C, AB, AC, BC, A^2, B^2 are significant model terms. Values greater than 0.1000 indicate the model terms are not significant. If there are many insignificant model terms (not counting those required to support hierarchy), model reduction to improve the model.

Table 4-21: Analysis of variance for tool life

Source	Sum of Squares	df	Mean Square	F-value	P-value		% contribution
Model	0.1578	9	0.0175	56.09	< 0.0001	significant	98.44%
A-Wheel Speed	0.0545	1	0.0545	174.24	< 0.0001		33.99%
B-Feed Rate	0.0410	1	0.0410	131.07	< 0.0001		25.57%
C-Depth of Cut	0.0040	1	0.0040	12.80	0.0072		2.49%
AB	0.0137	1	0.0137	43.81	0.0002		8.54%
AC	0.0025	1	0.0025	7.84	0.0232		1.56%
BC	0.0018	1	0.0018	5.76	0.0432		1.12%
A^2	0.0098	1	0.0098	31.22	0.0005		6.11%
B^2	0.0082	1	0.0082	26.23	0.0009		5.11%
C^2	0.0003	1	0.0003	0.8671	0.3790		0.18%
Residual	0.0025	8	0.0003				1.55%
Lack of Fit	0.3549	5	0.0710	0.0869	0.9789	not significant	
Pure Error	0.0000	3	0.0000				
Cor Total	0.1603	17					

Table 4-22: Fit statistics

Std. Dev.	0.0177	**R^2**	0.9844
Mean	1.21	**Adjusted R^2**	0.9668
C.V. %	1.46	**Predicted R^2**	0.8561
		Adeq Precision	28.1569

4.5.3 Regression model for tool life

This model was used to determine the statistical relationship between cutting parameters and tool life. The change in grinding parameters associated with the change in tool life was ascertained by using this model.

Regression Equation:

$$TL = 1.547 - 0.000142\ N(m/min) - 1.85\ f\ (mm/rev) - 1.00\ d\ (mm) \quad (4.4)$$

4.5.4 Parametric influence on tool life

The residuals follow a normal distribution and, therefore, a straight line, according to the graph of the normal probability plot vs. internally studentized residual in Figure 4-11a. If the residuals are regularly distributed, the points should fall close to the dotted line. The plot of the residuals against the ascending predicted response values in Figure 4.11b, which is used to test the assumption of constant variance, revealed a random scatter or constant range of residuals across the graph, indicating that no transformation is required. This is the graph of residuals vs. predicted. Therefore, the model is appropriate for doing analyses on how different factors affect tool life.

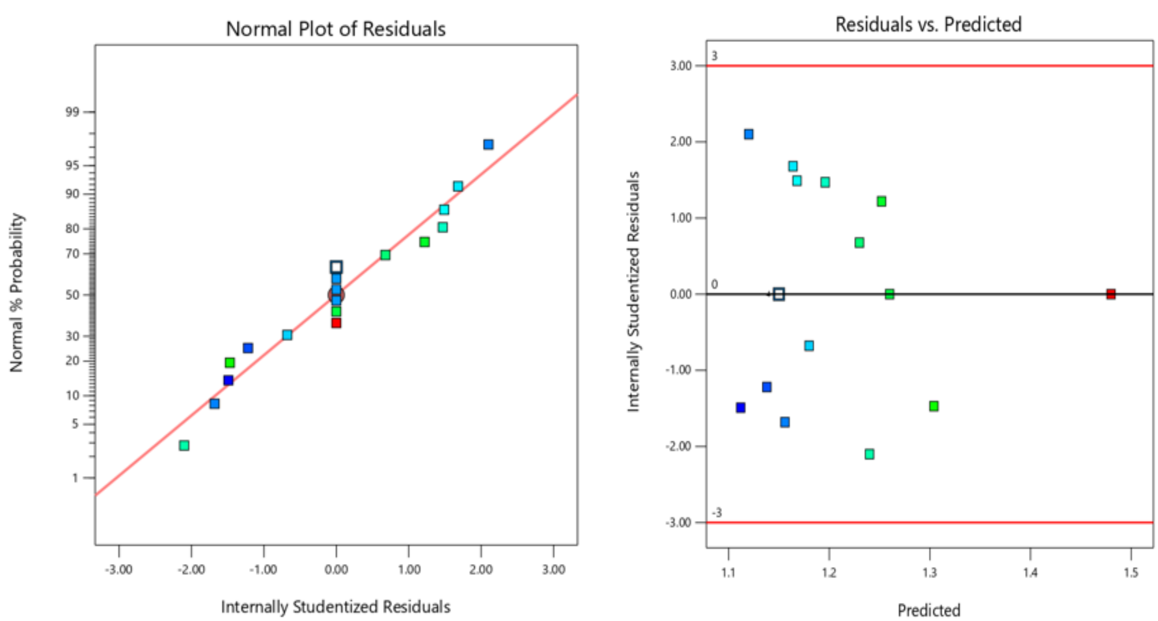

Figure 4-11: (a) Normal plot of residuals and (b) Residuals vs. Predicted

4.5.5 Effect of wheel speed on tool life

Wheel speed, or the rotational speed of the grinding wheel, affects the tool's life. The effect of wheel speed on tool life was shown in Figure 4-12. It was observed that as wheel speed increased at a constant feed rate and depth of cut, at the smallest speed of 1200 mm/min, the highest tool life was achieved, and the smallest tool life was found at the highest speed, which is 2100 mm/min. It was observed from the study and from the ANOVA wheel that there was a significant factor affecting tool life with a percentage contribution of 33.99%, and hence a similar result has been obtained and discussed by (Jeevanantham et al., 2017). Increased wheel speed means more material is in contact with the grinding work piece, which results in a higher grinding force to remove material at a faster rate, which results in the existence of vibration and friction, which leads to a lower tool life. The wheel speed has a considerable impact on the tool life in grinding operations. Higher wheel speeds could decrease tool life due to increased cutting forces and heat buildup. The relationship between wheel speed and tool life was quadratic, as suggested by the ANOVA model. Figure 4-12 shows the 3D surface projection of the contour plot graph for the interaction effects of wheel speed and feed rate on tool life.

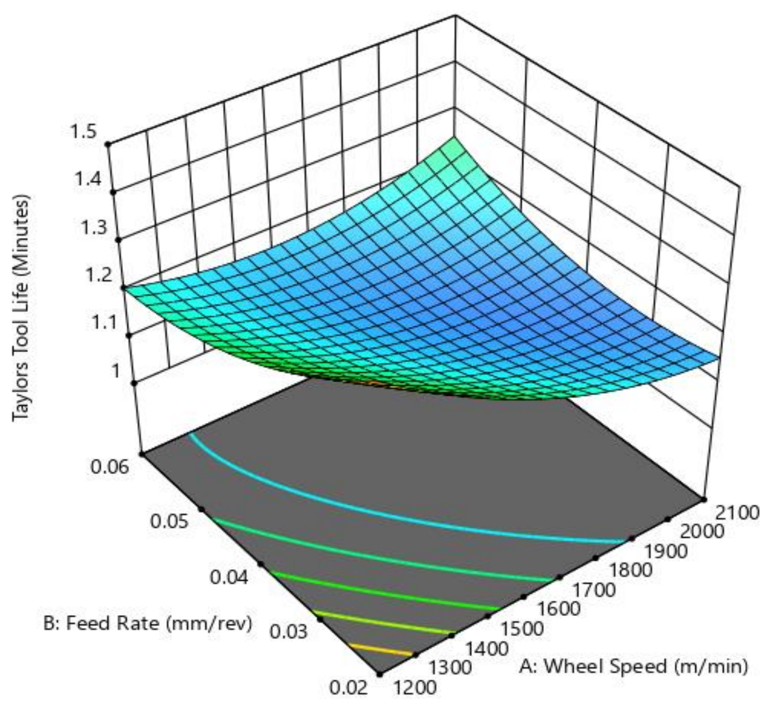

Figure 4-12: Interaction effects of wheel speed and feed rate on tool life

4.5.6 Effect of depth of cut and feed rate tool life

Figure 4-13 shows the 3D surface projection of the contour plot graph for the interaction effects of feed rate and depth of cut on tool life. Both feed rate and depth of cut are observed as insignificant factors that affect tool life, with a percentage contribution of 8.54% and 2.49%, respectively.

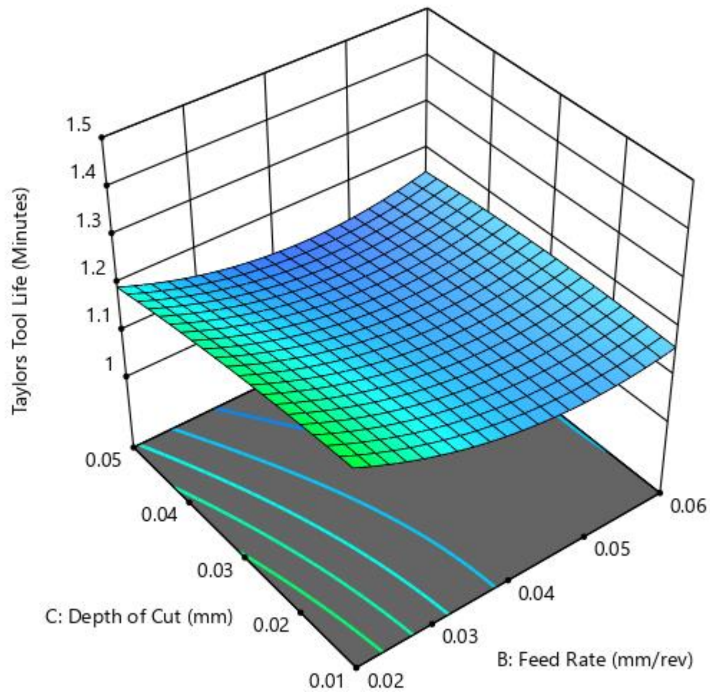

Figure 4-13: Interaction effects of feed rate and depth of cut on tool life.

4.6 Multi Response Grey Relational Analysis

Grey Relational Analysis (GRA) is a method for analyzing systems in which statistical approaches are ineffective due to inadequate, uncertain, or noisy data. It is a statistical strategy that optimizes multiple responses in the same process. To determine the ideal parameter combination for the best metal qualities, data from tests measuring surface roughness, tool life, MRR, and temperature signal-to-noise ratios were combined into a single.

Step 1: Determine the S/N ratio for the matching answers by applying equation 3.2, equation 3.3, and equation 3.4.

Step 2: Using Eq. 3.6, a grey connection that ranges from 0 to 1 is created during the normalization of the S/N values.

Table 4-23: S/N ratio values and normalized S/N ratio values

S/N ratios				Normalized Value			
Ra	MRR	Temp.	TL	Ra	MRR	Temp.	TL
6.375	21.966	-40.945	1.289	0.568	0.698	0.237	0.179
2.853	23.493	-41.237	1.214	0.295	0.980	0.126	0.154
10.173	19.851	-40.324	1.214	0.761	0.381	0.462	0.154
3.098	23.352	-41.077	1.656	0.714	0.952	0.187	0.308
12.765	23.009	-41.038	1.438	0.852	0.885	0.202	0.231
13.556	23.082	-40.035	1.727	0.875	0.899	0.561	0.333
11.701	16.663	-40.138	1.868	0.818	0.028	0.526	0.385
2.158	22.898	-41.489	1.062	0.227	0.864	0.026	0.103
11.373	20.473	-40.206	1.511	0.807	0.467	0.503	0.256
0.175	23.591	-41.555	2.007	0.000	0.000	0.000	0.436
16.478	18.244	-39.869	2.923	0.943	0.187	0.617	0.795
7.535	20.596	-40.859	0.749	0.636	0.484	0.269	0.000
6.936	20.693	-40.914	1.364	0.602	0.498	0.249	0.205
9.897	21.244	-40.407	1.214	0.750	0.581	0.433	0.154
20.000	16.351	-38.629	3.405	1.000	0.000	1.000	1.000
8.874	19.573	-40.547	1.214	0.705	0.345	0.383	0.154
8.636	20.531	-40.820	1.214	0.693	0.475	0.284	0.154
15.918	21.274	-39.789	2.076	0.932	0.586	0.643	0.462

Step 3: Calculation the grey relational coefficient using Eq.3.8.

Step 4: The grey relational grade using Eq.3.9.

Table 4-24: Grey relational co-efficient and grey relational grade values

Deviation Sequences				Grey Relation Coefficient					
Ra	MRR	Temp.	TL	Ra	MRR	Temp.	TL	GRG.	Rank
0.432	0.302	0.763	0.821	0.537	0.624	0.396	0.379	0.484	12
0.705	0.020	0.874	0.846	0.415	0.962	0.364	0.371	0.528	7
0.239	0.619	0.538	0.846	0.677	0.447	0.482	0.371	0.494	11
0.286	0.048	0.813	0.692	0.636	0.912	0.381	0.419	0.587	6
0.148	0.115	0.798	0.769	0.772	0.814	0.385	0.394	0.591	5
0.125	0.101	0.439	0.667	0.800	0.833	0.533	0.429	0.648	2
0.182	0.972	0.474	0.615	0.733	0.340	0.514	0.448	0.509	10
0.773	0.136	0.974	0.897	0.393	0.787	0.339	0.358	0.469	15
0.193	0.533	0.497	0.744	0.721	0.484	0.501	0.402	0.527	8
1.000	1.000	1.000	0.564	0.333	0.333	0.333	0.470	0.367	18
0.057	0.813	0.383	0.205	0.898	0.381	0.566	0.709	0.639	3
0.364	0.516	0.731	1.000	0.579	0.492	0.406	0.333	0.453	17
0.398	0.502	0.751	0.795	0.557	0.499	0.400	0.386	0.460	16
0.250	0.419	0.567	0.846	0.667	0.544	0.468	0.371	0.513	9
0.000	1.000	0.000	0.000	1.000	0.333	1.000	1.000	0.833	1
0.295	0.655	0.617	0.846	0.629	0.433	0.448	0.371	0.470	14
0.307	0.525	0.716	0.846	0.620	0.488	0.411	0.371	0.472	13
0.068	0.414	0.357	0.538	0.880	0.547	0.584	0.481	0.623	4

By analyzing the main effect of the grey relational grade value in Minitab 21 software, the optimal parameter was predicted for the best value of parameters for MRR, temperature, and surface roughness minimization properties. Higher GRG means better machinability conditions and product quality. Hence, based on the higher GRG or rank, the optimum process level can be achieved, as stated by (Shunmugesh & Kavan, 2017).

4.6.1 Optimization of process parameters for grey relational grade

Taguchi ratios of signal to noise (S/N) are log functions of the intended output that are used as objective functions in optimization, data analysis, and optimal result prediction. With the use of the mean and signal-to-noise (S/N) ratios, the Taguchi method was used to investigate the variation in GRG response.

Analysis of Mean for GRG

The mean value of GRG for each factor i.e., MRR, Temperature and surface roughness at each level was also obtained using Minitab 21 for GRG and the result was listed in Table 4-25:

Table 4-25: Response table for a mean of GRG

Level	Wheel Speed(rpm)	Feed Rate(mm/rev)	Depth of cut(mm)
1	**0.667**	**0.587**	**0.616**
2	0.487	0.524	0.522
3	0.487	0.531	0.504
Delta	0.180	0.063	0.112
Rank	**1**	**3**	**2**

The wheel speed of (Delta = 0.180, Rank = 1) had the biggest impact on the mean from Table 4.19 above. Feed rate (Rank = 3, Delta = 0.063) is the factor that has the least impact on the mean. In order to determine the expected value of the responses (GRG), the preceding linear regression equation was utilized (Panda et al., 2016).

$$Opt = A1+B1+C1 -2m \tag{4.5}$$

Optimum = 0.667+ 0.587+ 0.616-2 x 0.574

Opt = 0.776 (Predicted optimum value of GRG)

Where m is the average performance mean value for GRG (i.e.: m=0.574).

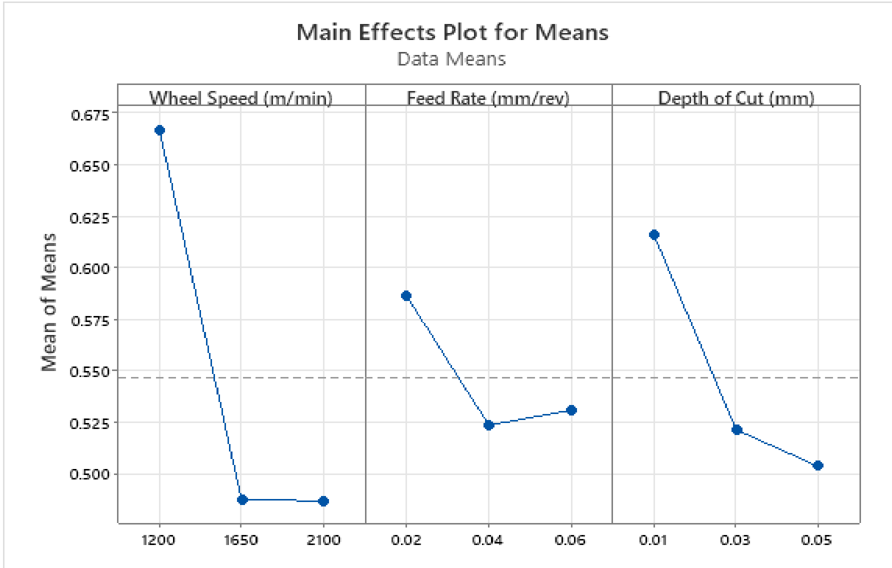

Figure 4-14: Main effect plot of mean for GRG

Figure 4-14 showed that within the scope of this study, the maximum points in the graph for each factor are the optimum conditions at which a larger GRG was obtained. The maximum point for wheel speed is at level 1, the lowest feed rate is at level 1, and the depth of cut is at level 1. This justified the optimum parameter at the lowest wheel speed, lowest feed rate, and lowest depth of cut as (**A1B1C1)**.

4.6.2 Analysis of S/N ratio for grey relational grade

Table 4-26 displays the signal-to-noise ratio obtained when the experiment's optimal value was achieved.

Table 4-26: Signal-to-Noise ratios for GRG (larger is better)

Level	**Wheel Speed(m/min)**	**Feed Rate (mm/rev)**	**Depth of Cut (mm)**
1	**-3.584**	**-4.847**	**-4.364**
2	-6.262	-5.672	-5.705
3	-6.350	-5.677	-6.123
Delta	2.766	0.830	1.756
Rank	1	3	2

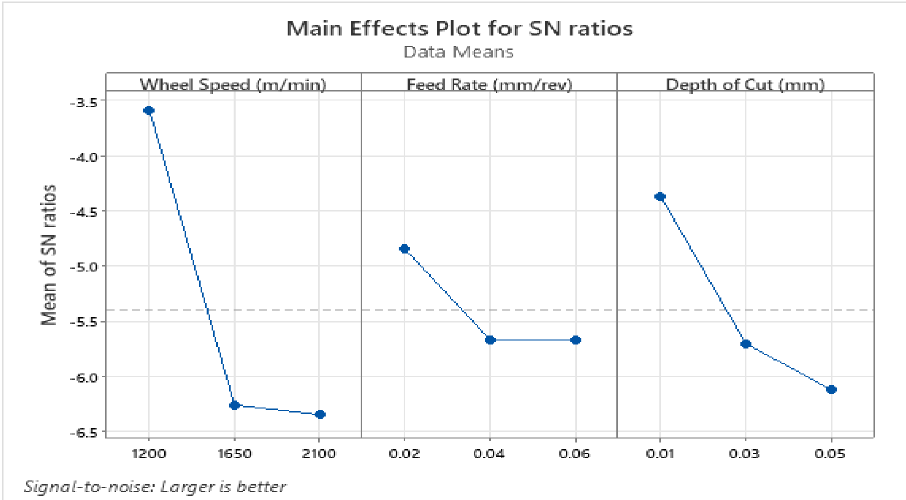

Figure 4-15: Main effect plots for S/N ratio of GRG response

Figure 4-15 shows the control factor's main effect plot for the S/N ratio and the optimal parameter combination on the GRG response (the larger, the better the GRG response). In the S/N ratio, the numerical value of the maximum point in each graph shows the best optimum combination of factors at that level, and the above Figure shows the maximum point for wheel speed at level 1 of 1200 m/min, for feed rate level 1 of 0.02 mm/rev, and for depth of cut at level 1 of 0.01 mm, that is **(A1B1C1)**, was selected. The most effective parameter for the GRG response is the wheel speed when compared with other factors and feed rate that have the least effect on the GRG response.

4.6.3 Determining optimum condition for GRG

The optimum prediction condition for the S/N ratio, in which the GRG response result of the material was obtained with the terms set, is shown in Table 4-27. The selected optimum parameters in this study were lowest wheel speed, a lowest feed rate, and a lowest depth of cut, which was **A1B1C1.**

Table 4-27: The optimum condition for GRG response result prediction-settings

Factors	**Levels**	**Value of level**	**Rank of affecting**	**Prediction Values**	
				S/N Ratio	**Mean**
Wheel speed(N)	1	1200m/min	1	-2.322	0.751
Feed rate(f)	1	0.02mm/rev	3		
Depth of cut(d)	1	0.01mm	2		

4.6.4 Analysis of variance for GRG

The relationship between the response variable and the suggested factors was examined using an ANOVA as an analytical tool to determine the significant factors in measurement. The proportion of contribution was determined using an ANOVA on behalf of because the Taguchi approach was unable to determine the impact of individual process parameters on the entire process. The results indicated that the wheel speed was the most important parameter, followed by depth of cut, and feed rate. This information was used to improve the cutting parameters and attain the optimal mix of quality properties, including surface roughness, material removal rate, and tool life.

Regression Equation for Grey Relational Grade (GRG):

$$\mathrm{GRG} = 1.0066 - 0.000200\,\mathrm{N}\,(\mathrm{m/min}) - 1.39\,\mathrm{f}\,(\mathrm{mm/rev}) - 2.80\,\mathrm{d}\,(\mathrm{mm}) \tag{4.6}$$

Table 4-28: Analysis of variance of GRG

Source	DF	Adj SS	Adj MS	F-Value	P-Value	%Contribution
Wheel Speed (m/min)	2	0.102303	0.048881	15.81	0.001	57.28**%**
Feed Rate (mm/rev)	2	0.01802	0.001373	2.914	0.043	10.09**%**
Depth of Cut (mm)	2	0.039243	0.0019622	6.35	0.015	21.98 **%**
Error	11	0.024258	0.003092			13.59 **%**
Total	17	0.178580				

Based on the ANOVA results displayed in Table 4-28, the wheel speed (57.28 percent) was determined to have the greatest influence on the grey relational grade, followed by the feed rate (10.09 percent) and depth of cut (21.98 percent).

4.7 Multi-objective Optimization by using Genetic Algorithm

The Multi-Objective Genetic Algorithm Solver, or GA gamultiobj function tool, was utilized to resolve this optimization issue. To solve the fitness function, genetic methods must be applied. The fitness function is a multi-objective (vector) function that requires optimization. In this work, the mathematical models utilized to ascertain the link between input and output were the ANOVA model and the regression model developed by Taguchi and Design Expert software. The developed mathematical model was converted into a MATLAB R2021 function. This function was placed in MATLAB R2021's General Toolbox as the objective function. Three variables were used, and upper and lower boundaries were defined based on the machining parameter values. When grinding Inconel 718, the goal function values are found for maximizing material removal rate and minimizing surface roughness.

4.7.1 Analysis of GRG, Ra, MRR, and temperature by genetic algorithm

In this approach, GA was used to optimize the mathematical model developed through the design of experiment-based response surface methodology by developing quadratic regression model surface roughness, Temp., MRR, and tool life by using MATLABR2021a software. To reduce surface roughness, increase material removal rate, decrease temperature, and discover the optimum grinding parameters for multi-responses, the genetic algorithm approach was used. The optimum setting for input factors was in range. The material removal rate value was analyzed using the larger-is-better desirability function, whereas surface roughness and temperature data were analyzed using the smaller-is-better desire function.

Table 0-29: Optimization GA parameter for MATLAB Code

Variable		**Value**
Fitness function		Regression Equations of 4.1, 4.2, 4.3, and 4.4
Boundary condition	Lowe bound	(0.01mm, 0.02mm/rev, 1200m/min)
	Upper bound	(0.05mm, 0.06mm/rev, and 2100m/min)
Total number of iterations		10
Population size		1000

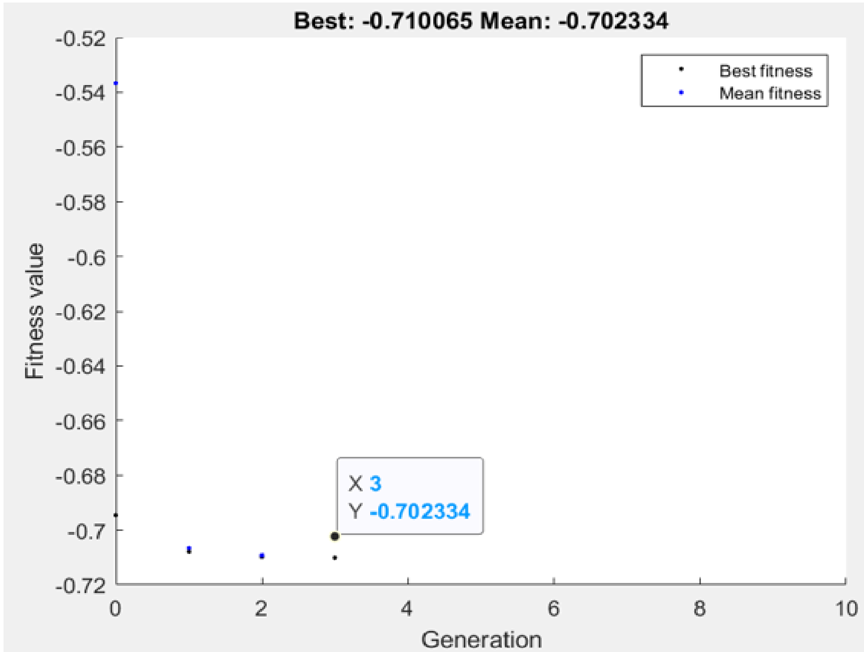

Figure 4-16: Fitness value versus Generation for GRG

Figure 4-16 explains the fitness value versus generation for grey relational grade (GRG), where the optimum value from MATLAB code generation based on the regression result obtained was 0.7106 at the third generation, with an optimum value of input parameters with a depth of cut of 0.01mm, feed rate of 0.02mm/rev, and wheel speed of 1200 m/min.

Table 4-30: MATLAB result generation for GRG

Generation	Func-count	Best f(x)	Max Constraint	Stall Generations
1	11550	0.70792	0	0
2	22100	0.70972	0	0
3	32650	0.710065	0	0

- Optimization Results: Grey Relational Analysis (GRG): 0.7106
- The optimal values at a depth of cut (mm), feed rate (mm/rev), and wheel speed (m/min) were found to be, respectively, 0.01, 0.02, and 1200.

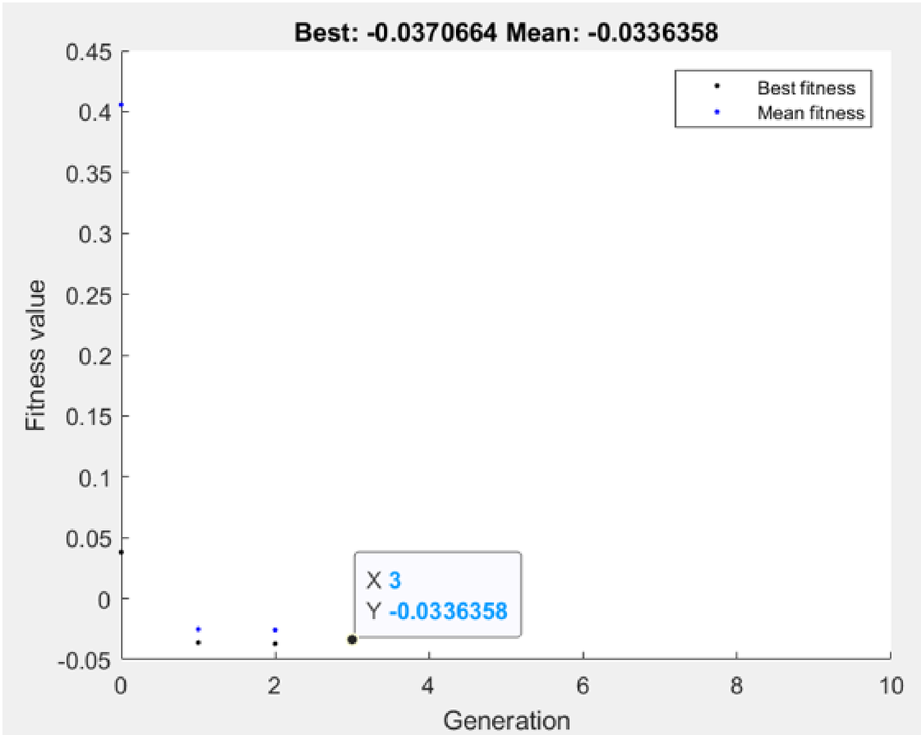

Figure 4-17: Fitness value versus Generation for Ra

Figure 4-17 explains the fitness value versus generation for surface roughness (Ra), where the optimum value from MATLAB code generation based on the regression result obtained was 0.0364 at the third generation, with an optimum value of depth of cut of 0.01mm, feed rate of 0.02mm/rev, and wheel speed of 1200m/min.

Table 4-31: MATLAB result generation for Ra

Generation	Func-count	Best f(x)	Max Constraint	Stall Generations
1	11550	0.0360914	0	0
2	22100	0.0361304	0	0
3	32650	0.0363745	0	0

- Optimization Results: Surface roughness in (µm): 0.036375
- The optimal values at a depth of cut (mm), feed rate (mm/rev), and wheel speed (m/min) were found to be, respectively, 0.01, 0.02, and 1200.

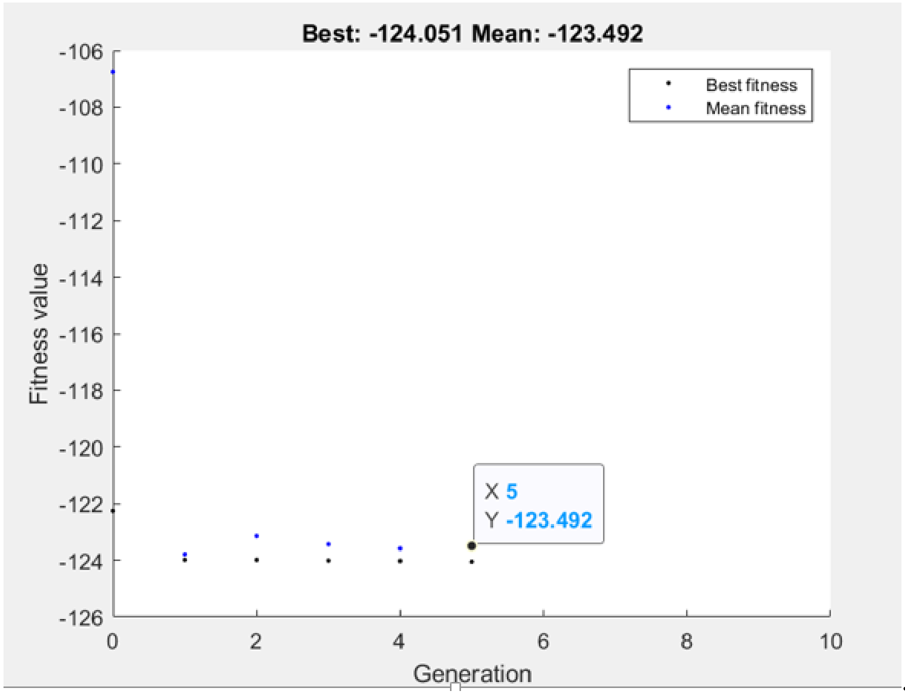

Figure 4-18: Fitness value versus Generation for Temperature.

Figure 4-18 shows that the obtained result was 124.0512°C at the fifth generation with an optimum value of depth of cut of 0.05mm, a feed rate of 0.06mm/rev, and a speed of 2100m/min.

Table 4-32: MATLAB result generation for Temperature

Generation	Func-count	Best f(x)	Max Constraint	Stall Generations
1	11550	123.984	0	0
2	22100	123.985	0	0
3	32650	124.012	0	0
4	43200	124.026	0	0
5	53750	124.051	0	0

- Optimization Results: Temperature in (°C): 124.0512
- The optimal values at a depth of cut (mm), feed rate (mm/rev), and wheel speed (m/min) were found to be, respectively,: 0.05, 0.06, 2100 respectively

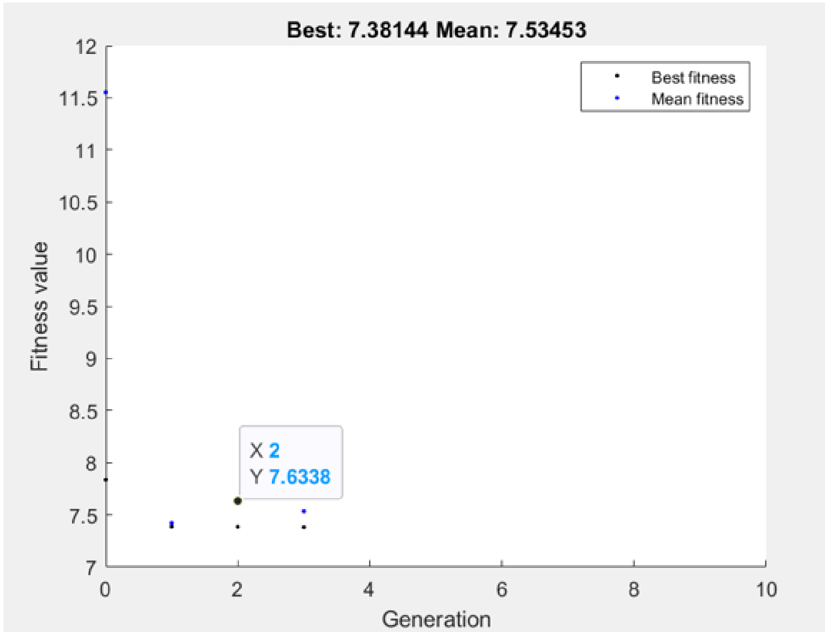

Figure 4-19: Fitness value versus Generation for MRR

Figure 4-19 explains the fitness value versus generation for material removal rate (MRR), where the optimum value from MATLAB code generation based on the regression result obtained was 7.372 mm^3/min at the third generation, with an optimum value of depth of cut of 0.01mm, feed rate of 0.02mm/rev, and wheel speed of 1200m/min.

Table 4-33: MATLAB result generation for MRR

Generation	Func-count	Best f(x)	Max Constraint	Stall Generations
1	11550	7.37308	0	0
2	22100	7.37202	0	0
3	32650	7.37202	0	1

- Optimization Results: Material removal rate: 7.372
- The optimal values at a depth of cut (mm), feed rate (mm/rev), and wheel speed (m/min) were found to be, respectively, 0.01, 0.02, and 1200.

4.8 Confirmation Test

The final step was to confirm that the projected outcome was within the range of the experimental results after determining the ideal process parameters and levels. There was no requirement for a confirmation test if the set of ideal process parameters matches any experimental trial array. These thesis studies validated the ideal combinations of process parameters for temperature, MRR, and surface roughness, unless further testing at that new level was conducted.

Table 4-34: Confirmation location from Grey Relational Grade (GRG) and Genetic Algorithm

Sr. No	Response	Optimal values	Predicted	Actual	Error %
1.	GRG	d, f, N: 0.01 , 0.02, 1200	0.71064	0.751	5.3%
2.	Ra(μm)	d, f, N: 0.01, 0.02, 1200	0.03637	0.080	5.4%
3.	Temp.(^{o}C)	d, f, N: 0.05 ,0.06, 2100	124.051	119.60	3.6%
4.	MRR (mm^3/min)	d, f, N: 0.01, 0.02, 1200	7.3720	7.100	3.8%

Table 4-34 shows that the average surface roughness, temperature, MRR, and GRG values had percentage errors of less than 10 percent. This means that the suggested approach is validated and used to simultaneously estimate the temperature, MRR, surface roughness average, and GRG with accuracy. As recommended by the experimental work, the standard qualities for the cylindrical grinding of the Inconel 718 workpiece were confirmed by conducting confirmation tests in accordance with the optimal set point. The response values obtained from the confirmation test are surface roughness = 0.08 µm, MRR = 7.10 mm^3/min, temperature = 85.4^{o}C, and tool life = 1.48 minutes at the lowest level of input parameters with wheel speed 1200 m/min, feed rate 0.02 mm/rev, and 0.01mm of depth of cut. The optimal scenario was expected using the 95% confidence interval, and the confirmation test's gray relational grade estimate indicates a 5% improvement above the average value. Because of this, it generates very accurate forecasts for temperature, tool life, MRR, and surface roughness during the cylindrical grinding of Inconel 718 work pieces when paired with the hybrid Taguchi-based Grey relational analysis and Genetic algorithm.

4.9 Finite Element Analysis

The investigation of the thermal impacts and temperature distribution that take place in the workpiece during the grinding process is known as heat analysis of a work piece during cylindrical grinding. Regarding an Inconel 718 work piece, Inconel 718 is a nickel-based alloy that is frequently used in gas turbine and aerospace applications. It is resistant to corrosion at high temperatures.

4.9.1 Johnson–Cook model

The Johnson-Cook model is employed in the calculation of the pressure distribution of a material as a mix of strain influences, thermal properties, and rate of strain due to the theoretical flexibility and precision of the method. The three variables describe the effect of hardness due to stress, rate of strain, and heat relaxing on the stress of the component's flow throughout deformation. Due to the obvious method's versatility in FEM analysis, it is used to assess the deformation inclinations of different materials.

The details was depend on the data shown in the graph, but the Johnson-Cook model is commonly used to explain the flow stress behavior of materials like Inconel 718 under various conditions. Inconel 718 exhibits dynamic behavior during grinding due to its significant strain-hardening characteristic. When it comes to flow stress behavior, materials under high strain rates and temperatures are described by the model. Compared to other machining techniques, grinding has a far higher strain rate, and as the strain rate rises, so does the shear stress. In this work, the yield stress for Inconel 718 at high strain rates has been estimated using the JC model (Sinha, Ghosh, et al., 2019b).

The Johnson–Cook model is (Soori & Arezoo, 2023).

$$\sigma = (A + B\varepsilon^{n})\,(1 + Cln\frac{\dot{\varepsilon}}{\dot{\varepsilon}0})\left[1 - (\frac{T-T0}{Tm-T0})^{m}\right] \tag{4.7}$$

where σ = flow stress

A (MPa) = yield strength

B (MPa) = hardening modulus

$\ddot{\varepsilon}$ = strain rate (s-1)

ε = plastic strain

$\dot{\varepsilon}0$ = reference plastic strain rate(s^{-1})

T (°C) = work piece temperature

To (°C) = room temperature,

Tm (°C) = melting temperature of work piece material

C = strain rate sensitivity coefficient

n = hardening coefficient

m = thermal softening coefficient

The first bracket is an elastic-plastic term, and it represents strain hardening. The second one is the viscosity term, and it shows that the flow stress of material increases when material is exposed to high strain rates. The last one is the temperature-softening term. This model assumes that flow stress depends on strain, strain rate, and temperature independently.

According to the Johnson-Cook model, the three influencing elements of strain, strain amplitude, and temperature are completely independent of each other, limiting any one of them from having a cumulative effect. Such strain rate dependence is difficult to anticipate using the usual J-C constitutive model. The modified Johnson-Cook model, which greatly enhances prediction accuracy over the original Johnson-Cook mode, investigates the interaction between deformation temperature and strain rate on flow stress (Soori & Arezoo, 2023).

The modified Johnson–Cook model is suggested by (Zhao et al., 2017) to address the problems of the Johnson–Cook model as Eq 4.7,

$$\sigma = (A_1+B_1\varepsilon +B_2\varepsilon^2)\ (1+Cln\underline{\varepsilon})\ \exp.[(\lambda 1 + \lambda 2 ln\varepsilon)(T - Tref)] \qquad (4.8)$$

where A_1, B_1, B_2, C_1, $\lambda 1$, and $\lambda 2$ are characteristics of material, and the other parameters have the same quantities as in the Johnson–Cook model.

Table 4-35:Johnson Cook model parameters for Inconel 718 (J. Wang et al., 2018)

A (Mpa)	B (Mpa)	C	n	m	$\dot{\varepsilon}o$ (S^{-1})	T_{melt} (^0C)	T_{room} (^0C)
450	1700	0.017	0.65	1.3	0.001	1320	20

The tests were performed with a nominal $\dot{\varepsilon}$= 0.01 Hz for Inconel 625, while Inconel 718 is tested with 0.01 < $\dot{\varepsilon}$< 1 Hz from (Malmelöv et al., 2020) and the plastic strain(ε) value up to 0.5 (X. Wang et al., 2013). Next, by applying the generic Johnson-Cook model formula to all of the model's parameters, the flow stress shown in the table below was obtained. The following value can be obtained in the flow stress table using equation 4.7 and the parameters from the John Soon Cook model.

Table 4-36 was predicted from the Johnson-Cook model parameters and formula to know the relationship between temperature and flow stress. Figure 4-20, 4-21 were drawn depending on this table and relationships.

Table 4-36: Analysis of Johnson Cook model

Temperature (ºC)	**Plastic strain (ε)**	**Strain rate($\dot{\varepsilon}$)**	**Reference strain rate($\dot{\varepsilon}0$)**	**Flow stress (σ) (MPa)**
25	0.05	0.01	0.001	720
100	0.10	0.1	0.001	865
200	0.15	0.2	0.001	950
300	0.20	0.3	0.001	995
400	0.25	0.4	0.001	1005
500	0.30	0.5	0.001	985
600	0.35	0.6	0.001	945
700	0.40	0.7	0.001	880
800	0.45	0.8	0.001	790
900	0.50	0.9	0.001	680

Figures 4-20 and 2-21 were drawn using Table 4-36, which provides an examination of the Johnson Cook model and was assessed using a variety of Johnson Cook models and formulas.

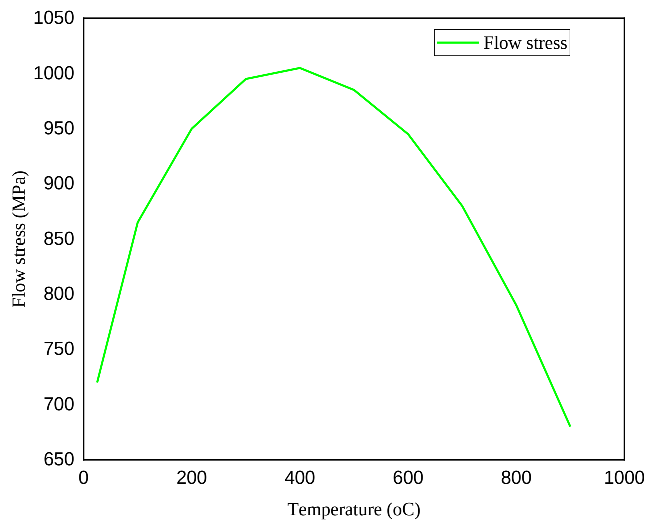

Figure 4-20: Interaction graph of temperature versus flow stress

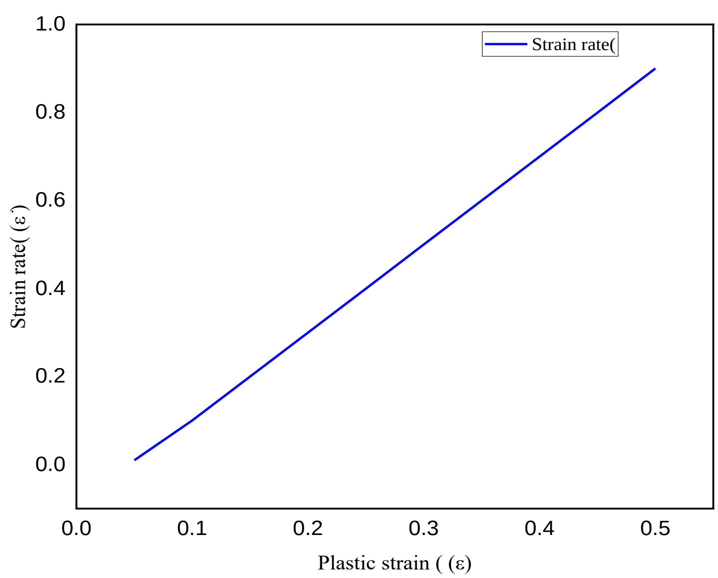

Figure 4-21: Interaction graph of strain rate versus and plastic strain

Based on the general property of temperature (maximum up to 900^{o}C), which was the basis for both Figures 4-20 and 4-21, Inconel 718 was analytically analyzed.

Figure 4-20: flow stress versus temperature from the analytical illustrates that as temperature rises, thermal activation increases and deformation resistance reduces, resulting in a decrease in flow stress. Because of the material's thermal softening at higher temperatures, the flow stress decreases. As temperature rises, thermal activation increases and deformation resistance reduces, resulting in a decrease in flow stress. To avoid thermal damage to the tool and workpiece, temperature monitoring is essential.

Figure 4-21 shows the link between Inconel 718's strain rate and plastic strain. Because the material has less time to distort at greater strain rates, plastic strain increases with increased strain rates.

In cylindrical grinding, a lower flow stress indicates better machinability and can lead to improved surface roughness. Therefore, at a lower flow stress on the graph, it achieves good surface roughness during cylindrical grinding. When temperatures are lower and strain rates are moderate, one often attain a good surface roughness value at lower flow stress levels. Combining these two methods yields a finer surface finish by removing material effectively without causing undue distortion or heat generation.

4.9.2 Mesh generation

Due to the grinding wheel's movement and the significant temperature differential in the area, only the grinding zone's mesh and the workpiece's surface layer are refined. The refined mesh and mesh analysis are shown in Figures 3-9 and 3-10, respectively.

The initial temperature of the workpiece was T=85^{o}C the final temperature of workpiece was T=125^{o}C for this mesh analysis, and thermal conductivity was 11.4 W/mk; Young's modulus was 208GPa; the Poisson's ratio was 0.3; and specific heat was 203 J/kg. In all, from mesh analysis, at the lowest temperature (in blue), good surface roughness was obtained, and at the highest temperature (in red)) worst surface roughness was obtained. According to Figure 3-9, the blue color (approximately a temperature of 85^{o}C-100^{o}C) indicates good surface roughness at the lowest temperature, and the red color indicates unexpected surface roughness at the maximum temperature in which it validates the experimental runs.

CHAPTER-5

CONCLUSIONS AND RECOMMENDATIONS

5.1 Conclusion

The research aimed to investigate surface finish, material removal rate, temperature, and tool life in a cylindrical grinding process of nickel-based super-alloy Inconel 718. The work piece was grinded with a CBN tool in a dry environment. The optimal design ranges of grinding conditions and the effect of grinding parameters on output responses were identified based on statistical analysis and graphical interpretations using Design Expert 13. The results indicated that grinding parameters influence surface roughness, material removal rate, temperature, and tool life. The main effect plots graphically present the response mean for each factor level.

1. The research findings close a gap in the body of knowledge about Inconel 718 cylindrical grinding in the literature. The research offers significant perspectives on the interplay between process variables, the optimization of several goals, and the use of ABAQUS analysis in the grinding procedure.
2. The identification of the best combinations of process parameters that simultaneously minimize temperature and surface roughness, maximize material removal rate, and prolong tool life was made possible by the integration of multi-objective optimization techniques such as genetic algorithms, Response surface methodology, and Grey relational analysis. This strategy provides an organized and effective means of attaining increased work piece quality and increased grinding efficiency.
3. The plot graphs clearly show that the minimum value of surface roughness was obtained at the lowest grinding parameters, and wheel speed is observed to be a significant factor in surface roughness for similar values of feed rate and depth of cut, which have a percentage contribution of 78.18%. A minimum surface roughness of 0.080μm was achieved at the lowest value of grinding parameters (0.01mm depth of cut, 0.02mm/rev, and 1200m/min of wheel speed).
4. The factor with the most significant influence on temperature was wheel speed, which had a contribution of 57.03%, followed by a depth of cut 17.98% of the contribution. This justifies the fact the fact that during operations, as surface roughness increases, the temperature also increases.

5. The factor with the most significant influence on material removal rate was feed rate, which had a contribution of 36.65%, followed by wheel speed (22.14% contribution) and depth of cut, which had an insignificant influence. The maximum MRR doesn't show economical machining because tool wear increases, surface roughness increases as wheel speed increases, and feed rate increases. The acceptable or recommended MRR was at optimum wheel speed, feed rate, and depth of cut, where the minimum Ra value was obtained.
6. Feed rate was the second most significant factor on tool life with a contribution of 25.57%, next to wheel speed as the most significant factor with a percentage of contribution of 33.99%, with a very small influence by depth of cut with a percentage of contribution of 2.49%.
7. In the present research, multi-objective optimization of wheel speed, feed rate, and depth of cut from the point of their effect on the surface roughness, temperature, tool life, and material removal rate is conducted rather than optimizing individual values.
8. The desirability function was used by Design Expert 13 to produce a single set of optimal parameters; however, Grey Relational Analysis and Genetic Algorithms in MATLAB 2021 produced many sets of optimal input process parameters.
9. Based on experimental researches, the arithmetical mean roughness of the surface is in the range Ra = 0.08 – 0.98μm. This means that by an appropriate choice of the input process parameters exceptionally high quality of a machined surface can be obtained, but worse quality as well.
10. The material removal rate, which varies from 7.10 to 15.12 mm^3/min and is proportionate to productivity, also varies significantly. The ideal output responses were cross-checked and the influence of the optimal input parameters on them was the same as for experimental research.
11. The mesh analysis at the lowest temperature (about 85^{o}C –100^{o}C) produced the best surface roughness result value because there was less friction at that temperature, and good surface roughness was acquired at that friction level. Reduced flow stress can result in improved surface roughness and better machinability.
12. A confirmation experiment is carried out to verify the model's validity. Since these errors guarantee that the grinding operation is carried out within the machining tolerances and the geometric product specifications, the model is regarded as usable in practice when the percentage of error achieved is less than 10%. The results of the study's confirmation experiments confirmed that the conclusions obtained through optimization were valid.

5.2 Recommendation

The applied methodology is limited to the conditions, equipment, and parameters used in performing this experimental investigation and to the workpiece material, Inconel 718. This presents its basic limitation. However, the methodology is entirely generalized and universal, so with additional experimental research, it can also be applied to other machining operations, workpiece materials, conditions of machining, etc. In addition, all types of wear mechanisms and chip morphology should be analyzed in detail in future research.

5.3 Scope for Future Work

- Future research could be directed toward considering a higher number of input process parameters. This will contribute to the optimization of the process, considering a higher number of criteria.
- The impact of grinding parameters such as feed rate, depth of cut, and wheel speed was investigated in this study. Additional factors such as grinding wheel type, coolant type and coolant flow rate, material composition, coating material, abrasive grain size lubricants, and so on could be considered in future research.
- Grinding forces, tool wear rate, and power usage could be measured in future experiments.
- Numerical simulation and modeling could be employed in the future to investigate stress, strain, and force analysis because those characteristics are difficult to investigate experimentally.
- Future research work also be directed towards applying the minimum quantity lubrication technique to further study the effect of grinding parameters and analyze them.
- In order to conduct a thorough investigation into the behavior of chips, further research using Scanning Electron Microscope could be included in the study of chip morphology.

SPECIAL ACKNOWLEDGEMENT

This research work is funded by Adama Science and Technology University under the grant number of ASTU/SM-R/1071/24, Adama, Ethiopia.

REFERENCES

Adiloğlu, S., Fajardo, S., García-Galvan, R., F., Barranco, V., Galvan, J. C., & Batlle, S. F. (2016). https://doi.org/http://dx.doi.org/10.5772/57353

Alagan, N. T., Beno, T., & Wretland, A. (2016). Investigation of modified cutting insert with forced coolant application in machining of alloy 718. Procedia Cirp, 42, 481–486.

Baksa, T., Hronek, O., Farsky, J., & Zetek, M. (2017a). Influence of Cutting Conditions on the Surface Quality snd Grinding Wheel Wear During Cylindrical Grinding of Inconel 718.

Baksa, T., Hronek, O., Farsky, J., & Zetek, M. (2017b). Influence of cutting conditions on the surface quality and grinding wheel wear during cylindrical grinding of inconel 718. https://doi.org/10.2507/28th.

Bedada, B. D., Woyesssa, G. K., Jiru, M. G., Fetene, B. N., & Gemechu, T. (2021). Experimental investigation on the advantages of dry machining over wet machining during turning of AISI 1020 steel. Journal of Modern Mechanical Engineering and Technology, 8, 12–25.

Botcha, B., Rajagopal, V., Babu, R. R., & Bukkapatnam, S. T. S. (2018). Process-machine interactions and a multi-sensor fusion approach to predict surface roughness in cylindrical plunge grinding process. https://doi.org/10.1016/j.promfg.2018.07.080

Canacoo, S. K. (2022). ScholarWorks @ UTRGV A Study of the Surface Properties of Additive Manufactured Inconel 718 After Laser Surface Treatment and CNC Grinding.

Chelladurai, S. J. S., Murugan, K., Ray, A. P., Upadhyaya, M., Narasimharaj, V., & Gnanasekaran, S. (2020). https://doi.org/10.1016/j.matpr.2020.06.466

Code, B. (2018). To Secure Your Paper As Per UGC Guidelines We Are Providing A Electronic Optimization Of Process Parameters On Cylindrical Grinding Machine Using Taguchi Method. 07.

Curtis, D., Krain, H., Winder, A., & Novovic, D. (2021). Impact of grinding wheel specification on surface integrity and residual stress when grinding Inconel 718. https://doi.org/10.1177/0954405420961209

Das, S., Pandivelan, C., Reddy, M., … D. K.-A. C., & 2021, undefined. (n.d.). Optimisation of ultrasonic assisted grinding of inconel 718 using grey relational analysis. Pubs.Aip.Org. Retrieved November 12, 2023, from https://pubs.aip.org/aip/acp/article-abstract/2341/1/040019/651993

Dawood Professor, Aks. (2016a). Prediction and Optimization of Process Parameters for Cylindrical Grinding of Inconel718 Alloy using Taguchi Approach. 3(26), 274–279. www.ijert.org

Dawood Professor, Aks. (2016b). Prediction and Optimization of Process Parameters for Cylindrical Grinding of Inconel718 Alloy using Taguchi Approach. 274–279. www.ijert.org

De Bartolomeis, A., Newman, S. T., Jawahir, I. S., Biermann, D., & Shokrani, A. (2021). Future research directions in the machining of Inconel 718. Journal of Materials Processing Technology, 297, 117260.

de Martini Fernandes, L., Lopes, J. C., Ribeiro, F. S. F., Gallo, R., Razuk, H. C., de Angelo Sanchez, L. E., de Aguiar, P. R., de Mello, H. J., & Bianchi, E. C. (2019). Thermal model for surface grinding application. The International Journal of Advanced Manufacturing Technology, 104, 2783–2793.

de Souza Ruzzi, R., de Paiva, R. L., da Silva, L. R. R., Abrão, A. M., Brandão, L. C., & da Silva, R. B. (2021). Comprehensive study on Inconel 718 surface topography after grinding. Tribology International, 158, 106919.

de Souza Ruzzi, R., de Paiva, R. L., Machado, A. R., & da Silva, R. B. (2021). Analysis of temperature and surface finish of Inconel 718 during grinding utilizing different grinding wheels. Journal of the Brazilian Society of Mechanical Sciences and Engineering, 43, 1–12.

Deshpande, Y. V., Andhare, A. B., Padole, P. M., & Sahu, N. K. (2018). Application of advanced algorithms for enhancement in machining performance of inconel 718. Indian Journal of Engineering and Materials Sciences, 25(5), 366–376.

Esmaeili, H., Adibi, H., & Rezaei, S. M. (2021). Study on surface integrity and material removal mechanism in eco-friendly grinding of Inconel 718 using numerical and experimental investigations. International Journal of Advanced Manufacturing Technology, 112(5–6), 1797–1818. https://doi.org/10.1007/S00170-020-06528-8

Halim, N. H. A., Haron, C. H. C., Ghani, J. A., & Azhar, M. F. (2019). Tool wear and chip morphology in high-speed milling of hardened Inconel 718 under dry and cryogenic CO 2 conditions. Wear, 426–427(September 2018), 1683–1690. https://doi.org/10.1016/j.wear.2019.01.095

Hatami, O., Adibi, H., & Rezaei, S. M. (2022). Application of a compressed air jet for cleaning of wheel surface in grinding nickel-based super alloy Inconel 718. CIRP Journal of Manufacturing Science and Technology, 37, 233–244. https://doi.org/10.1016/J.CIRPJ.2022.02.004

Henry, N., Akinlabi, E. T., & Ozoegwu, C. G. (2020). Optimization techniques applied to machinability studies for turning aluminium metal matrix composites : A literature review Materials Today : Proceedings Optimization techniques applied to machinability studies for turning aluminium metal matrix composit. Materials Today: Proceedings, 44(July 2021), 1124–1129. https://doi.org/10.1016/j.matpr.2020.11.228

Jafarian, F., Umbrello, D., Golpayegani, S., & Darake, Z. (2016). Experimental investigation to optimize tool life and surface roughness in Inconel 718 machining. Materials and Manufacturing Processes, 31(13), 1683–1691.

Jeevanantham, S., Robinson Smart, D. S., Sivaram, N. M., Nallusamy, S., & Manikanda Prabu, N. (2017). Effect of machining parameters on MRR and surface roughness in internal grinding using EN8, EN31 steel. International Journal of Applied Engineering Research, 12(11), 2963–2968.

Katoch, S., Chauhan, S. S., & Kumar, V. (2021). A review on genetic algorithm: past, present, and future. In Multimedia Tools and Applications (Vol. 80, Issue 5). Multimedia Tools and Applications. https://doi.org/10.1007/s11042-020-10139-6

Khuri, A. I., & Cornell, J. A. (2018). Response surfaces: designs and analyses. CRC press.

Kishore, K., Chauhan, S. R., & Sinha, M. K. (2023). Application of machine learning techniques in environmentally benign surface grinding of Inconel 625. Tribology International, 188, 108812. https://doi.org/10.1016/J.TRIBOINT.2023.108812

Kumar, A. K., & Venkataramaiah, P. (2022a). Experimental investigation on surface integrity of Inconel 718 under hot machining and optimisation of its process parameters.

Kumar, A. K., & Venkataramaiah, P. (2022b). Experimental investigation on surface integrity of Inconel 718 under hot machining and optimisation of its process parameters. https://doi.org/10.1080/2374068X.2020.1860503

Li, F., Li, X., Wang, T., Rong, Y. K., & Liang, S. Y. (2020). In-process residual stresses regulation during grinding through induction heating with magnetic flux concentrator. International Journal of Mechanical Sciences, 172, 105393.

Li, G., Liang, G., Shen, X., Lv, M., Liu, D., Hao, X., & Huang, Y. (2021). Investigation of the wear behavior of abrasive grits in a dry machining Inconel 718 narrow-deep-groove with a single-layer cubic boron nitride grinding wheel.

Li, G., Liang, G., Shen, X., Lv, M., Liu, D., Hao, X., Huang, Y., Tochukwu, O. P., & Al-Nehari, M. (2021). Investigation of the wear behavior of abrasive grits in a dry machining Inconel 718 narrow-deep-groove with a single-layer cubic boron nitride grinding wheel. International Journal of Advanced Manufacturing Technology, 117(3–4), 1061–1076. https://doi.org/10.1007/s00170-021-07823-8

Li, X., Wang, Y., Xu, R., Yang, S., Guan, C., & Zhou, Y. (2019). Influence of surface integrity on fatigue behavior of Inconel 718 and Ti6Al4V workpieces with CBN electroplated wheel. International Journal of Advanced Manufacturing Technology, 102(5–8), 2345–2356. https://doi.org/10.1007/s00170-019-03345-6

Liu, H., Han, H., Jiang, Q., He, M., & Zhang, B. (2024). Characterization and Analysis of Inconel 718 Alloy Ground at Different Speeds. Chinese Journal of Mechanical Engineering (English Edition), 37(1). https://doi.org/10.1186/s10033-024-01017-5

Lu, X., Wang, F., & Wang, X. (2018). Modelling and optimisation of cutting parameters on surface roughness in micro-milling Inconel 718 using response surface methodology and genetic algorithm Modeling and Optimization of cutting parameters on surface roughness in micro-milling Inconel 718 u. September. https://doi.org/10.1504/IJNM.2018.089178

Lyu, Y., Jang, K., Lee, R., Lyu, Y., Ay, H., & Huang, Y. (2023). Prediction of Surface Residual Stress in Grinding Process Prediction of Surface Residual Stress in Grinding. 0–22.

Malmelöv, A., Fisk, M., Lundbäck, A., & Lindgren, L.-E. (2020). Mechanism based flow stress model for alloy 625 and alloy 718. Materials, 13(24), 5620.

Martin, N., Nataa, N., & Hitoshi, O. (2016). Grinding of the Alloy INCONEL 718 and Final Roughness of the Surface. Key Engineering Materials, 686, 212–217. https://doi.org/10.4028/www.scientific.net/KEM.686.212

Materials, M. A. (2017). An Investigation into Vibratory Grinding Of Difficult to Machine Aerospace Materials Elsiddig Eldaw Ibrahim. November.

Nukman, Y., Farooqi, A., Al-Sultan, O., Alnasser, A. R. A., & Bhuiyan, M. S. H. (2017). A Strategic Development of Green Manufacturing Index (GMI) Topology Concerning the Environmental Impacts. Procedia Engineering, 184, 370–380.

https://doi.org/10.1016/j.proeng.2017.04.107

Nwobi-Okoye, C. C., & Uzochukwu, C. U. (2020). RSM and ANN modeling for production of Al 6351/ egg shell reinforced composite: Multi objective optimization using genetic algorithm. Materials Today Communications, 22(August), 100674. https://doi.org/10.1016/j.mtcomm.2019.100674

Panda, A., Sahoo, A., & Rout, R. (2016). Multi-attribute decision making parametric optimization and modeling in hard turning using ceramic insert through grey relational analysis: A case study. Decision Science Letters, 5(4), 581–592.

Park, E., Kim, D. M., Park, H. W., Park, Y. Bin, & Kim, N. (2020). Evaluation of Tool Life in the Dry Machining of Inconel 718 Parts from Additive Manufacturing (AM). https://doi.org/10.1007/s12541-019-00275-x

Pedroso, A. F. V., Sebbe, N. P. V., Costa, R. D. F. S., Barbosa, M. L. S., Sales-Contini, R. C. M., Silva, F. J. G., Campilho, R. D. S. G., & de Jesus, A. M. P. (2024). INCONEL® Alloy Machining and Tool Wear Finite Element Analysis Assessment. https://doi.org/10.3390/jmmp8010037

Ruzzi, R. de S., da Silva, R. B., da Silva, L. R. R., Machado, Á. R., Jackson, M. J., & Hassui, A. (2020). Influence of grinding parameters on Inconel 625 surface grinding. https://doi.org/10.1016/j.jmapro.2020.04.002

Serra, R., Chibane, H., & Duchosal, A. (2018). Multi-objective optimization of cutting parameters for turning AISI 52100 hardened steel. The International Journal of Advanced Manufacturing Technology, 99, 2025–2034.

Sheth, M., Gajjar, K., Jain, A., Shah, V., Patel, H., Chaudhari, R., & Vora, J. (2021). Multi-objective optimization of inconel 718 using Combined approach of taguchi—Grey relational analysis.

Shunmugesh, K., & Kavan, P. (2017). Investigation and optimization of machining parameters in drilling of carbon fiber reinforced polymer (CFRP) composites. Pigment and Resin Technology, 46(1), 21–30. https://doi.org/10.1108/PRT-03-2016-0029

Siddik, A. J., Kumar, A. A., Gurumoorthy, G., Mattuvarkulali, M., & Rekha, R. (2017). Effect of machining parameters on Material Removal Rate (MRR) and surface roughness in cylindrical grinding of Inconel 718. International Journal of Advanced Research Methodology in Engineering and Technology, 1(2), 152.

Sinha, M. K. (2018). Experimental investigations in grinding of inconel718 using different environments and modelling of specific grinding energy.

Sinha, M. K., Ghosh, S., & Paruchuri, V. R. (2019a). Modelling of specific grinding energy for Inconel 718 superalloy. https://doi.org/10.1177/0954405417741513

Sinha, M. K., Ghosh, S., & Paruchuri, V. R. (2019b). Modelling of specific grinding energy for Inconel 718 superalloy. Proceedings of the Institution of Mechanical Engineers, Part B: Journal of Engineering Manufacture, 233(2), 443–460.

Sinha, M. K., Kishore, K., & Sharma, P. (2023). Surface integrity evaluation in ecological nanofluids assisted grinding of Inconel 718 superalloy. Proceedings of the Institution of Mechanical Engineers, Part E: Journal of Process Mechanical Engineering, April. https://doi.org/10.1177/09544089231171042

Sinha, M. K., Madarkar, R., Ghosh, S., & Paruchuri, V. R. (2019). Some investigations in grindability improvement of Inconel 718 under ecological grinding. Proceedings of the Institution of Mechanical Engineers, Part B: Journal of Engineering Manufacture, 233(3), 727–744. https://doi.org/10.1177/0954405417752513

Slowik, A., & Kwasnicka, H. (2020). Evolutionary algorithms and their applications to engineering problems. https://doi.org/10.1007/s00521-020-04832-8

Soori, M., & Arezoo, B. (2022). Minimization of surface roughness and residual stress in grinding operations of Inconel 718. Journal of Materials Engineering and Performance, 1–10.

Soori, M., & Arezoo, B. (2023). Minimization of Surface Roughness and Residual Stress in Grinding Operations of Inconel 718. https://doi.org/10.1007/s11665-022-07721-4

Tawakoli, T., & Daneshi, A. (2019). Advanced Grinding. Modern Manufacturing Processes, 351–375.

Taylor, E., & Slatter, T. (2017). Role of temperature parameters in achieving precision traverse cylindrical grinding of chrome- plated ferrous metal rolls. https://doi.org/10.1115/1.4037889

Tebaldo, V., di Confiengo, G. G., & Faga, M. G. (2017). Sustainability in machining:“Eco-friendly” turning of Inconel 718. Surface characterisation and economic analysis. Journal of Cleaner Production, 140, 1567–1577.

Thankachan, T., Soorya Prakash, K., & Kamarthin, M. (2018). Optimizing the Tribological

Behavior of Hybrid Copper Surface Composites Using Statistical and Machine Learning Techniques. Journal of Tribology, 140(3). https://doi.org/10.1115/1.4038688

Tufa, K. A. (2024). Multi-Objective Electric Discharge Machining Process Parameters Optimization of Inconel 718 by using Machine Learning Techniques . 1–38.

Unune, D. R., & Mali, H. S. (2016). Optimization of Multi-Performance Characteristics in Abrasive Mixed Electro-Discharge Diamond Cut-off Grinding of Inconel 718 using Taguchi Grey Relational Analysis.

Upadhyay, V. V. (2020). Machining Parameters Optimization By Grey Relational Analysis of Alloy Steel Aisi 4140. Pjaee, 17(7), 4107–4121.

Varma, N. S. K., Varma, I., Rajesh, S., Raju, K. S. R., & Raju, V. V. M. K. (2018). Prediction of surface roughness and MRR in grinding process on Inconel 800 alloy using neural networks and ANFIS. Materials Today: Proceedings, 5(2), 5445–5451.

Wang, J., Yu, T., Ding, W., Fu, Y., & Bastawros, A. F. (2018). Wear evolution and stress distribution of single CBN superabrasive grain in high-speed grinding. Precision Engineering, 54, 70–80.

Wojtewicz, M., Nadolny, K., Kapłonek, W., Rokosz, K., Matýsek, D., & Ungureanu, M. (2019). Experimental studies using minimum quantity cooling (MQC) with molybdenum disulfide and graphite-based microfluids in grinding of Inconel® alloy 718. https://doi.org/10.1007/s00170-018-2935-4

Xie, W., Yang, F., Ding, L., & Scarpa, F. (2019). Predictive models and experiments for high-velocity and high-temperature impacts in Inconel-alloy panels. Materials & Design, 182, 108032.

Yin, G., & Marinescu, I. D. (2017). A heat transfer model of grinding process based on energy partition analysis and grinding fluid cooling application. https://doi.org/10.1115/1.4037241

Zahoor, S., Ameen, F., Abdul-Kader, W., & Stagner, J. (2020). Environmentally conscious machining of Inconel 718: surface roughness, tool wear, and material removal rate assessment. https://doi.org/10.1007/s00170-019-04550-z

Zhao, Y., Sun, J., Li, J., Yan, Y., & Wang, P. (2017). A comparative study on Johnson-Cook and modified Johnson-Cook constitutive material model to predict the dynamic behavior laser additive manufacturing FeCr alloy. Journal of Alloys and Compounds, 723, 179–187.

APPENDIX-I: Report Tables of Responses

I. Surface Roughness

Report on surface roughness is descriptions of each case statistic. The values in this report table were used to produce the diagnostics graphs.

Report

Run Order	Actual Value	Predicted Value	Residual	Leverage	Internally Studentized Residuals	Externally Studentized Residuals	Cook's Distance	Influence on Fitted Value DFFITS	Standard Order
1	0.4800	0.4763	0.0037	0.794	0.404	0.382	0.063	0.751	2
2	0.7200	0.7198	0.0002	0.505	0.013	0.013	0.000	0.013	10
3	0.3100	0.3412	-0.0312	0.155	-1.682	-1.957	0.052	-0.837	16
4	0.7000	0.7063	-0.0063	0.794	-0.688	-0.663	0.182	-1.303	4
5	0.2300	0.2343	-0.0043	0.794	-0.469	-0.445	0.085	-0.874	7
6	0.2100	0.2143	-0.0043	0.794	-0.469	-0.445	0.085	-0.874	3
7	0.2600	0.2738	-0.0138	0.505	-0.973	-0.969	0.096	-0.978	11
8	0.7800	0.7763	0.0037	0.794	0.404	0.382	0.063	0.751	6
9	0.2700	0.2638	0.0062	0.505	0.436	0.413	0.019	0.417	13
10	0.9800	0.9813	-0.0013	0.794	-0.142	-0.133	0.008	-0.261	8
11	0.1500	0.1443	0.0057	0.794	0.623	0.597	0.150	1.173	5
12	0.4200	0.4238	-0.0038	0.505	-0.268	-0.252	0.007	-0.255	14
13	0.4500	0.4338	0.0162	0.505	1.141	1.166	0.133	1.177	12
14	0.3200	0.3412	-0.0212	0.155	-1.143	-1.168	0.024	-0.500	18
15	0.0800	0.0793	0.0007	0.794	0.077	0.072	0.002	0.141	1
16	0.3600	0.3412	0.0188	0.155	1.014	1.016	0.019	0.435	17
17	0.3700	0.3412	0.0288	0.155	1.554	1.739	0.044	0.744	15
18	0.1600	0.1578	0.0022	0.505	0.154	0.145	0.002	0.146	9

Current Transform: Surface Roughness

Recommended Transform: None

Best Lambda	95% CI Low	95% CI High
0.9800	-0.4300	1.50

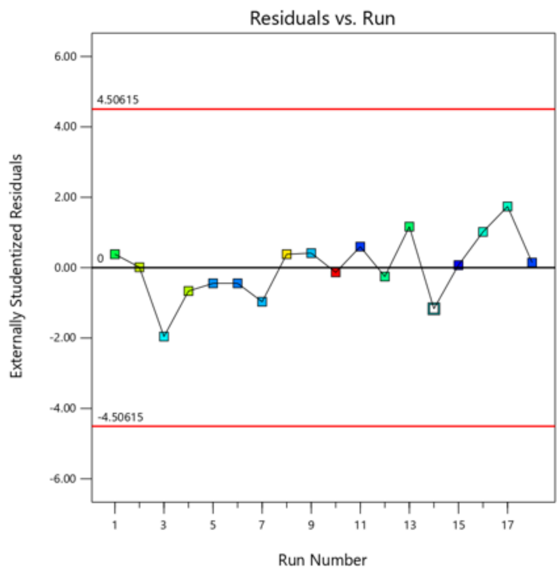

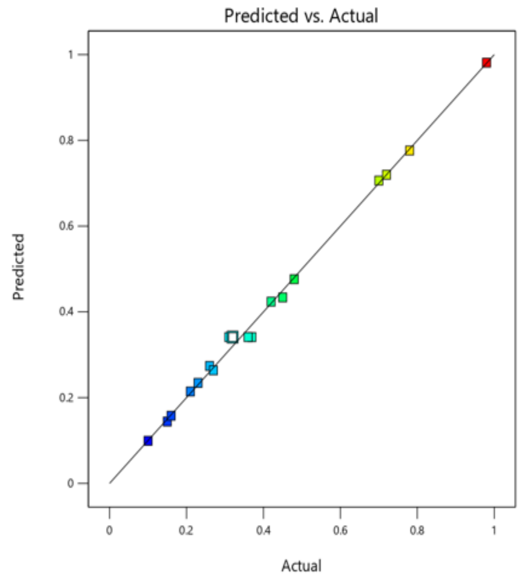

II. Material Removal Rate

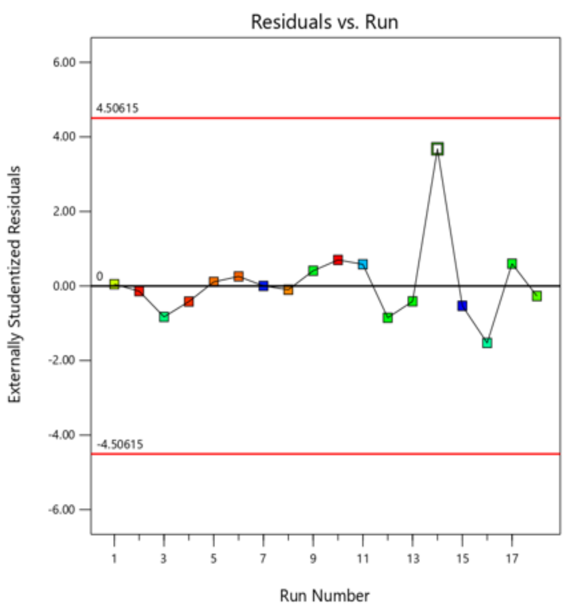

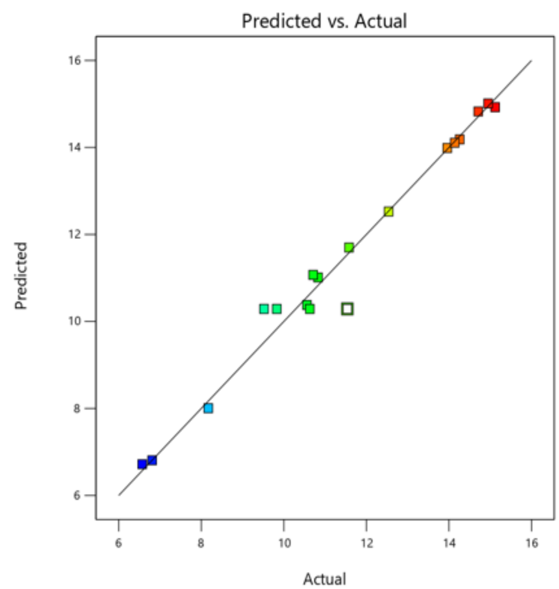

Report on material removal rate is descriptions of each case statistic. The values in this report table were used to produce the diagnostics graphs.

Report

Run Order	Actual Value	Predicted Value	Residual	Leverage	Internally Studentized Residuals	Externally Studentized Residuals	Cook's Distance	Influence on Fitted Value DFFITS	Standard Order
1	12.54	12.53	0.0136	0.794	0.050	0.047	0.001	0.093	2
2	14.95	15.01	-0.0612	0.505	-0.147	-0.138	0.002	-0.139	10
3	9.83	10.29	-0.4598	0.155	-0.845	-0.828	0.013	-0.354	16
4	14.71	14.83	-0.1184	0.794	-0.441	-0.417	0.075	-0.820	4
5	14.14	14.11	0.0316	0.794	0.117	0.110	0.005	0.216	7
6	14.26	14.19	0.0736	0.794	0.274	0.257	0.029	0.505	3
7	6.81	6.81	0.0008	0.505	0.002	0.002	0.000	0.002	11
8	13.96	13.99	-0.0284	0.794	-0.106	-0.099	0.004	-0.195	6
9	10.56	10.38	0.1808	0.505	0.434	0.411	0.019	0.415	13
10	15.12	14.93	0.1946	0.794	0.724	0.701	0.202	1.376	8
11	8.17	8.01	0.1636	0.794	0.609	0.583	0.143	1.145	5
12	10.71	11.07	-0.3612	0.505	-0.867	-0.852	0.077	-0.860	14
13	10.83	11.01	-0.1812	0.505	-0.435	-0.412	0.019	-0.416	12
14	11.54	10.29	1.25	0.155	2.297	3.680	0.097	1.575	18
15	7.1	7.23	-0.1494	0.794	-0.556	-0.531	0.119	-1.042	1
16	9.52	10.29	-0.7698	0.155	-1.414	-1.527	0.037	-0.653	17
17	10.63	10.29	0.3402	0.155	0.625	0.599	0.007	0.256	15
18	11.58	11.70	-0.1192	0.505	-0.286	-0.269	0.008	-0.272	9

Current Transform: Material Removal Rate

Recommended Transform: None

Best Lambda	95% CI Low	95% CI High
1.21	-0.1800	2.83

Report on temperature is descriptions of each case statistic. The values in this report table were used to produce the diagnostics graphs.

Report

Run Order	Actual Value	Predicted Value	Residual	Leverage	Internally Studentized Residuals	Externally Studentized Residuals	Cook's Distance	Influence on Fitted Value DFFITS	Standard Order
1	111.50	111.00	0.5044	0.731	0.586	0.567	0.133	0.934	2
2	115.30	115.23	0.0744	0.156	0.049	0.047	0.000	0.020	10
3	103.80	106.86	-3.06	0.056	-1.895	-2.201	0.030	-0.534	16
4	113.20	113.01	0.1944	0.731	0.226	0.216	0.020	0.355	4
5	112.70	111.92	0.7844	0.731	0.911	0.903	0.321	1.487	7
6	100.40	99.97	0.4344	0.731	0.504	0.487	0.099	0.801	3
7	101.60	102.73	-1.13	0.156	-0.738	-0.722	0.014	-0.310	11
8	118.70	117.85	0.8544	0.731	0.992	0.991	0.381	1.632	6
9	102.40	102.16	0.2444	0.156	0.160	0.153	0.001	0.066	13
10	119.60	119.06	0.5444	0.731	0.632	0.614	0.155	1.011	8
11	98.50	97.41	1.09	0.731	1.270	1.311	0.625	2.159[1]	5
12	110.40	111.56	-1.16	0.156	-0.758	-0.742	0.015	-0.318	14
13	111.10	110.99	0.1144	0.156	0.075	0.072	0.000	0.031	12
14	104.80	106.86	-2.06	0.056	-1.275	-1.316	0.014	-0.319	18
15	85.40	84.66	0.7444	0.731	0.864	0.853	0.289	1.405	1
16	106.50	106.86	-0.3556	0.056	-0.220	-0.211	0.000	-0.051	17
17	109.90	106.86	3.04	0.056	1.888	2.189	0.030	0.531	15
18	97.60	98.49	-0.8856	0.156	-0.581	-0.562	0.009	-0.241	9

Current Transform: Temperature

Recommended Transform: None

Best Lambda	95% CI Low	95% CI High
-0.4500	-2.33	1.91

APPENDIX-II: Surface Roughness Report from Instrument

Zeta Analysis Report			
	Ra	Rq	Rz
1	0.10	0.13	0.59
2	0.15	0.18	0.71
3	0.16	0.21	0.96
4	0.21	0.26	1.25
5	0.23	0.29	1.34
6	0.26	0.32	1.28
7	0.27	0.36	1.40
8	0.31	0.40	1.81
9	0.32	0.10	1.55
10	0.36	0.83	2.82
11	0.37	0.43	1.75
12	0.42	0.83	3.29
13	0.45	0.94	4.12
14	0.48	0.96	4.55
15	0.70	1.18	4.62
16	0.72	1.22	5.43
17	0.78	1.48	6.17
18	0.98	1.56	7.58

Interaction Plot for GRG (Grey relational grade)

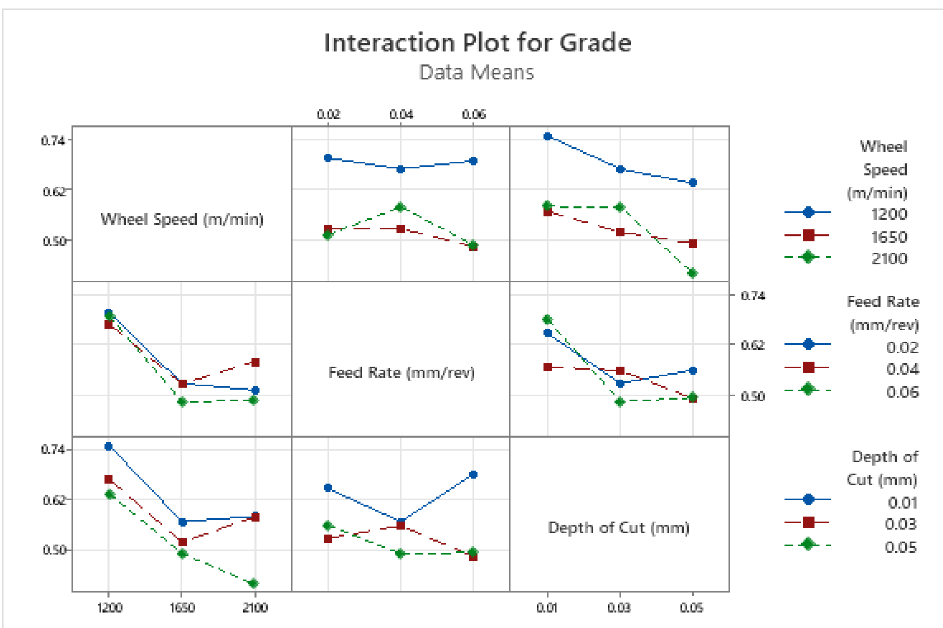

APPENDIX-III: CNC Cylindrical Grinding Code

The G-Code developed for work piece material on a vertical CNC Cylindrical grinding machine.

PROGRAM	**O0250 N000**
O0250 …………………………………………………………………. Program Name	
O0250; N100 G90 N102 G54 N106 G0 XO YO XO N108 G1 Z-100 F200 N110 G1 X15 N112 G1 X30 N114 G1 Y30 N116 G1 Z-100 F50 N118 G1 X30 N120 G1 Z-100 F200 N122 G1 X15 N124 G1 YO N126 G1 Z-100 F50 N128 G1 X30 N130 G1 Z-100 F200 N132 G1 X15 N134 G0 Z10 N136 G0 X0 YO M30 %	

APPENDIX-IV: MATLAB R2021 Code Generation for Ra

```
clear all
clc
close all

%% Define Objective Function and Constraints
SURFACEROUGHNESS = @(x) -(0.906 - 0.000624.* x(3)-
4.00.*x(2)- 4.00.*x(1)); % minimize objective function

g1 = @(x) x(1) - 0.05; % constraint 4
g2 = @(x) x(2) - 0.06; % constraint 2
g3 = @(x) x(3) - 2100; % constrain

%% Define Genetic Algorithm Parameters
nvars = 3; % number of decision variables
lb = [0.01, 0.02, 1200]; % lower bounds of decision
variables
ub = [0.05, 0.06, 2100]; % upper bounds of decision
variables
options = optimoptions('ga', 'Display', 'iter',
'PopulationSize', 1000, ...
    'MaxGenerations', 10, 'FunctionTolerance', 1e-6,
'PlotFcn', @gaplotbestf);

%% Run Genetic Algorithm
[x, fval] = ga(SURFACEROUGHNESS, nvars, [], [], [], [],
lb, ub, ...
    @(x) deal([g1(x), g2(x), g3(x)], []), options);

%% Display Results
disp('Optimization Results:')
disp(['SURFACEROUGHNESS In (?m): ', num2str(-fval)])
disp(['OPTIMUM VALUE OF d, f, N: ', num2str(x)])
```

```
Command Window

                              Best         Max          Stall
Generation   Func-count        f(x)      Constraint   Generations
    1          11550     -0.0360288          0         0
    2          22100     -0.0370054          0         0
    3          32650     -0.0370664          0         0
Optimization terminated: average change in the fitness value less than options.FunctionTolerance
 and constraint violation is less than options.ConstraintTolerance.
Optimization Results:
SURFACEROUGHNESS In (?m): 0.037066
OPTIMUM VALUE OF d, f, N: 0.010033397           0.02           1200
fx >>
```

Workspace

Name	Value
fval	-0.0371
g1	@(x)x(1)-0.05
g2	@(x)x(2)-0.06
g3	@(x)x(3)-2100
lb	[0.0100,0.020...
nvars	3
options	*1x1 GaOptions*
SURFACER...	@(x)-(0.906-0...
ub	[0.0500,0.060...
x	[0.0100,0.020...

APPENDIX-V: MATLAB R2021 Code Generation for GRG

```
clear all

clc

close all

%% Define Objective Function and Constraints

GRG= @(x) -(1.0066 - 0.000200.*x(3) - 1.39.* x(2)-
2.80.*x(1)); % maximize objective function

g1 = @(x) x(1) - 0.05; % constraint 4

g2 = @(x) x(2) - 0.06; % constraint 2

g3 = @(x) x(3) - 2100; % constrain

%% Define Genetic Algorithm Parameters

nvars = 3; % number of decision variables

lb = [0.01, 0.02, 1200]; % lower bounds of decision
variables

ub = [0.05, 0.06, 2100]; % upper bounds of decision
variables

options = optimoptions('ga', 'Display', 'iter',
'PopulationSize', 1000, ...

    'MaxGenerations', 10, 'FunctionTolerance', 1e-6,
'PlotFcn', @gaplotbestf);

%% Run Genetic Algorithm

[x, fval] = ga(GRG, nvars, [], [], [], [], lb, ub, ...

    @(x) deal([g1(x), g2(x), g3(x)], []), options);

%% Display Results
```

```
disp('Optimization Results:')

disp(['GRG: ', num2str(-fval)])

disp(['OPTIMUM VALUE OF d, f, N: ', num2str(x)])
```